

<https://www.mdc-berlin.de/de/veroeffentlichungstypen/clinical-journal-club>

## The weekly Clinical Journal Club by Dr. Friedrich C. Luft

Usually every Wednesday 17:00 - 18:00



### Klinische Forschung

Experimental and Clinical Research Center (ECRC) von MDC und Charité

Als gemeinsame Einrichtung von MDC und Charité fördert das Experimental and Clinical Research Center die Zusammenarbeit zwischen Grundlagenwissenschaftlern und klinischen Forschern. Hier werden neue Ansätze für Diagnose, Prävention und Therapie von Herz-Kreislauf- und Stoffwechselerkrankungen, Krebs sowie neurologischen Erkrankungen entwickelt und zeitnah am Patienten eingesetzt. Sie sind eingeladen, uns beizutreten. [Bewerben Sie sich!](#)



A previously healthy 42-year-old man presented with a 20-day history of an expanding, asymptomatic rash on his trunk. The initial lesion had been a red spot on the patient's left side. Ten days after that spot had first appeared, smaller lesions had developed elsewhere. The patient reported no viral prodrome. The skin examination — including the initial lesion that had appeared — is shown. What is the diagnosis?

Nummular eczema

Pityriasis rosea

Secondary syphilis

Tinea corporis

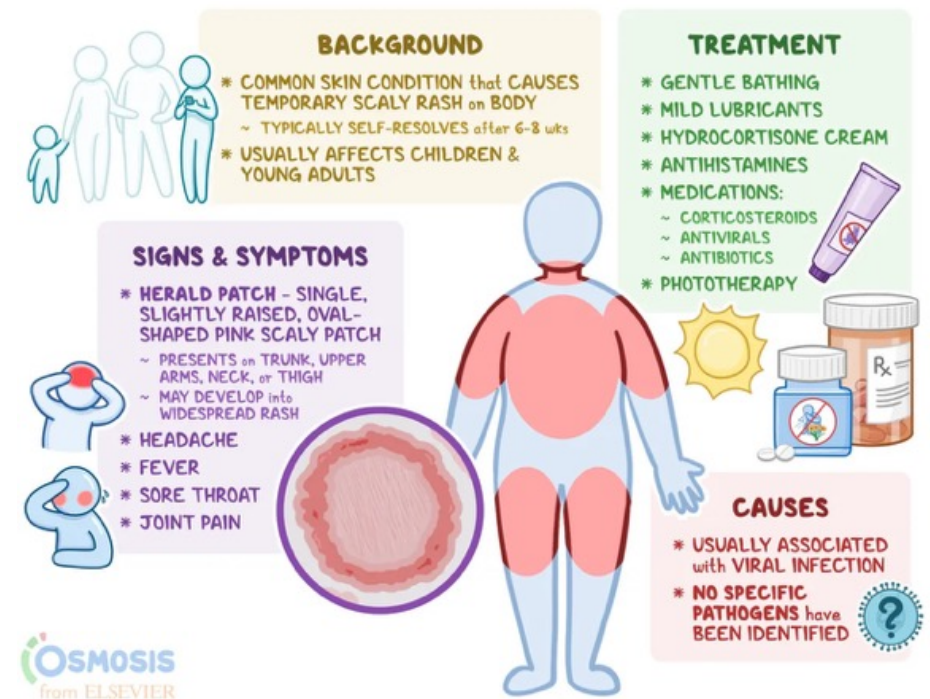
Tinea versicolor



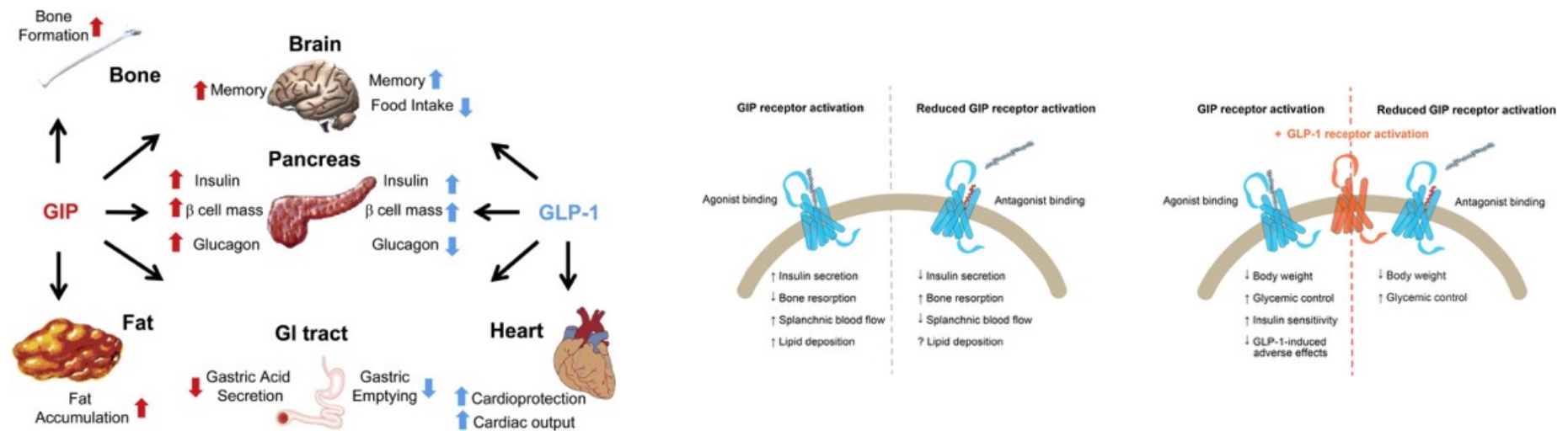
On the basis of the finding of a “herald – **primär Fleck**” patch in the patient's midaxillary line on the left side, a diagnosis of pityriasis rosea was made. Pityriasis rosea is a self-limiting disorder that typically affects children, adolescents, and young adults. The cause of pityriasis rosea remains unclear. It may be related to viral reactivation of human herpes virus 6 or 7.

Die Röschenflechte ist eine nicht ansteckende Hauterkrankung, welche in den meisten Fällen 6 bis 8 Wochen dauert, in einigen Fällen sogar bis zu einem halben Jahr. Sie tritt meistens bei Kindern und jüngeren Erwachsenen zwischen dem 10. und 35. Lebensjahr auf, vor allem im Frühjahr und Herbst.

Die Ursachen für diese Krankheit sind bisher unbekannt. Da sie unbedenklich ist und eher ein kosmetisches Problem für den Patienten darstellt, wurde bisher auch wenig hierzu geforscht. Es wurde vermutet, dass es sich um einen Virusinfekt handelt, der von einem humanen Herpesvirus, möglicherweise HHV-6 (B) oder HHV-7, hervorgerufen wird. Belege gibt es für diese Hypothese keine. Die Krankheit tritt häufig in Kombination mit Allergien und Stress auf. Zuerst bildet sich das rötliche, etwa einen Zentimeter große, sogenannte Primärmedaillon (auch Primärfleck, Plaque mère oder Herald Patch), am Körperstamm; es wurde aber auch schon an der Innenseite des Unterarmes, auf dem Rücken, am Unterschenkel, auf dem Bauch, an den Oberschenkeln oder am Haaransatz beobachtet.



GIP (glucose-dependent insulinotropic polypeptide) and GLP-1 (glucagon-like peptide-1) are both incretin hormones released by the gut after a meal to stimulate insulin secretion, but they have different origins and some differing actions. GIP promotes fat deposition and bone formation, while GLP-1 suppresses appetite, slows gastric emptying, and inhibits bone absorption. Dual GIP/GLP-1 receptor agonists, like tirzepatide, leverage the complementary effects of both hormones for improved glycemic control and weight loss in type 2 diabetes.



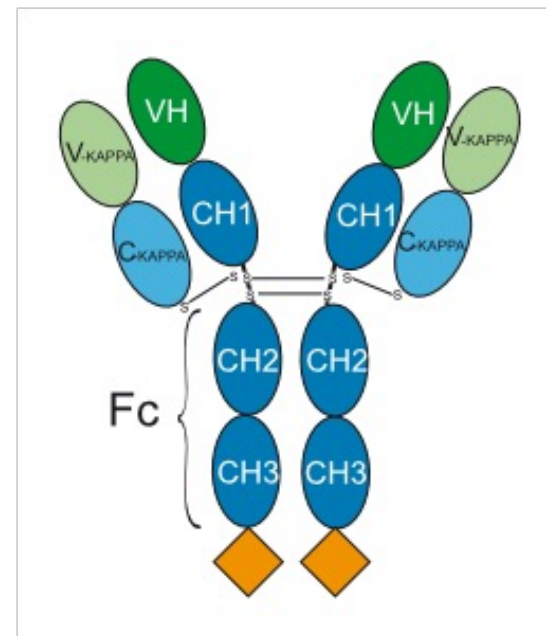
Tirzepatid wirkt als hochselektiver Agonist an Rezeptoren der Inkretine GLP-1 (Glucagon-Like Peptide 1) und GIP (Glucoseabhängiges Insulinotropes Peptid). Der Wirkstoff erhöht auf die gleiche Weise wie GIP und GLP-1 glukoseabhängig die Insulinmenge, die die Bauchspeicheldrüse als Reaktion auf Nahrung freisetzt.



Maridebart cafraglutide (MariTide) is an investigational once-monthly weight-loss drug developed by Amgen that acts as both a GLP-1 receptor agonist and a GIP receptor antagonist. It has shown promising results in Phase 2 trials, with patients losing up to 20% of their body weight in one year and experiencing improvements in metabolic health markers. While it is generally well-tolerated, common side effects include mild gastrointestinal symptoms like nausea and vomiting. AMG 133 (maridebart cafraglutide) is a bispecific molecule engineered by conjugating a fully human monoclonal anti-human GIPR antagonist antibody to two GLP-1 analogue agonist peptides using amino acid linkers.

The gastric inhibitory polypeptide receptor (GIP-R), also known as the glucose-dependent insulintropic polypeptide receptor, is a protein that in humans is encoded by the GIPR gene. GIP-R is a member of the class B family of G protein coupled receptors. GIP-R is found on beta-cells in the pancreas where it serves as the receptor for the hormone Gastric inhibitory polypeptide (GIP).

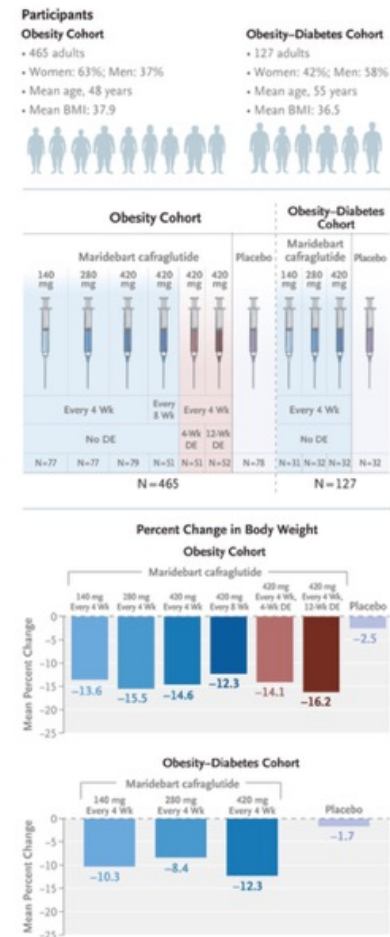
Glucose-dependent insulintropic polypeptide receptor and the gastric inhibitory polypeptide receptor (GIP-R) are the same thing. Fortunately, the abbreviation is the same.



# Once-Monthly Maridebart Cafraglutide for the Treatment of Obesity — A Phase 2 Trial

Maridebart cafraglutide (known as MariTide) is a long-acting peptide–antibody conjugate that combines glucagon-like peptide-1 receptor agonism and glucose-dependent insulintropic polypeptide receptor antagonism and that is intended for the treatment of obesity.

We conducted a phase 2, double-blind, randomized, placebo-controlled, dose-ranging trial that included 11 groups as two cohorts. Participants with obesity (obesity cohort) were randomly assigned in a 3:3:3:2:2:2:3 ratio to receive maridebart cafraglutide subcutaneously at a dose of 140, 280, or 420 mg every 4 weeks without dose escalation; 420 mg every 8 weeks without dose escalation; 420 mg every 4 weeks with 4-week dose escalation; 420 mg every 4 weeks with 12-week dose escalation; or placebo. Participants with obesity with type 2 diabetes (obesity–diabetes cohort) were randomly assigned in a 1:1:1:1 ratio to receive maridebart cafraglutide at a dose of 140, 280, or 420 mg every 4 weeks (all without dose escalation) or placebo. The primary end point was the percent change in body weight from baseline to week 52.



Once-monthly therapeutics for obesity may offer sustainable treatment for persons with this highly prevalent, chronic disease. Once-weekly nutrient-stimulated hormone receptor modulators, such as semaglutide and tirzepatide, target the neurometabolic pathophysiological pathways of obesity, resulting in substantial weight reduction while also addressing obesity-related complications. However, access and adherence remain barriers to treatment. Medication at less frequent intervals may improve adherence and reduce barriers, potentially facilitating improvements in long-term health outcomes.

Maridebart cafraglutide (known as MariTide or AMG133; Amgen) is a long-acting molecule that combines glucagon-like peptide-1 (GLP-1) receptor agonism and glucose-dependent insulinotropic polypeptide (GIP) receptor antagonism.

### **Participants**

The obesity cohort included participants with a BMI of 30 or more, or 27 or more with at least one obesity-related complication, and a glycated hemoglobin level of less than 6.5%. The obesity–diabetes cohort included participants with a BMI of 27 or more and an established diagnosis of type 2 diabetes.

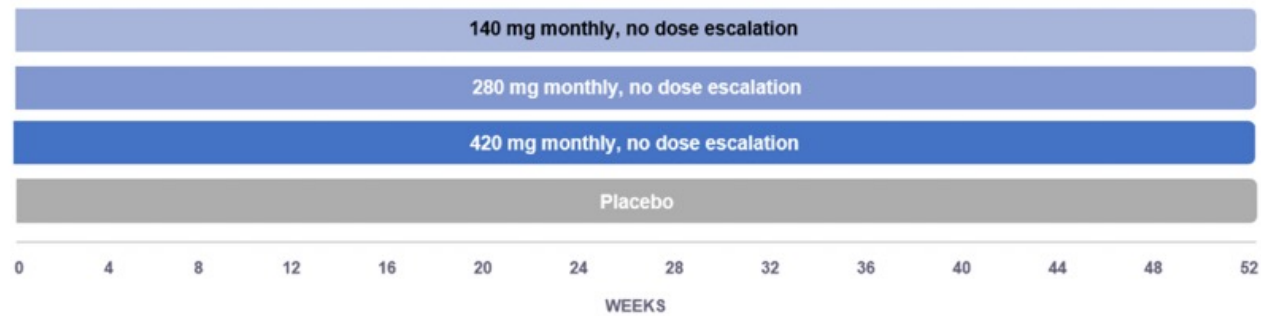
### **Procedures**

Participants in the obesity cohort were randomly assigned in a 3:3:3:2:2:2:3 ratio to receive 52 weeks of maridebart cafraglutide subcutaneously at a dose of 140, 280, or 420 mg every 4 weeks; or 420 mg every 8 weeks without dose escalation; or 420 mg every 4 weeks with a 4-week dose escalation; or 420 mg every 4 weeks with a 12-week dose escalation; or placebo, respectively. Participants in the obesity–diabetes cohort were randomly assigned in a 1:1:1:1 ratio to receive 52 weeks of maridebart cafraglutide at a dose of 140, 280, or 420 mg every 4 weeks (all without dose escalation) or placebo, respectively.

A. Study design - obesity cohort (n = 465)



B. Study design - obesity+diabetes cohort (n = 127)





## Demographic and Clinical Characteristics of the Participants at Baseline.

Characteristic	Obesity Cohort							Obesity+Diabetes Cohort					
	Maridebart Cafraglutide, No Dose Escalation				Maridebart Cafraglutide, Dose Escalation (DE)		Placebo (N=78)	Total (N=465)	Maridebart Cafraglutide, No Dose Escalation			Placebo (N=32)	Total (N=127)
	140 mg Every 4 Wk (N=77)	280 mg Every 4 Wk (N=77)	420 mg Every 4 Wk (N=79)	420 mg Every 8 Wk (N=51)	420 mg Every 4 Wk, with 4-Wk DE (N=51)	420 mg Every 4 Wk, with 12-Wk DE (N=52)			140 mg Every 4 Wk (N=31)	280 mg Every 4 Wk (N=32)	420 mg Every 4 Wk (N=32)		
Age — yr	45.6±12.2	49.4±12.6	49.1±13.0	47.6±11.0	49.0±11.4	48.2±12.5	47.0±12.9	47.9±12.3	54.9±12.8	56.8±11.7	55.3±10.3	53.5±10.2	55.1±11.2
Female sex — no. (%)	48 (62)	48 (62)	50 (63)	33 (65)	31 (61)	33 (64)	49 (63)	292 (63)	13 (42)	14 (44)	13 (41)	13 (41)	53 (42)
Race or ethnic group — no. (%)†													
American Indian or Alaska Native	0	0	0	0	0	1 (2)	1 (1)	2 (<0.5)	0	0	0	0	0
Asian	13 (17)	20 (26)	15 (19)	11 (22)	14 (27)	16 (31)	14 (18)	103 (22)	6 (19)	6 (19)	9 (28)	10 (31)	31 (24)
Black	6 (8)	4 (5)	4 (5)	3 (6)	6 (12)	2 (4)	7 (9)	32 (7)	2 (6)	2 (6)	0	5 (16)	9 (7)
White	53 (69)	52 (68)	59 (75)	33 (65)	30 (59)	32 (62)	51 (65)	310 (67)	23 (74)	24 (75)	22 (69)	17 (53)	86 (68)
Native Hawaiian or other Pacific Islander	1 (1)	1 (1)	0	1 (2)	0	0	1 (1)	4 (1)	0	0	0	0	0
Multiple	2 (3)	0	0	2 (4)	0	0	1 (1)	5 (1)	0	0	0	0	0
Other	2 (3)	0	1 (1)	1 (2)	1 (2)	1 (2)	3 (4)	9 (2)	0	0	1 (3)	0	1 (1)
Hispanic or Latino ethnic group — no. (%)†	6 (8)	8 (10)	9 (11)	4 (8)	7 (14)	9 (17)	19 (24)	62 (13)	6 (19)	4 (12)	3 (9)	4 (12)	17 (13)
Body weight — kg	109.9± 26.7	103.4± 18.3	108.6± 25.3	106.9± 28.4	109.3± 21.9	102.3± 19.7	110.1± 31.7	107.4± 25.2	106.0± 24.6	101.0± 16.8	106.7± 26.5	101.8± 18.0	103.9± 21.7
Mean BMI	38.3±7.6	36.6±5.8	38.8±7.8	38.0±8.7	38.3±6.9	36.2±6.2	38.9±8.9	37.9±7.5	36.5±6.8	35.8±6.6	37.1±8.5	36.4±6.3	36.5±7.0
BMI category — no. (%)													
<30	6 (8)	8 (10)	7 (9)	7 (14)	1 (2)	6 (12)	7 (9)	42 (9)	5 (16)	7 (22)	7 (22)	6 (19)	25 (20)
30 to <35	25 (32)	25 (32)	20 (25)	14 (27)	18 (35)	21 (40)	28 (36)	151 (32)	9 (29)	8 (25)	7 (22)	8 (25)	32 (25)
35 to <40	20 (26)	24 (31)	22 (28)	14 (27)	15 (29)	13 (25)	12 (15)	120 (26)	9 (29)	10 (31)	9 (28)	11 (34)	39 (31)
≥40	26 (34)	20 (26)	30 (38)	16 (31)	17 (33)	12 (23)	31 (40)	152 (33)	8 (26)	7 (22)	9 (28)	7 (22)	31 (24)
Waist circumfer- ence — cm	114.9± 16.3	113.1± 13.2	117.3± 16.4	114.4± 18.4	117.4± 14.8	112.0± 12.8	116.8± 19.6	115.2± 16.2	117.8± 15.7	116.4± 11.8	119.7± 16.2	115.0± 13.8	117.2± 14.4
Prediabetes — no. (%)‡	26 (34)	27 (35)	24 (30)	18 (35)	23 (45)	11 (21)	24 (31)	153 (33)	NA	NA	NA	NA	NA
Glycated hemoglo- bin — %	5.5±0.4	5.5±0.4	5.5±0.4	5.5±0.4	5.5±0.4	5.5±0.4	5.5±0.4	5.5±0.4	7.8±0.6	7.8±0.7	7.8±0.6	8.0±0.9	7.9±0.7
Systolic blood pressure — mm Hg	125.0± 14.3	126.3± 16.1	128.6± 14.8	126.6± 14.1	130.0± 13.1	126.2± 11.9	125.9± 13.7	126.8± 14.2	128.3± 13.2	131.3± 15.6	131.0± 19.5	133.9± 16.0	131.1± 16.2
Diastolic blood pressure — mm Hg	80.5±10.5	79.0±11.4	80.4±10.3	80.9±8.9	82.4±9.9	81.2±8.6	81.9±9.3	80.8±10.0	81.8±8.6	84.5±8.5	80.1±10.5	83.6±9.2	82.5±9.3

## Primary and Select Key Secondary End Points.

End Point	Obesity Cohort						Obesity-Diabetes Cohort				
	Maridebart Cafraglutide, No Dose Escalation				Maridebart Cafraglutide, Dose Escalation (DE)		Placebo (N = 76)	Maridebart Cafraglutide, No Dose Escalation			Placebo (N = 32)
	140 mg Every 4 Wk (N = 77)	280 mg Every 4 Wk (N = 77)	420 mg Every 4 Wk (N = 79)	420 mg Every 8 Wk (N = 51)	420 mg Every 4 Wk, with 4-Wk DE (N = 51)	420 mg Every 4 Wk, with 12-Wk DE (N = 52)		140 mg Every 4 Wk (N = 31)	280 mg Every 4 Wk (N = 32)	420 mg Every 4 Wk (N = 32)	
estimate (95% CI)											
Treatment policy estimand											
Primary end point											
Mean percent change in body weight	-13.6 (-15.5 to -11.7)	-15.5 (-17.7 to -13.4)	-14.6 (-16.8 to -12.4)	-12.3 (-15.0 to -9.7)	-14.1 (-16.2 to -12.1)	-16.2 (-18.9 to -13.5)	-2.5 (-4.2 to -0.7)	-10.3 (-13.2 to -7.4)	-8.4 (-11.0 to -5.7)	-12.3 (-15.3 to -9.2)	-1.7 (-2.9 to -0.6)
Mean difference vs. placebo — percentage points	-11.1 (-13.6 to -8.7)	-13.1 (-15.6 to -10.6)	-12.2 (-14.8 to -9.5)	-9.9 (-12.8 to -6.9)	-11.7 (-14.3 to -9.1)	-13.8 (-16.8 to -10.7)	NA	-8.6 (-11.6 to -5.6)	-6.6 (-9.3 to -3.9)	-10.5 (-13.6 to -7.4)	NA
Key secondary end points											
Change in glycated hemoglobin — percentage points	-0.3 (-0.4 to -0.3)	-0.4 (-0.5 to -0.3)	-0.3 (-0.3 to -0.2)	-0.3 (-0.4 to -0.2)	-0.3 (-0.4 to -0.3)	-0.3 (-0.4 to -0.3)	0.0 (-0.1 to 0.1)	-1.6 (-1.9 to -1.2)	-1.2 (-1.7 to -0.7)	-1.5 (-1.9 to -1.0)	0.1 (-0.4 to 0.5)
Change in mean fasting serum insulin — $\mu$ U/ml	-1.7 (-4.0 to 0.7)	-4.0 (-5.6 to -2.4)	-3.8 (-5.4 to -2.2)	-2.0 (-4.1 to 0.1)	-4.2 (-6.0 to -2.4)	-5.1 (-6.6 to -3.7)	0.0 (-3.4 to 3.4)	-1.7 (-4.7 to 1.3)	0.4 (-2.9 to 3.6)	-2.2 (-5.7 to 1.4)	0.1 (-2.6 to 2.9)
Change in mean fasting plasma glucose — mg/dl	-8.6 (-10.8 to -6.5)	-9.2 (-11.2 to -7.2)	-9.0 (-11.5 to -6.5)	-7.7 (-10.2 to -5.3)	-10.6 (-12.9 to -8.2)	-9.1 (-12.3 to -5.9)	-0.6 (-3.7 to 2.6)	-33.9 (-48.7 to -19.2)	-25.5 (-42.5 to -8.5)	-35.1 (-52.7 to -17.5)	9.2 (-16.8 to 35.1)
Efficacy estimand											
Primary end point											
Mean percent change in body weight	-16.3 (-17.5 to -15.2)	-19.9 (-21.1 to -18.6)	-18.9 (-20.2 to -17.6)	-17.7 (-19.3 to -16.1)	-16.7 (-18.0 to -15.4)	-19.9 (-21.4 to -18.4)	-2.6 (-3.6 to -1.5)	-12.3 (-14.1 to -10.4)	-12.1 (-14.2 to -10.1)	-17.0 (-18.8 to -15.3)	-1.4 (-2.5 to -0.3)
Mean difference vs. placebo — percentage points	-13.8 (-15.3 to -12.2)	-17.3 (-18.9 to -15.7)	-16.3 (-18.0 to -14.6)	-15.1 (-17.1 to -13.2)	-14.2 (-15.8 to -12.5)	-17.4 (-19.2 to -15.6)	NA	-10.9 (-13.0 to -8.7)	-10.7 (-13.1 to -8.4)	-15.7 (-17.8 to -13.6)	NA
Key secondary end points											
Change in glycated hemoglobin — percentage points	-0.4 (-0.5 to -0.3)	-0.4 (-0.5 to -0.4)	-0.4 (-0.4 to -0.3)	-0.4 (-0.5 to -0.3)	-0.4 (-0.5 to -0.3)	-0.4 (-0.5 to -0.3)	0.0 (-0.1 to 0.1)	-1.9 (-2.1 to -1.6)	-2.0 (-2.2 to -1.8)	-2.2 (-2.4 to -2.0)	0.1 (-0.4 to 0.6)
Change in mean fasting serum insulin — $\mu$ U/ml	-1.4 (-4.1 to 1.2)	-5.2 (-6.4 to -4.0)	-5.0 (-6.9 to -3.1)	-2.7 (-5.2 to -0.3)	-6.0 (-8.0 to -3.9)	-6.1 (-7.1 to -5.1)	-0.5 (-3.2 to 2.2)	-2.0 (-5.4 to 1.4)	-0.1 (-4.8 to 4.5)	-3.1 (-8.4 to 2.3)	1.2 (-1.6 to 3.9)
Change in mean fasting plasma glucose — mg/dl	-11.4 (-13.3 to -9.5)	-12.3 (-13.8 to -10.9)	-12.7 (-15.1 to -10.3)	-11.7 (-14.0 to -9.5)	-13.0 (-15.3 to -10.7)	-11.7 (-15.3 to -8.1)	-0.5 (-3.7 to 2.7)	-43.6 (-56.1 to -31.0)	-46.4 (-56.5 to -36.4)	-58.2 (-67.4 to -49.0)	22.0 (-8.9 to 53.0)

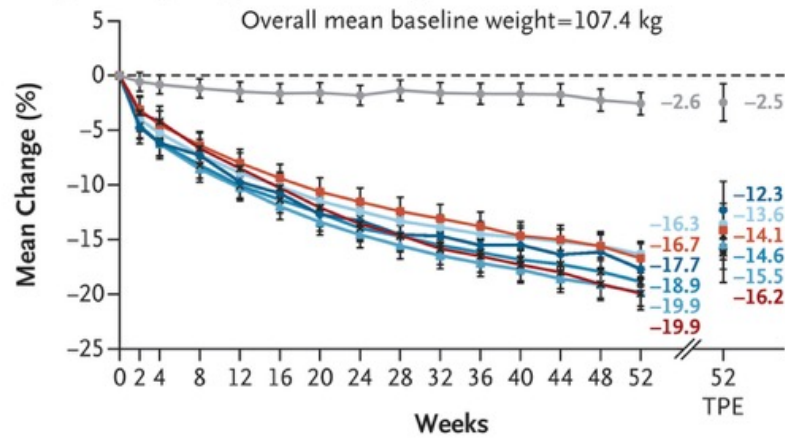
## Safety and Adverse Events.

Event	Obesity Cohort						Obesity+Diabetes Cohort					
	Maridebart Cafraglutide, No Dose Escalation				Maridebart Cafraglutide, Dose Escalation (DE)		Placebo (N=76)	Maridebart Cafraglutide, No Dose Escalation			Placebo (N=32)	
	140 mg Every 4 Wk (N=77)	280 mg Every 4 Wk (N=77)	420 mg Every 4 Wk (N=79)	420 mg Every 8 Wk (N=51)	420 mg Every 4 Wk, with 4-Wk DE (N=51)	420 mg Every 4 Wk, with 12-Wk DE (N=52)		140 mg Every 4 Wk (n=31)	280 mg Every 4 Wk (N=32)	420 mg Every 4 Wk (N=32)		
	number of participants (percent)											
Overall												
Any adverse event	73 (95)	75 (97)	78 (99)	49 (96)	46 (90)	49 (94)	52 (68)	29 (94)	29 (91)	31 (97)	26 (81)	
Serious adverse event	4 (5)	4 (5)	5 (6)	7 (14)	0	3 (6)	5 (7)	1 (3)	2 (6)	4 (12)	0	
Death†	0	0	0	0	0	1 (2)	0	0	1 (3)	0	0	
Adverse events leading to discontinuation of trial regimen	11 (14)	11 (14)	17 (22)	15 (29)	5 (10)	6 (12)	1 (1)	4 (13)	6 (19)	5 (16)	1 (3)	
GI adverse event leading to dis- continuation	10 (13)	9 (12)	13 (16)	14 (27)	4 (8)	4 (8)	0	2 (6)	5 (16)	4 (12)	0	
Most frequent adverse events leading to discontinua- tion‡												
Vomiting	9 (12)	8 (10)	12 (15)	12 (24)	3 (6)	1 (2)	0	1 (3)	3 (9)	4 (12)	0	
Nausea	6 (8)	7 (9)	11 (14)	8 (16)	3 (6)	1 (2)	0	1 (3)	2 (6)	1 (3)	0	
Retching	2 (3)	1 (1)	1 (1)	3 (6)	0	0	0	0	0	0	0	
Headache	1 (1)	1 (1)	2 (3)	2 (4)	0	0	0	0	0	0	0	
Diarrhea	0	1 (1)	3 (4)	0	1 (2)	0	0	1 (3)	1 (3)	0	0	
Fatigue	1 (1)	1 (1)	2 (3)	1 (2)	0	0	0	0	0	0	0	
Constipation	2 (3)	1 (1)	1 (1)	0	0	0	0	0	0	0	0	
GERD	2 (3)	0	0	1 (2)	0	0	0	0	0	0	0	
Injection-site reaction	1 (1)	0	1 (1)	0	1 (2)	0	0	0	0	0	0	
Malaise	0	2 (3)	1 (1)	0	0	0	0	0	0	0	0	

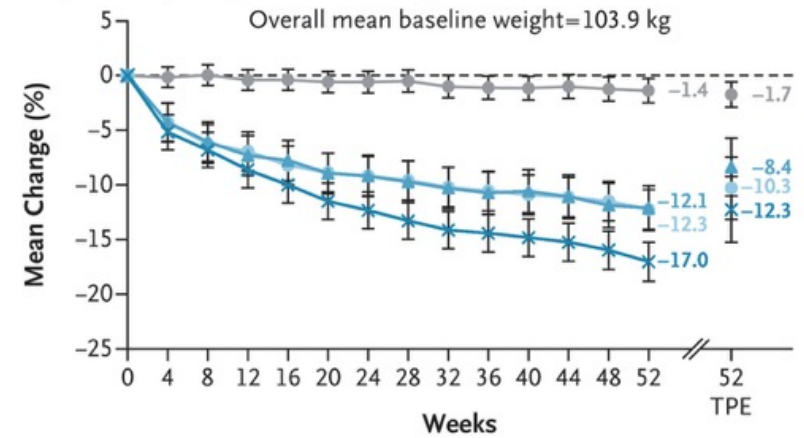
<b>Most frequent adverse events§</b>											
Nausea	59 (77)	60 (78)	69 (87)	42 (82)	36 (71)	38 (73)	19 (25)	18 (58)	13 (41)	19 (59)	3 (9)
Vomiting	52 (68)	56 (73)	69 (87)	47 (92)	22 (43)	23 (44)	2 (3)	14 (45)	16 (50)	24 (75)	2 (6)
Constipation	23 (30)	19 (25)	19 (24)	18 (35)	12 (24)	11 (21)	4 (5)	4 (13)	3 (9)	6 (19)	0
Retching	13 (17)	11 (14)	18 (23)	11 (22)	5 (10)	8 (15)	1 (1)	1 (3)	2 (6)	2 (6)	0
Diarrhea	8 (10)	5 (6)	17 (22)	6 (12)	7 (14)	10 (19)	4 (5)	3 (10)	5 (16)	5 (16)	3 (9)
Headache	11 (14)	8 (10)	13 (16)	10 (20)	3 (6)	5 (10)	5 (7)	1 (3)	1 (3)	3 (9)	4 (12)
GERD	8 (10)	8 (10)	8 (10)	7 (14)	4 (8)	7 (13)	0	2 (6)	2 (6)	2 (6)	0
<b>Adverse events of special inter- est¶</b>											
Hypersensitivity	3 (4)	4 (5)	2 (3)	3 (6)	4 (8)	4 (8)	3 (4)	1 (3)	1 (3)	1 (3)	0
Injection-site reactions	10 (13)	5 (6)	8 (10)	0	8 (16)	6 (12)	2 (3)	2 (6)	3 (9)	1 (3)	2 (6)
Severe or serious GI events	6 (8)	2 (3)	9 (11)	5 (10)	1 (2)	1 (2)	0	0	1 (3)	3 (9)	0
Acute renal events	0	0	0	1 (2)	0	0	0	0	0	0	0
Diabetic retinopathy	0	0	0	0	0	0	0	0	0	0	0
Acute pancreatitis	0	0	0	0	0	0	0	0	0	0	0
Acute gallbladder diseases	1 (1)	1 (1)	5 (6)	1 (2)	0	2 (4)	0	0	1 (3)	0	0
C-cell hyperplasia or thyroid cancer	0	0	0	0	0	0	0	0	0	0	0
Heart-rate increase	0	4 (5)	0	1 (2)	1 (2)	0	1 (1)	0	2 (6)	0	2 (6)
Depressive disorder or suicidal behavior or ideation]	1 (1)	0	4 (5)	5 (10)	1 (2)	0	0	0	0	0	1 (3)
Severe or serious adverse event	0	0	0	1 (2)	0	0	0	0	0	0	0

140 mg every 4 wk (no DE)    280 mg every 4 wk (no DE)    420 mg every 4 wk (no DE)    420 mg every 8 wk (no DE)  
 420 mg every 4 wk, with 4-wk DE    420 mg every 4 wk, with 12-wk DE    Placebo

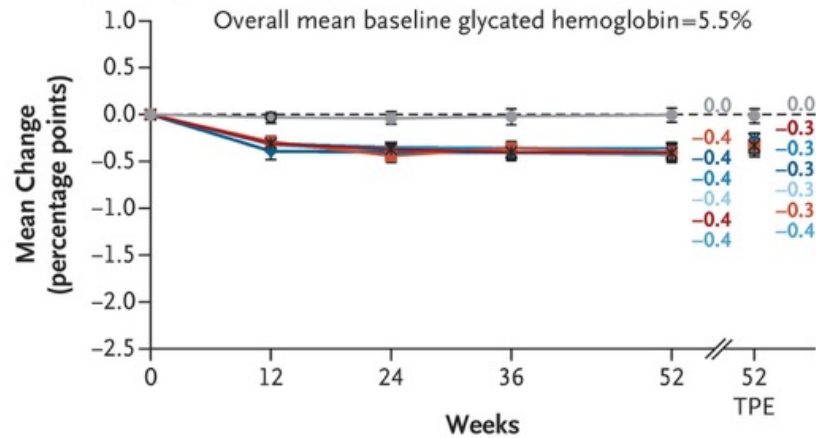
**A Change in Body Weight in the Obesity Cohort**



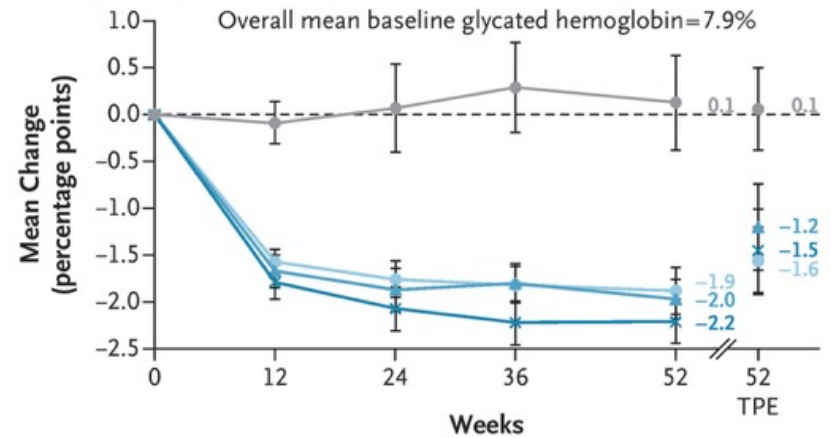
**B Change in Body Weight in the Obesity-Diabetes Cohort**



**C Change in Glycated Hemoglobin Level in the Obesity Cohort**

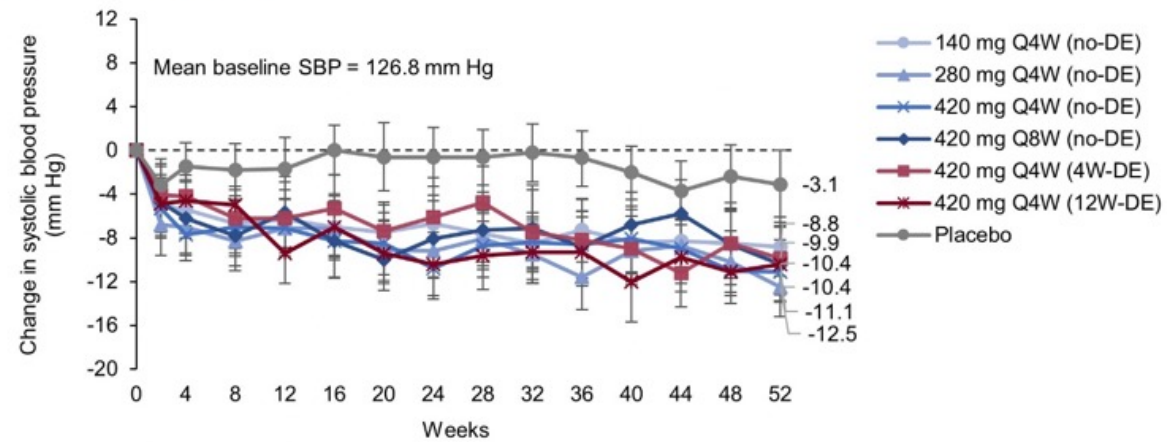


**D Change in Glycated Hemoglobin Level in the Obesity-Diabetes Cohort**

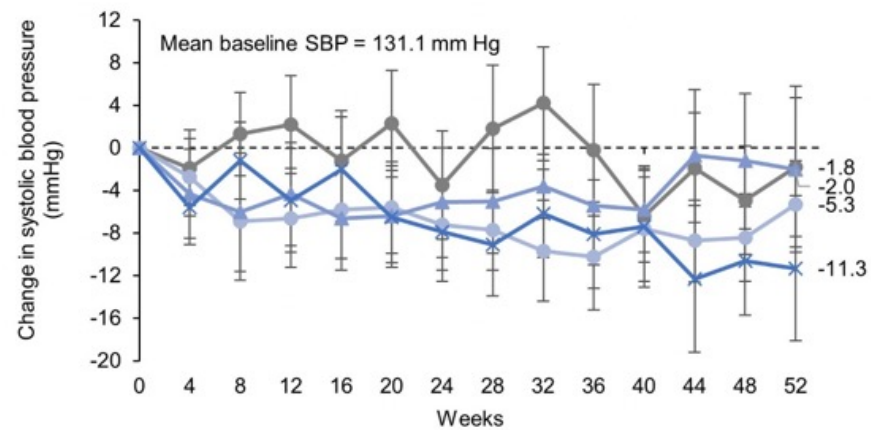


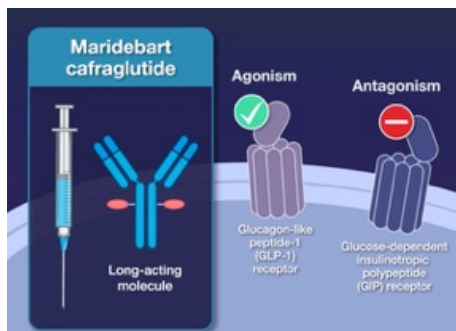
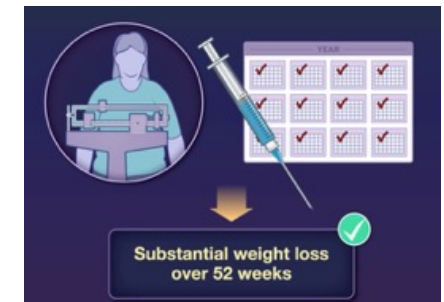
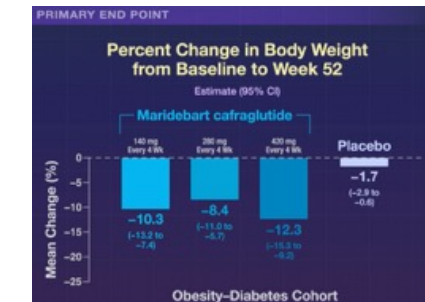
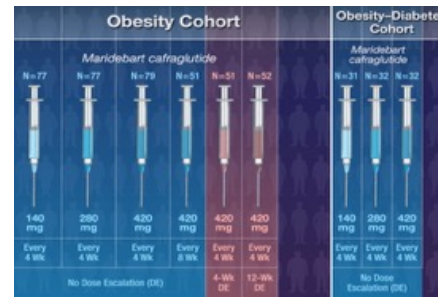


### A. Systolic blood pressure - obesity cohort



### B. Systolic blood pressure - obesity-diabetes cohort





Zimislecel (VX-880) is an investigational, allogeneic, stem cell-derived islet cell therapy developed by Vertex Pharmaceuticals for Type 1 Diabetes. In a Phase 1/2 study, a single infusion of zimislecel restored endogenous insulin production, with 10 of 12 participants achieving insulin independence at one year, offering hope for a functional cure for T1D by addressing the underlying cause of the disease.

### How it Works

#### •Stem Cell-Derived Islets:

•Zimislecel is a type of allogeneic cell therapy, meaning it uses cells from a donor (in this case, stem cells) to create fully differentiated, insulin-producing pancreatic islets.

#### Restores Insulin Production:

These infused cells are engrafted into the patient's body and begin to produce and release insulin in response to blood glucose levels.

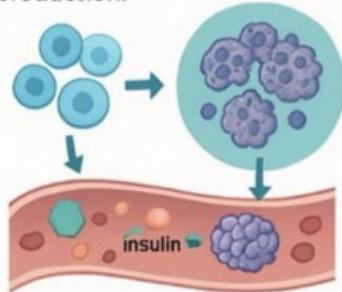
#### Functional Cure Potential:

By restoring the body's ability to produce its own insulin, zimislecel aims to resolve the root cause of Type 1 Diabetes rather than just managing its symptoms.

# Stem Cell–Derived Islets: A Breakthrough in Type 1 Diabetes?

## How It Works

Zimislecel: Allogeneic stem cell-derived fully differentiate islets infused via portal vein to restore endogenous insulin production.



## Key Takeaway

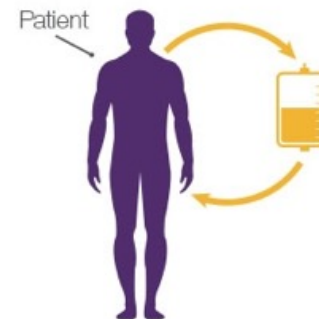
Zimislecel restored physiologic islet function, eliminating severe hypoglycemia & enabling insulin independence in most patients.



@Updates\_in\_Medicine

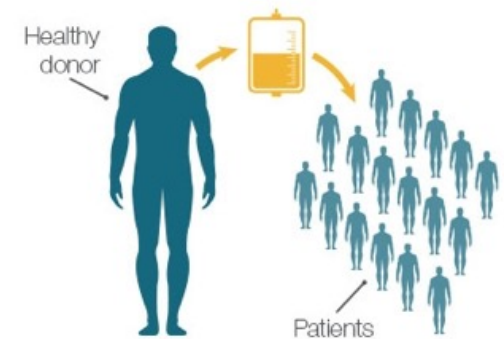
## Autologous

Cell therapy



## Allogeneic

Cell therapy





## **Stem Cell–Derived, Fully Differentiated Islets for Type 1 Diabetes**

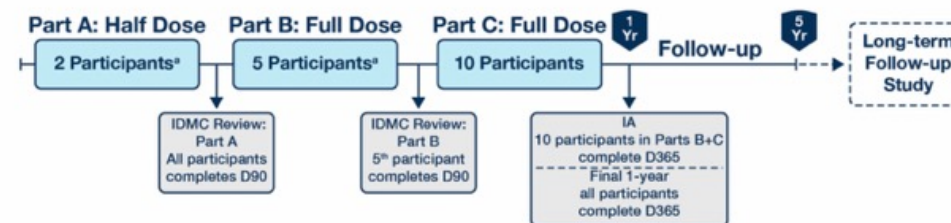
Zimislecel is an allogeneic stem cell–derived islet-cell therapy. Data on the safety and efficacy of zimislecel in persons with type 1 diabetes are needed.

We conducted a phase 1–2 study of zimislecel in persons with type 1 diabetes. In part A, participants received a half dose of zimislecel ( $0.4 \times 10^9$  cells) as a single infusion into the portal vein, with an option for a second half dose within 2 years. In parts B and C, participants received a full dose of zimislecel ( $0.8 \times 10^9$  cells) as a single infusion. All the participants also received glucocorticoid-free immunosuppressive therapy. The primary end point in part A was safety. The primary end point in part C was freedom from severe hypoglycemic events during days 90 through 365, with a glycated hemoglobin level of less than 7% or a decrease of at least 1 percentage point from baseline in the glycated hemoglobin level at one or more time points between days 180 and 365. Secondary end points in part C included safety and insulin independence between days 180 and 365. Assessment of the primary and secondary end points in part C involved the participants who received the full dose of zimislecel as a single infusion in part B or C. Detection of serum C-peptide during a 4-hour mixed-meal tolerance test was used to assess engraftment and islet function. All the analyses were interim and not prespecified.

### **Conclusions**

The results of this small, short-term study involving persons with type 1 diabetes support the hypothesis that zimislecel can restore physiologic islet function, warranting further clinical investigation.

Pluripotent stem cells can be differentiated into therapeutic cells to replace damaged or destroyed cells during disease. Studies have shown that stem cells can be differentiated into insulin-expressing beta cells and glucagon-expressing alpha cells capable of reversing diabetes in preclinical models. Using an approach based on this discovery, we developed zimislecel (VX-880), a treatment composed of allogeneic stem cell–derived, fully differentiated islets. We hypothesized that administering zimislecel by means of procedures used in the transplantation of islets from a deceased donor would lead to regulated secretion of endogenous insulin, improved glycemic control, elimination of severe hypoglycemic events, and insulin independence in humans. We report interim data from a phase 1–2 study evaluating the effects of a single infusion of zimislecel in persons with type 1 diabetes who have recurrent severe hypoglycemic events and impaired awareness of hypoglycemia despite appropriate disease management.



Note: Enrollment and dosing of the phase 1/2 portion of the trial is complete

D: day; IA: interim analysis; IDMC: independent data monitoring committee

<sup>a</sup> Participants in Parts A and B were dosed in a staggered manner. Part A and B enrolled and dosed 2 and 5 participants, respectively. One participant enrolled and received zimislecel as two half-doses, per protocol, and is thus counted in both Parts A and B (once for receiving a half dose in Part A and once for receiving a full dose in Part B).

Part A was designed to assess the safety of zimislecel, part B to assess safety and islet function, and part C to further assess safety and efficacy in additional participants. Persons 18 to 65 years of age who had type 1 diabetes with impaired awareness of hypoglycemia (defined by a reduced ability to perceive the onset of hypoglycemia), at least two severe hypoglycemic events in the previous year, and insulin dependence for at least 5 years were eligible. All the participants had received appropriate diabetes care, defined as standard insulin therapy by means of multiple daily injections or an insulin pump, under the direction of an endocrinologist, diabetologist, or diabetes specialist (an internist, physician assistant, or nurse practitioner experienced in the management of diabetes); all the participants had undergone at least three clinical evaluations documented by a diabetes specialist during the 12 months before screening.

### **End Points**

The primary end point in part A was safety. The primary end point in part C was freedom from severe hypoglycemic events from day 90 through day 365 after zimislecel infusion, with a glycated hemoglobin level of less than 7% or a reduction of at least 1 percentage point from baseline in the glycated hemoglobin level at one or more visits between day 180 and day 365.

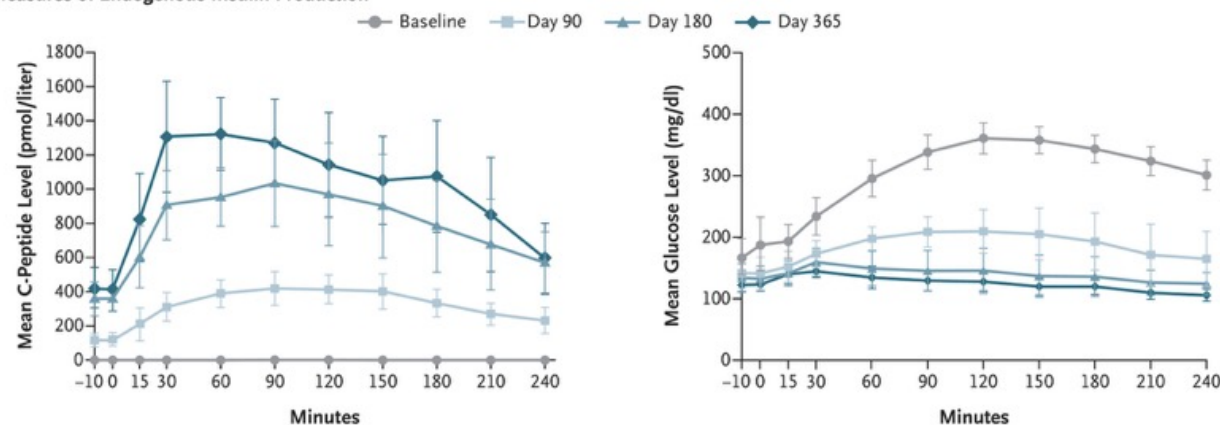
Characteristic	Participants (N = 12)
Mean age at screening (range) — yr	42.7 (24–60)
Female sex — no. (%)	4 (33)
White race — no. (%)†	12 (100)
Mean weight (range) — kg	74.1 (56.0–97.5)
Mean body-mass index (range)‡	25.0 (21.7–28.5)
Mean duration of type 1 diabetes (range) — yr	22.3 (7.8–47.4)
Mean glycated hemoglobin level (range) — %	7.8 (7.1–9.9)
Percentage of time in target glucose range (range)§	49.5 (19.0–66.2)
Mean fasting C-peptide level (range) — pmol/liter¶	Undetectable
Mean total daily insulin dose (range) — U	40.9 (19.8–52.0)
Mean daily insulin need (range) — U/kg	0.55 (0.35–0.64)
Mean no. of severe hypoglycemia events per year (range)	2.7 (2–4)
Use of insulin pump at prescreening or screening visit — no. (%)	8 (67)
Use of hybrid closed-loop system at prescreening or screening visit — no. (%)	6 (50)

## Adverse Events.

Event	Participants (N = 14)
	<i>no. (%)</i>
Diarrhea	11 (79)
Headache	10 (71)
Nausea	9 (64)
Covid-19	7 (50)
Mouth ulceration	7 (50)
Neutropenia	6 (43)
Rash	6 (43)



### A Measures of Endogenous Insulin Production



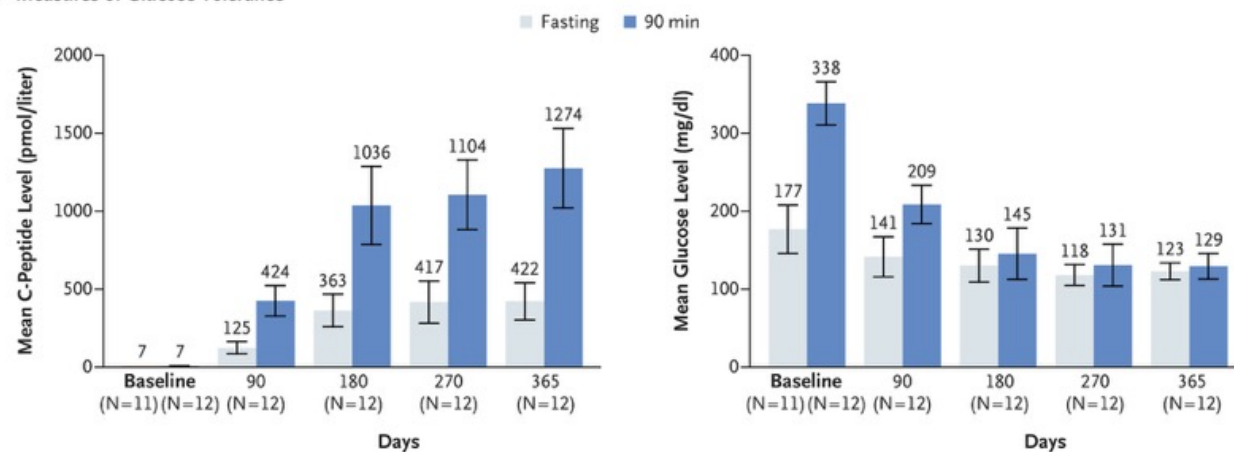
No. of  
Participants

Day 365	12	12	11	12	12	12	12	12	12	12
Day 180	12	11	10	11	11	12	11	11	11	11
Day 90	12	12	12	12	12	12	12	12	12	11
Baseline	11	11	12	12	12	12	11	12	12	12

No. of  
Participants

Day 365	12	12	12	12	12	12	12	12	12	12
Day 180	11	11	11	11	11	12	11	11	10	11
Day 90	12	12	12	12	12	12	12	12	11	12
Baseline	11	11	12	11	12	12	12	12	12	12

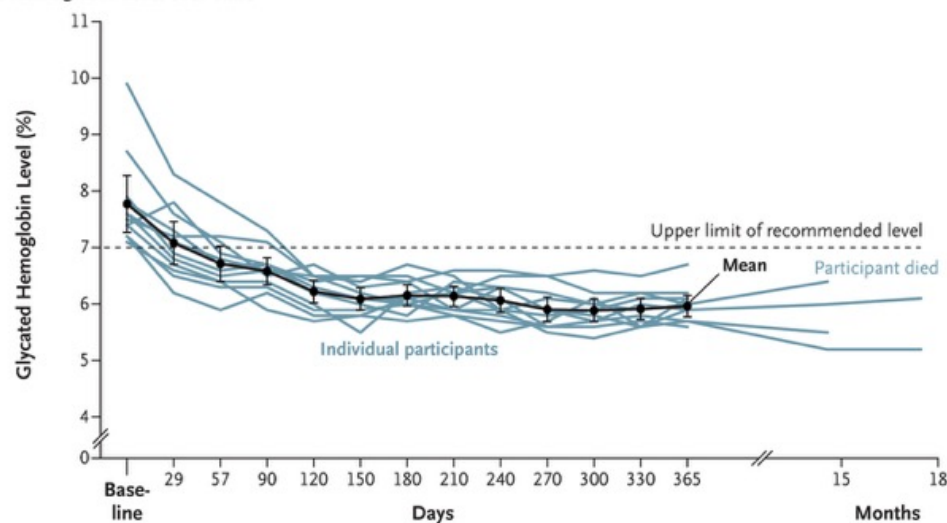
### B Measures of Glucose Tolerance



### Endogenous Insulin Production and Glucose Tolerance.

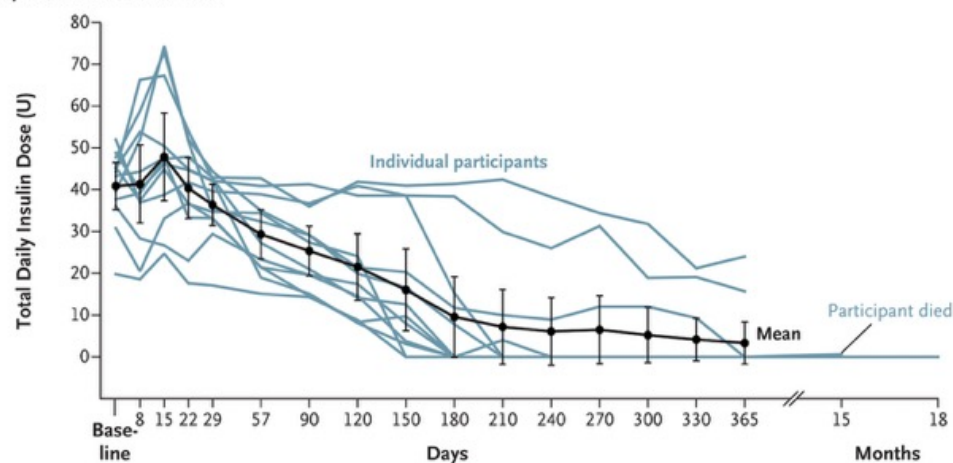
Panel A shows the mean C-peptide levels (lower limit of detection, 13 pmol per liter) (left) and mean glucose levels (right) over time during a 4-hour mixed-meal tolerance test at baseline and at day 90 and day 180 after zimislecel infusion. Panel B shows the mean fasting C-peptide level and mean mixed-meal-stimulated C-peptide level at 90 minutes (left) and the mean fasting glucose level and mean mixed-meal-stimulated glucose level at 90 minutes (right) at baseline and at day 90, day 180, day 270, and day 365 after zimislecel infusion. Data are shown for the 12 participants who received the full dose of zimislecel ( $0.8 \times 10^9$  cells) as a single infusion and completed at least 12 months of follow-up. Fasting C-peptide and glucose levels were calculated as the mean of the level at 10 minutes before the mixed-meal tolerance test and the level at the start of the test. I bars indicate 95% confidence intervals.

**A Glycated Hemoglobin Level over Time**



No. of Participants	12	12	12	12	12	12	12	12	12	12	12	12	12	12	4	2

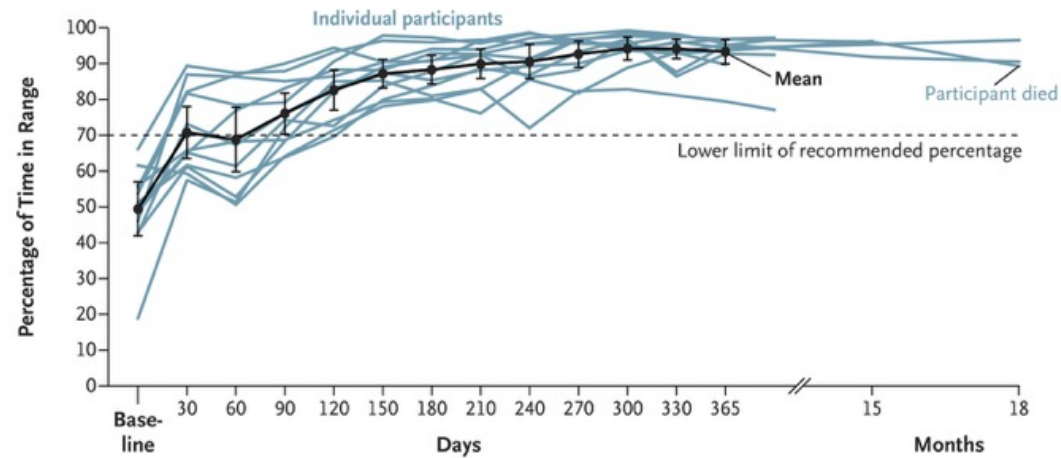
**B Total Daily Insulin Dose over Time**



### Glycated Hemoglobin Level and Total Daily Insulin Dose.

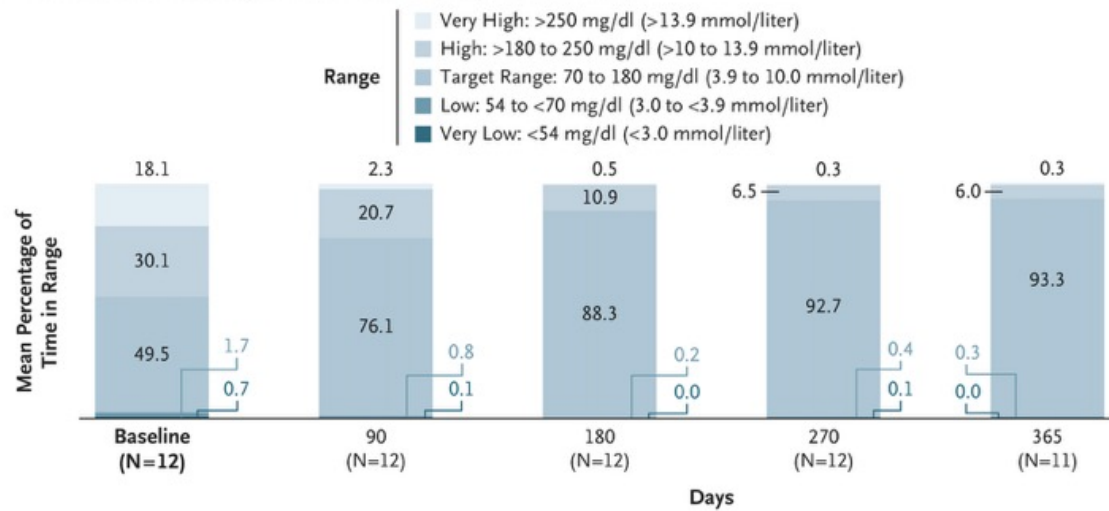
Panel A shows the glycated hemoglobin level over time. Blue lines indicate the glycated hemoglobin level in individual participants, the solid black line indicates the mean glycated hemoglobin during visits with data obtained from at least 5 participants, and the dashed line indicates the upper limit of the glycated hemoglobin level recommended by the American Diabetes Association (ADA) and European Association for the Study of Diabetes (EASD). Panel B shows total daily insulin dose over time. Blue lines indicate the total daily insulin dose in individual participants, and the solid black line indicates the mean total daily insulin dose during visits with data obtained from at least 5 participants. Data are shown for the 12 participants who received the full dose of zimislecel as a single infusion and completed at least 12 months of follow-up. I bars indicate 95% confidence intervals.

### A Percentage of Time in Target Glucose Range



No. of Participants	12	12	12	12	12	12	12	12	12	12	11	11	11	4	3

### B Distribution of Percentage of Time Relative to Target Glucose Range



### Time Spent in the Target Glucose Range.

Panel A shows the percentage of time in which the glucose level was in the target range of 70 to 180 mg per deciliter (3.9 to 10 mmol per liter) recommended by the ADA and EASD during the follow-up period. Blue lines indicate the percentage of time that individual participants spent in the target glucose range, the solid black line indicates the mean time in the target range during visits with data obtained from at least 5 participants, and the dashed line indicates the lower limit of the percentage of time in the target range recommended by the ADA and EASD for persons with type 1 diabetes. Panel B shows the mean distribution of the percentage of time spent below, within, and above the target glucose range. Percentages may not sum to 100 because of rounding. Data are shown for the 12 participants who received the full dose of zimislecel as a single infusion and completed at least 12 months of follow-up. I bars indicate 95% confidence intervals.

## **Discussion**

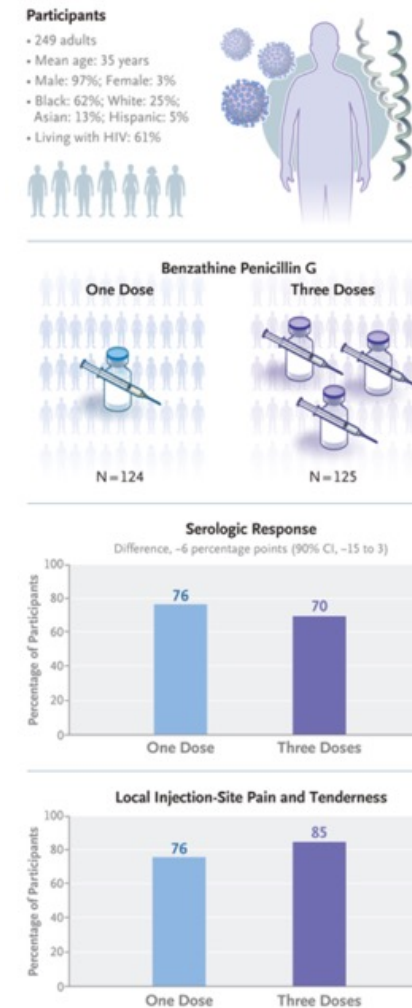
We report on the use of zimislecel, a fully differentiated, allogeneic pluripotent stem cell–derived islet-cell therapy for type 1 diabetes. Directed differentiation of pluripotent stem cells into specialized cell types can potentially provide an inexhaustible supply of replacement tissues for serious diseases. Our study showed that stem cell–derived islets engrafted, produced endogenous insulin, and restored the physiologic function of islets, leading to improved glycemic control, elimination of severe hypoglycemic events, and insulin independence in persons with type 1 diabetes.

The results of this unplanned interim analysis of our single-group, phase 1–2 study support further investigation of zimislecel in larger, longer studies involving diverse populations. These results also support our hypothesis that zimislecel can restore physiologic islet function, improve glycemic control, and eliminate the shortcomings of insulin-replacement therapy, including treatment-related adverse events and the burden of managing the insulin dose. More generally, these findings provide evidence that pancreatic islets can be effectively produced from pluripotent stem cells and used to treat type 1 diabetes.

# One Dose versus Three Doses of Benzathine Penicillin G in Early Syphilis


Controversy persists regarding the appropriate duration of therapy with benzathine penicillin G in persons with early (i.e., primary, secondary, or early latent) syphilis (*Treponema pallidum* infection).

In a multicenter, randomized, controlled, noninferiority trial, we assigned persons who had early syphilis, with or without human immunodeficiency virus (HIV) infection, to receive intramuscular injections of benzathine penicillin G in a one-time dose of 2.4 million units or in doses of 2.4 million units administered at three successive weekly intervals. The primary end point was seroreversion to nonreactive status or a decrease in the rapid plasma reagin titer by two or more dilutions at 6 months, referred to here as a serologic response (noninferiority margin, 10 percentage points). A key secondary end point was a serologic response within subgroups defined according to HIV status, also assessed in a noninferiority analysis.

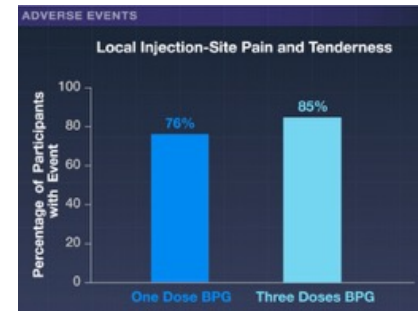




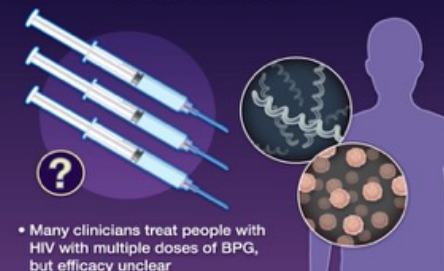
### Patients with Early Syphilis



- Single dose of benzathine penicillin G (BPG) is standard therapy
- Concerns about treatment for people with HIV are longstanding




### Patients with Early Syphilis



- Many clinicians treat people with HIV with multiple doses of BPG, but efficacy unclear



### Patients with Early Syphilis



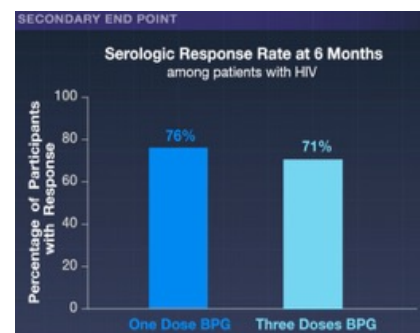
Treatment with more than a single dose of 2.4 million units of BPG **offers no benefit** at 6 months post-treatment, regardless of HIV infection status, and was associated with more pain.

### Trial

- Randomized
- Controlled
- Multicenter
- Noninferiority

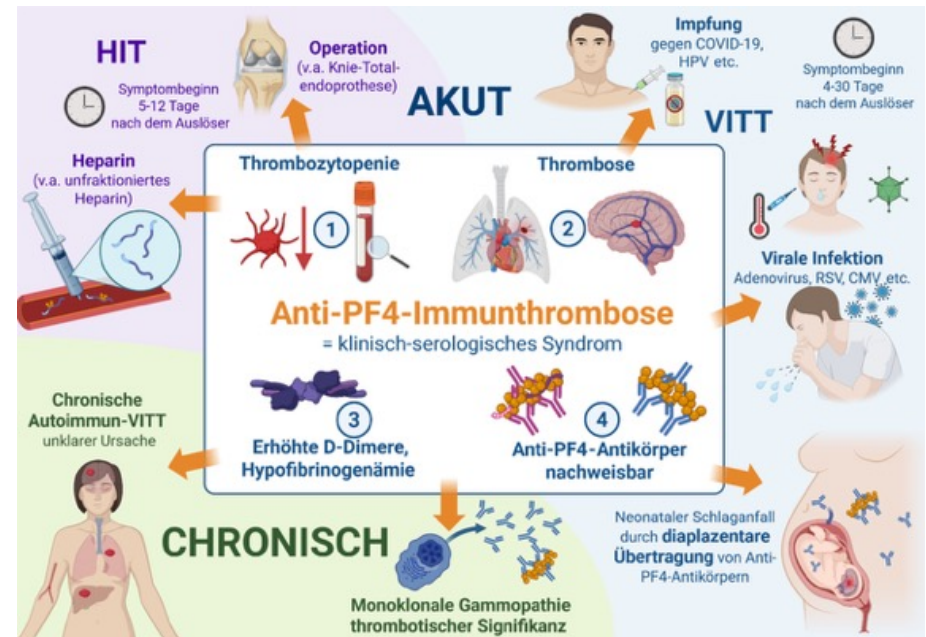
**249 Adults**

- With uncomplicated, early syphilis
- With or without HIV



Plättchenfaktor 4, kurz PF4, ist ein von Thrombozyten gebildetes Chemokin, das bei der Thrombozytenaggregation freigesetzt wird. Plättchenfaktor 4 ist ein Protein, das aus 70 Aminosäuren gebildet wird. Es hat eine hohe Affinität zu Heparin und spielt eine wichtige Rolle bei der Blutgerinnung. Es neutralisiert Heparin-ähnliche Moleküle an der Endotheloberfläche der Blutgefäße und hemmt dadurch die Aktivität des Antithrombins. Da PF4 neutrophile Granulozyten und Fibroblasten anzieht, fördert es die Entzündungsreaktion und die Wundheilung. Plättchenfaktor 4 bildet zusammen mit Heparin auf der Thrombozytenmembran ein Neoantigen, das die Zielstruktur der Antikörper darstellt, die bei Heparin-induzierter Thrombozytopenie Typ II (HIT II) gebildet werden.

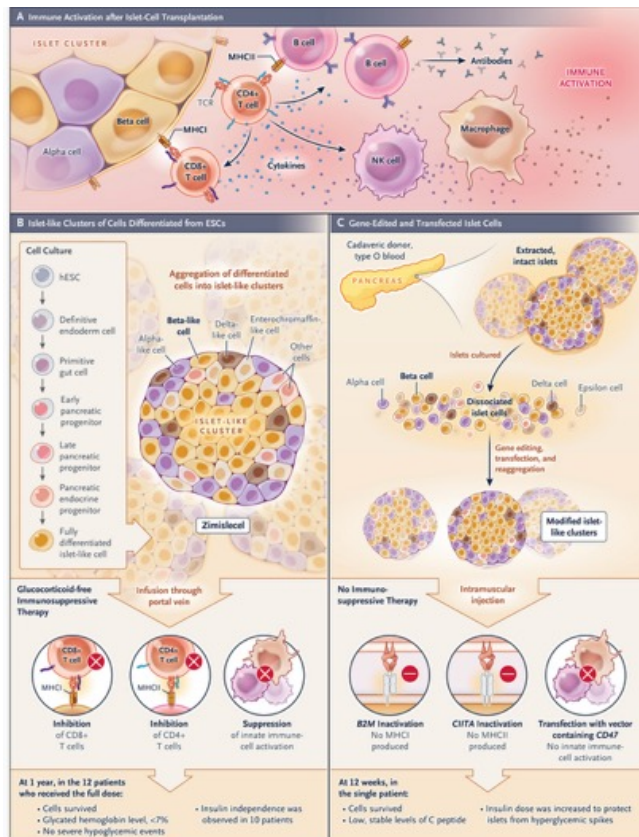
Das KKO-Epitop ist eine spezifische Bindungsstelle auf dem humanen Plättchenfaktor 4 (hPF4), das sich in der Nähe von Pro34 und dem N-Terminus des Proteins befindet und ein gemeinsames Antigen für HIT/HITT-Antikörper darstellt, die bei der Heparin-induzierten Thrombozytopenie (HIT) auftreten. Es ist ein wichtiger Bestandteil des KKO-Maus-Monoklonals, das das HIT-Syndrom nachahmt, und hilft, die Struktur des PF4-Proteins zu definieren, das für die Selbstimmunität bei HIT relevant ist.



"KKO-Maus Monoklonale" bezieht sich wahrscheinlich auf monoklonale Antikörper, die aus einer Maus stammen. Der Begriff "KKO-Maus" ist unklar, aber ein häufiger Herstellungsprozess für monoklonale Antikörper beinhaltet die Immunisierung von Mäusen, gefolgt von der Isolierung von Antikörper-produzierenden Zellen (Splenozyten) und deren Fusion mit Myelomzellen, um sogenannte Hybridome zu erzeugen. Diese Hybridome produzieren dann spezifische monoklonale Antikörper, die aus der Maus stammen.

## Making Beta Cells from Stem Cells

Reichman et al. report results from patients with type 1 diabetes who received zimislecel, clusters of islet cells differentiated from a line of human embryonic stem cells. They administered the clusters of differentiated islet cells by infusion into the portal vein, coupled with glucocorticoid-free immunosuppression.



## Overcoming Barriers to Replacement of Beta Cells.

Immune recognition of transplanted cells involves the coordinated activity of adaptive and innate immune cells (Panel A). CD8+ T cells can recognize class I major histocompatibility complex (MHC) molecules and kill the graft, but there is also presentation of antigens that are derived from the graft and of class II MHC molecules to CD4+ T cells, with release of cytokines, activation of B cells that can produce antibodies against MHC molecules on the graft, and innate immune cells. Reichman et al.<sup>3</sup> describe the derivation of differentiated isletlike clusters from a line of human embryonic stem cells (hESC) line, involving culture with specific agents and associations with specific gene-expression signatures as they pass through six stages (Panel B).<sup>6</sup> They then infused the clustered islet cells into the portal vein of patients with type 1 diabetes. To prevent rejection of the transplanted clusters through the recognition of the cells by the recipients' immune systems, the study participants were given

immunosuppressive therapy before receiving the cells and as a maintenance therapy after infusion. Carlsson et al.<sup>4</sup> harvested islets of Langerhans from the pancreas from an organ donor, dissociated the cells, and then altered them to render them resistant to rejection by the recipient's immune system (Panel C). More specifically, they shut down the expression of class I and II MHC genes through the inactivation of the genes *B2M* and *CIITA* and then transfected the edited cells with a gene encoding *CD47*, which inhibits innate immune cells. These "hypimmune islets" produced insulin for 12 weeks in the absence of immunosuppression in one patient after implantation in the forearm muscle. ESC denotes embryonic stem cell, NK natural killer, and TCR T-cell receptor.

# Monoclonal Antibodies in the Pathogenesis of Heparin-Induced Thrombocytopenia

Heparin-induced thrombocytopenia (HIT) is an immune-mediated platelet disorder caused by antibodies that target complexes of platelet factor 4 (PF4) and heparin. HIT has been characterized as a polyclonal immune response; however, studies of other rare anti-PF4 disorders have identified clonally restricted antibodies.

## Methods

In this study, we investigated the clonality of pathogenic HIT antibodies. Antibodies against PF4–heparin were affinity-purified with the use of PF4–heparin beads from serum samples obtained from nine patients with clinically and serologically confirmed HIT. Antibody clonality was assessed by means of immunofixation electrophoresis and mass spectrometry. Antibody binding to PF4 was evaluated by an enzyme immunoassay, and functional platelet activation was evaluated with the use of a P-selectin expression assay. HIT antibody epitopes were mapped in two patients with the use of a PF4 mutant library.

## Conclusions

The pathogenic antibodies in all nine patients with HIT were found to be monoclonal. This finding provides insight into the pathogenesis of HIT and has implications for improved diagnostics and targeted therapeutics. (Funded by the Canadian Institutes of Health Research and the National Institutes of Health.)

Heparin-induced thrombocytopenia (HIT), an immune-mediated reaction to heparin treatment, is characterized by a reduced platelet count and an increased risk of thrombosis. HIT is caused by IgG antibodies that recognize complexes of platelet factor 4 (PF4; also known as CXCL4) and heparin. These immune complexes activate platelets through Fc receptors (FcγRIIa), which leads to the release of procoagulant platelet microparticles and the generation of thrombin. The HIT immune response has several unusual features, including rapid development of anti-PF4–heparin IgG antibodies without a preceding IgM response and transient antibodies that last up to 100 days without evidence of immunologic memory on heparin readministration.

Like most immune responses, HIT antibodies have long been considered polyclonal. This position is supported by observations that patients produce a mixture of pathogenic and nonpathogenic anti-PF4–heparin antibodies.

However, the antibodies in other rare anti-PF4 disorders, including vaccine-induced immune thrombocytopenia and thrombosis (VITT) after adenoviral vector–based vaccination against severe acute respiratory syndrome coronavirus 2 or adenoviral infection, have been shown to be monoclonal or oligoclonal. Similar findings have been reported for VITT-like monoclonal gammopathy of thrombotic significance, in which the monoclonal IgG protein (M protein) had platelet-activating anti-PF4 activity. In light of these observations, we investigated whether HIT, the most common anti-PF4 disorder, may also be caused by clonally restricted anti-PF4–heparin antibodies.

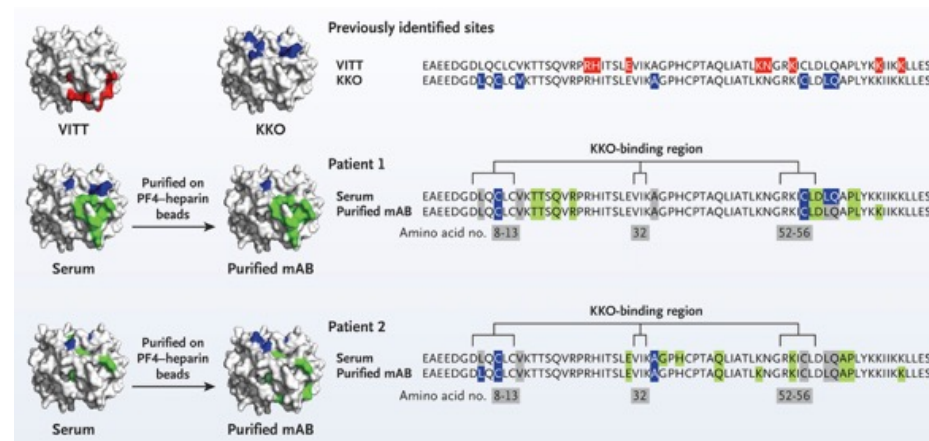


## **Patients**

Nine patients with HIT were included in this study, among whom two (22%) were women and seven (78%) were men. The mean age was 63 years (range, 45 to 77 years). All the serum samples from these patients tested positive in the anti-PF4-heparin enzyme immunoassay, with a mean OD<sub>405</sub> of 1.9 (range, 1.1 to 2.4); all the samples also tested positive in the serotonin-release assay, with a mean serotonin release of 87.7% (range, 60.0 to 99.0) at a heparin concentration of 0.1 U per milliliter and 90.7% (range, 74.0 to 99.0) at a heparin concentration of 0.3 U per milliliter. Platelet activation in the absence of heparin (with buffer alone) was observed in five of nine samples (56%), with a mean serotonin release of 71.4% (range, 45.0 to 100.0). This finding indicated a near-equal distribution of heparin-dependent platelet activation (in four samples) and heparin-independent platelet activation (in five samples) in vitro.

Among the five patients (56%) with HIT for whom clinical data were available, the median 4Ts score was 5 (interquartile range, 4 to 6), which indicates intermediate or high probability of HIT. HIT-associated thrombosis, including pulmonary embolism, deep-vein thrombosis, and right atrial thrombus, developed in three of these five patients (60%). None of the patients with HIT had a known history of monoclonal gammopathy. None of the control samples from patients who were hospitalized and had received recent heparin administration (four samples) or from healthy volunteers (seven samples) had detectable anti-PF4-heparin antibodies.

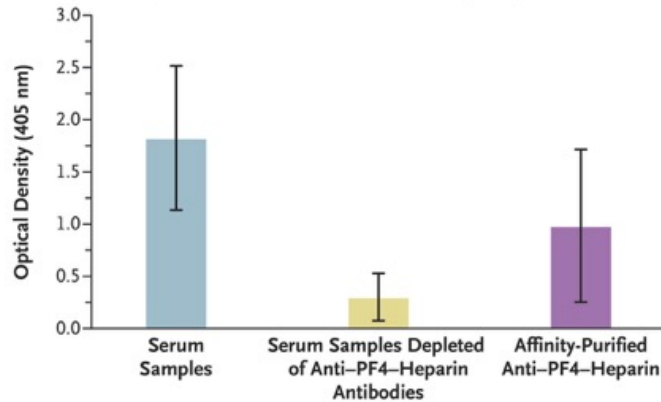
Characteristic	Patients with HIT (N=9)
Mean age (range) — yr	63 (45–77)
Female sex — no. (%)	2 (22)
Platelet count nadir (range) — mm <sup>3</sup>	76,200 (33,000–172,000)
D-Dimer level (range) — mg/liter	12,752 (6196–21,921)
Fibrinogen level (range) — g/liter	4.7 (2.3–6.8)
Median 4Ts score (IQR) <sup>†</sup>	5 (4–6)
Thrombosis — no. of patients/total no. (%)	3/5 (60)
Days from receipt of heparin to sample collection (range)	17 (10–29)
Mean OD of serum samples (range) <sup>‡</sup>	1.9 (1.1–2.4)
Mean serotonin release (range) — % <sup>§</sup>	
Heparin, 0.0 U/ml	40.6 (0–100)
Heparin, 0.1 U/ml	87.7 (60.0–99.0)
Heparin, 0.3 U/ml	90.7 (74.0–99.0)
Heparin, 100.0 U/ml	0 (0–3.0)
Serum M protein detected — no. of patients <sup>¶</sup>	6
Heavy-chain isotype — no. of patients <sup>  </sup>	
IgG	6
IgM	1
IgA	0
Ratio of kappa to lambda light chains <sup>**</sup>	3:4



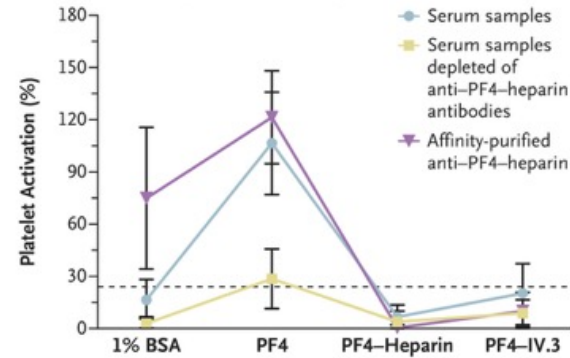
### Mapping of Epitopes on PF4.

Epitopes recognized by purified monoclonal anti-PF4-heparin antibodies from two patients with HIT who were positive for M protein were mapped on PF4, and the maps were compared with those for the original serum samples. Maps for affinity-purified fractions showed overlap with serum epitope maps at 10 of 11 PF4-binding residues (91%) and 7 of 10 PF4-binding residues (70%). Binding sites for vaccine-induced immune thrombocytopenia and thrombosis (VITT) antibodies (red) and KKO monoclonal antibodies (blue) are shown for comparison. Gray shading indicates amino acids that were present in the KKO epitope but not the epitope recognized by the serum sample or purified antibody fraction; green shading indicates amino acids present in the epitope recognized by the serum sample or purified antibody fraction but not in the KKO epitope. Amino acids shaded in blue were present in both the KKO epitope and the epitope recognized by the serum sample or purified antibody fraction. The abbreviation mAB denotes monoclonal antibodies.

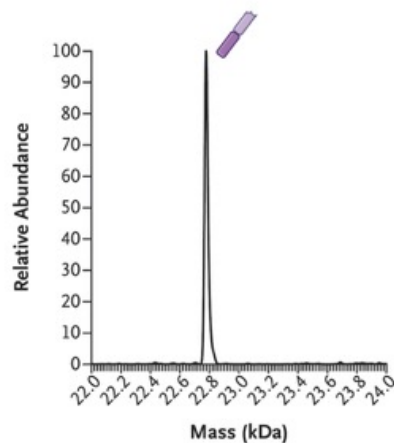
**A Anti-PF4-Heparin Antibodies in Patients with HIT (N=9)**



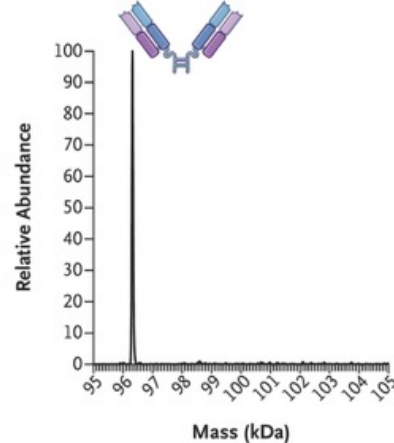
**B Functional Activity of Anti-PF4-Heparin Antibodies**



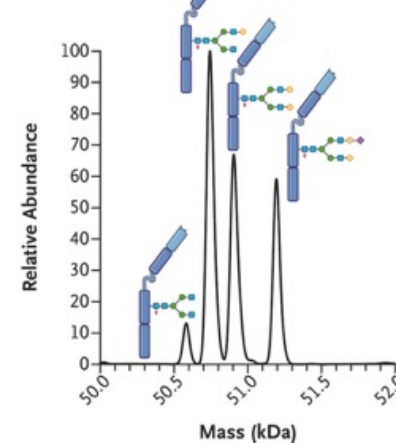
**C Mass Distribution of the Light Chains**



**D Mass Distribution of the F(ab')<sub>2</sub> Fragment**



**E Mass Distribution of the Heavy Chains**



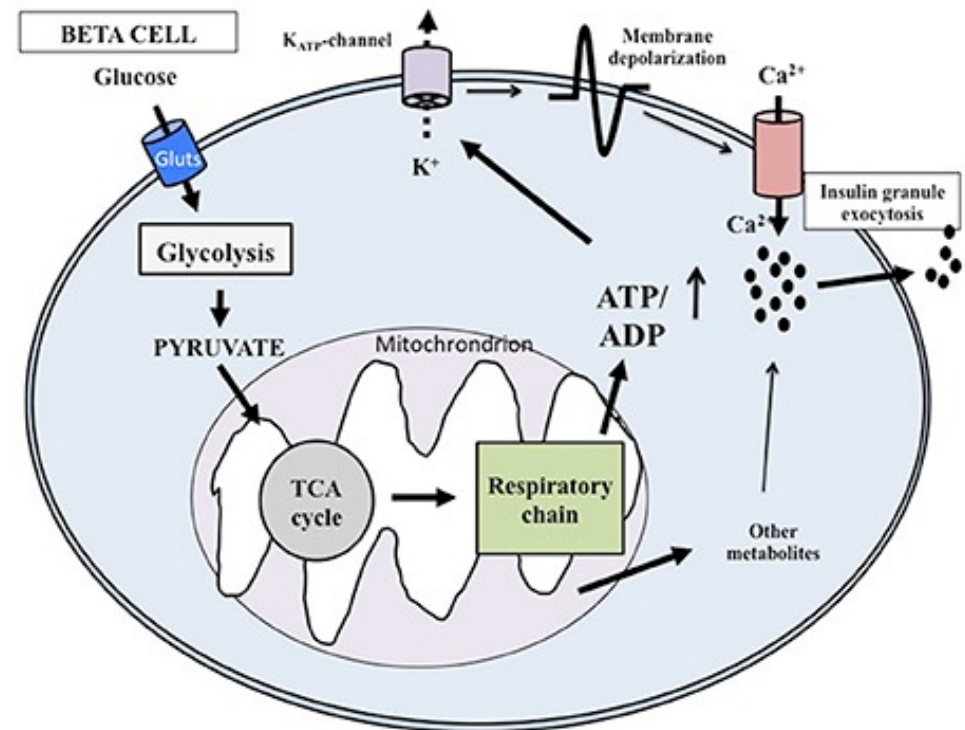
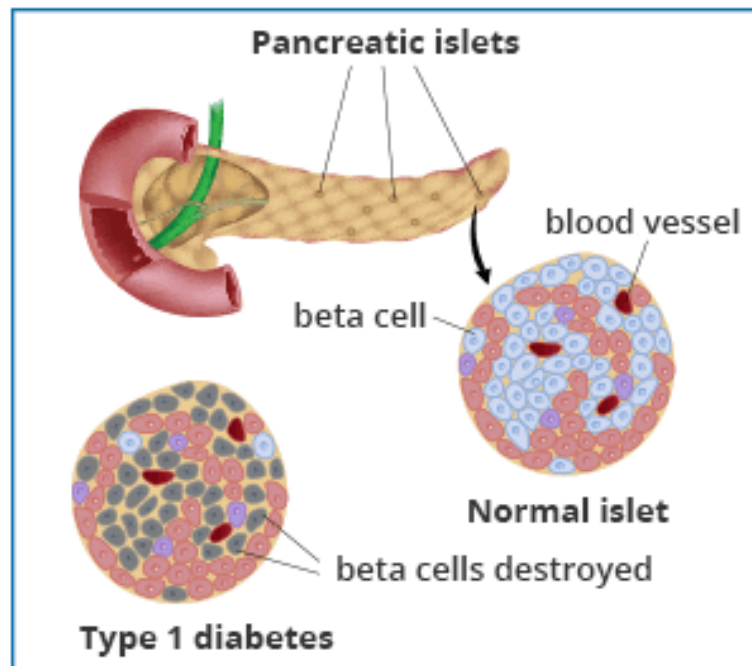
#### Detection and Function of Anti-PF4-Heparin Antibodies from Patients with HIT.

An anti-platelet factor 4 (PF4)-heparin IgG-IgA-IgM enzyme immunoassay was used to determine the levels of anti-PF4-heparin antibodies in serum samples from nine patients with heparin-induced thrombocytopenia (HIT) (Panel A). Results for affinity-purified fractions were compared with those for the original serum samples and antibody-depleted serum samples. The functional activity of anti-PF4-heparin antibodies was assessed with the use of the P-selectin expression assay (Panel B). Platelet activation under various conditions — in the presence of buffer alone (1% bovine serum albumin [BSA]), PF4, PF4 plus heparin at a concentration of 125 U per milliliter, or PF4 plus IV.3 (an FcγRIIa-blocking antibody) — was measured as a percentage of platelet activation by thrombin receptor activator peptide 6 (TRAP-6). I bars represent standard deviation. The dashed line indicates the level above which samples were considered to be positive for platelet activation. Pathogenic anti-PF4-heparin antibodies in serum samples from the patients with HIT were assessed for clonality. The affinity-purified fraction from a representative sample that screened positive for an M protein was analyzed by mass spectrometry. The mass distribution of the light chains showed a single sharp peak at 22.8 kDa, which corresponded to a single polypeptide of the lambda isotype (Panel C). The mass distribution of the F(ab')<sub>2</sub> fragment showed a single peak, which confirmed antibody monoclonality (Panel D). The mass distribution of the heavy chains showed multiple peaks that represented N-glycosylated polypeptides with varying glycan chain maturity, a finding characteristic of IgG monoclonal antibodies (Panel E).

## Discussion

Our study indicates that the pathogenic antibodies in HIT are monoclonal. In six patients, serum M proteins were detected by immunofixation electrophoresis, and affinity-purified anti-PF4-heparin IgG antibodies from serum samples from all nine patients with HIT were shown to activate platelets in the P-selectin expression assay and were confirmed to be monoclonal by mass spectrometry. Depleted serum did not retain pathogenic anti-PF4-heparin antibodies. Epitope mapping showed that serum samples and purified anti-PF4-heparin antibody fractions from the same samples bound to the same amino acids on PF4, which indicates that they represent the same antibodies. These findings showed that the isolated, platelet-activating anti-PF4-heparin antibodies from all the patients with HIT in this study were monoclonal.

Current test methods for HIT rely on anti-PF4-heparin enzyme immunoassays, which are sensitive but lack specificity because they cannot differentiate between pathogenic and nonpathogenic antibodies<sup>9</sup> and often yield false positive results. Functional platelet-activation assays are accurate but technically demanding and not widely accessible. Our findings provide new insights into the pathogenesis of HIT with implications for improved diagnostic tests and therapeutics targeting the pathogenic monoclonal antibody.



## **Survival of Transplanted Allogeneic Beta Cells with No Immunosuppression**

### **Summary**

The need to suppress a patient's immune system after the transplantation of allogeneic cells is associated with wide-ranging side effects. We report the outcomes of transplantation of genetically modified allogeneic donor islet cells into a man with long-standing type 1 diabetes. We used clustered regularly interspaced short palindromic repeats (CRISPR)–CRISPR-associated protein 12b (Cas12b) editing and lentiviral transduction to genetically edit the cells to avoid rejection; the cells were then transplanted into the participant's forearm muscle. He did not receive any immunosuppressive drugs and, at 12 weeks after transplantation, showed no immune response against the gene-edited cells. C-peptide measurements showed stable and glucose-responsive insulin secretion. A total of four adverse events occurred, none of which were serious or related to the study drug.



## Case Report

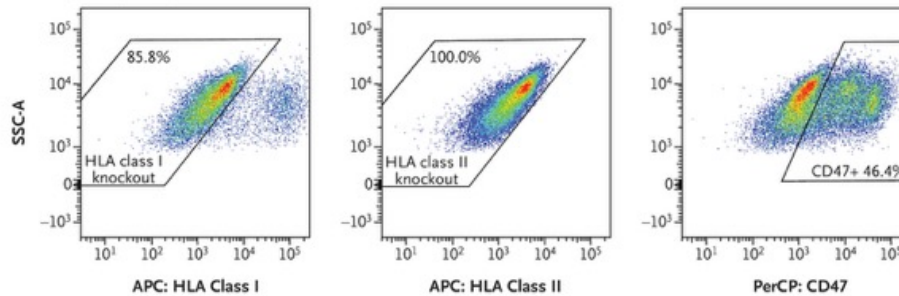
A 42-year-old man with a 37-year history of type 1 diabetes provided written informed consent to participate in the study. He fulfilled eligibility criteria. No additional patients were enrolled in this study. The participant had a glycated hemoglobin level of 10.9% (96 mmol per mole), undetectable endogenous insulin production (i.e., no measurable C-peptide), and detectable glutamic acid decarboxylase and islet antigen 2 autoantibodies (indicators of an autoimmune cause of his disease) and was receiving a daily insulin dose of 32 units.

A blood type O–matched pancreas from a 60-year-old donor with a glycated hemoglobin level of 6.0% (42 mmol per mole) became available, and islets were isolated after 5 hours 11 minutes of cold ischemia at Uppsala University Hospital. These islets had a glucose-stimulated insulin secretion index of 16.7 and a purity of 87%. The islets were shipped to Oslo University Hospital for **gene editing**. At the manufacturing facility of the hospital, the islets were dissociated into single cells, and the **genes *B2M* (encoding a component of class I HLA) and *CIITA* (encoding a master regulator of class II HLA transcription) were inactivated** with the use of the nuclease Cas12b (clustered regularly interspaced short palindromic repeats [CRISPR]–CRISPR-associated protein 12b) and guide RNAs. **The cells were then allowed to recluster and rest before they were again dissociated and transduced with a lentiviral vector containing *CD47* complementary DNA.**

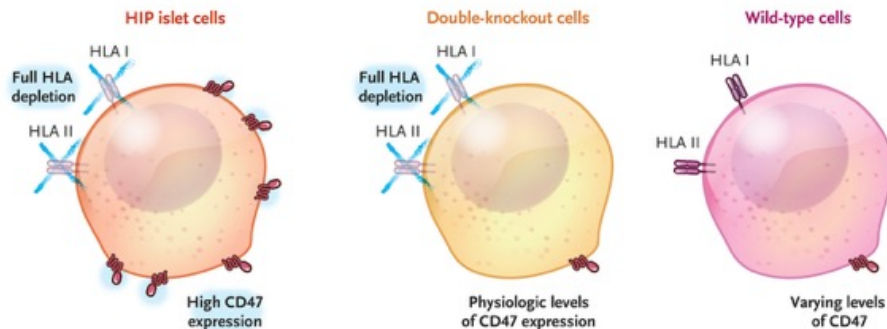
Of the edited islet cells, 85.8% were negative for HLA class I, 100% were negative for HLA class II, and 46.4% had high CD47 expression ([Figure 1A](#)). The final cellular product (UP421) thus contained fully edited HLA-depleted HIP islet cells with high CD47 expression, some HLA class I and II double-knockout cells with endogenous CD47 levels, and islet cells with retained HLA expression (wild type) and varying CD47 levels ([Figure 1B](#)). Gene editing did not change the composition of the islets. Approximately 66% of the islet cells in the study were beta cells ([Figure 1C](#)).

The engineered islet cells were then shipped to Uppsala University Hospital for implantation. With the participant under general anesthesia, a small (3.8 cm) skin incision was made over the participant's left brachioradialis muscle ([Figure 1D](#)). A total of 79.6 million engineered HIP islet cells were prepared into 17 syringes and delivered through 17 injections into the muscle. In each injection, the islets were distributed in a linear pearl-on-string pattern while the syringe was slowly pulled back. The participant remained hospitalized overnight to monitor for immediate complications and was discharged the following day. The participant did not receive any glucocorticoids or antiinflammatory or immunosuppressive medications.

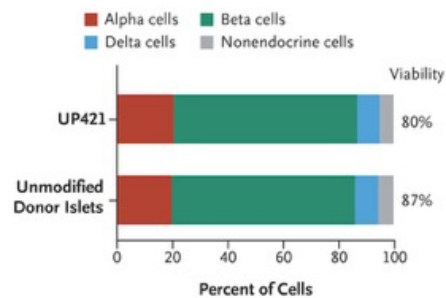
### A Flow Cytometry Analyses



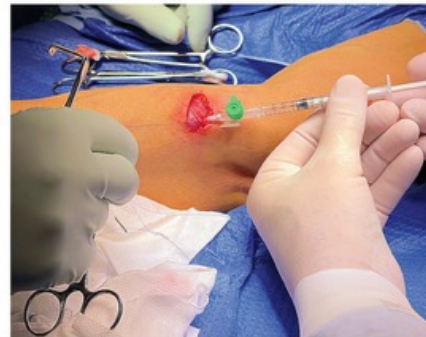
### B Islet-Cell Phenotypes Generated in UP421



### C Cell-Type Compositions

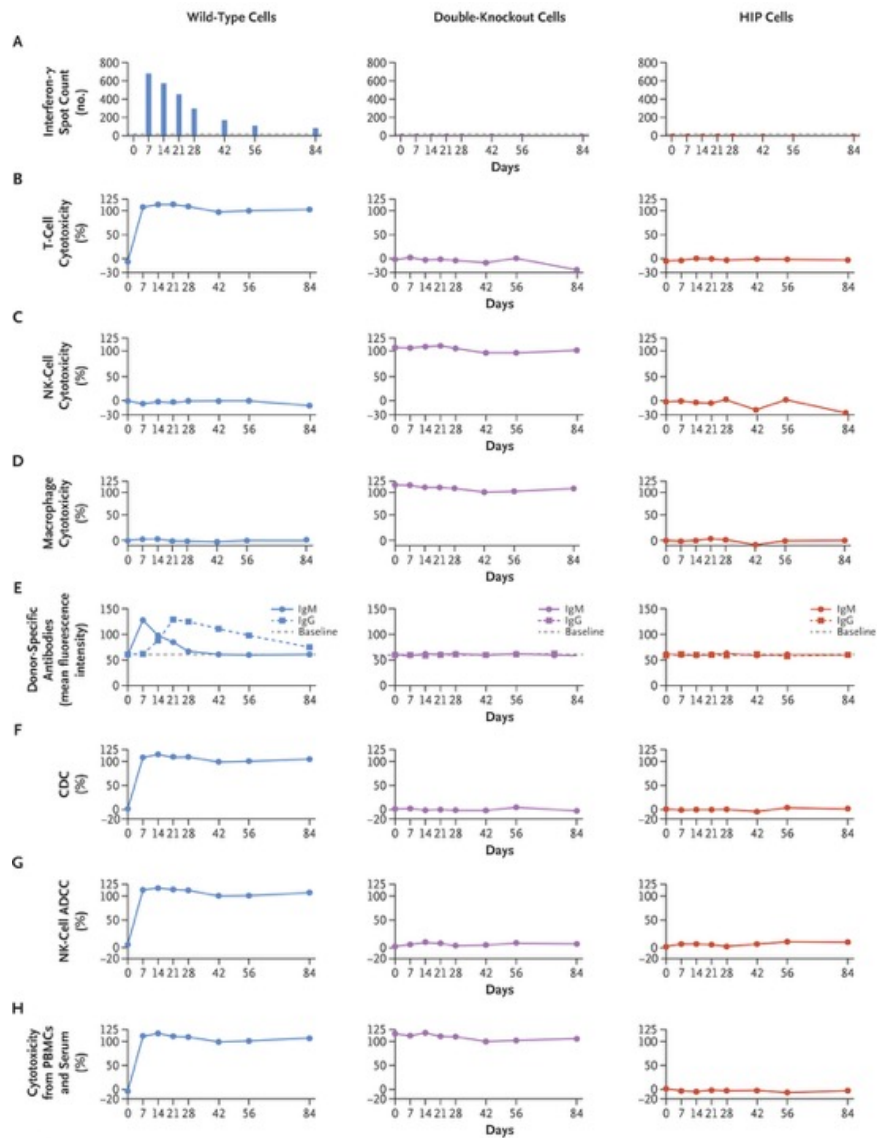


### D UP421 Injection into the Left Brachioradialis Muscle



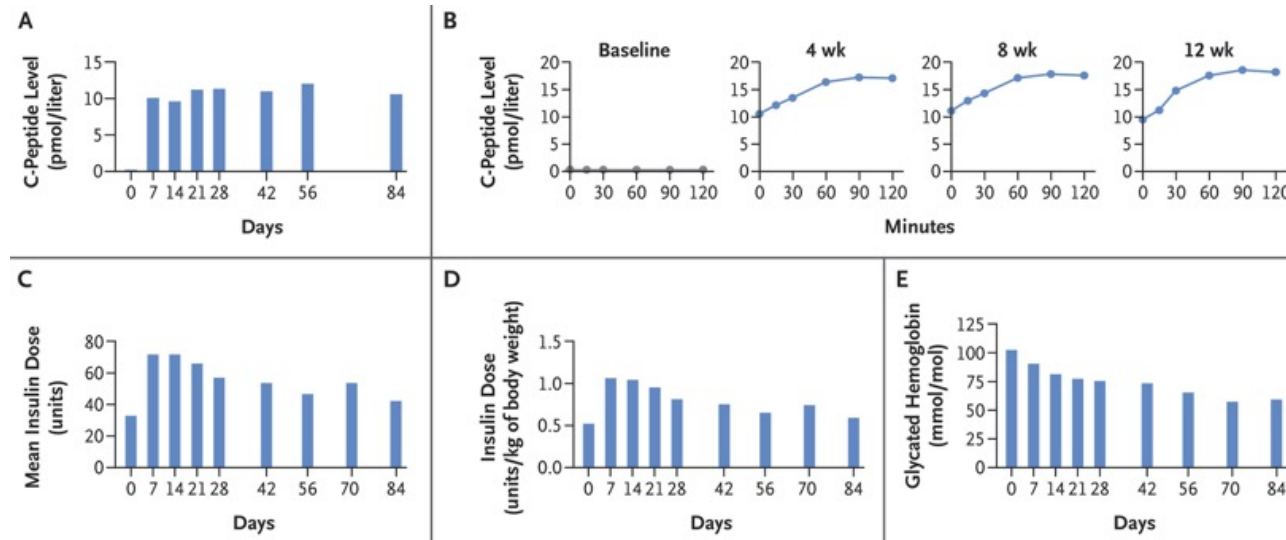
### Characterization and Transplantation of the Engineered Allogeneic Islet-Cell Product UP421.

Panel A shows the results of the flow cytometry analyses of the final gene-edited islet-cell product (UP421) for the surface expression of HLA class I, HLA class II, and CD47, with the percentages for HLA class I and II depletion and CD47 overexpression. Panel B shows the three islet-cell phenotypes that were generated in the UP421 product. The hypoimmune platform (HIP) islet cells showed both full HLA depletion and CD47 overexpression, whereas HLA class I- and class II-depleted double-knockout islet cells showed physiologic CD47 expression. Wild-type islet cells retained physiologic HLA expression and showed varying levels of CD47 expression. Panel C shows the cell-type compositions of the unmodified donor islets and the final UP421 cell product. Gene editing did not change the cell makeup of the islets. Panel D shows 1 of the 17 injections into the left brachioradialis muscle in the participant. APC denotes allophycocyanin, PerCP peridinin-chlorophyll-protein, and SSC-A side scatter area.



### Cellular and Humoral Immune Components in the Participant over 12 Weeks.

Panel A shows interferon- $\gamma$  enzyme-linked immunosorbent spot (ELISpot) data from the assessment of the participant's T-cell activation on restimulation with one of the three islet-cell subpopulations. Strong T-cell activation that peaked at approximately 7 days was seen only against wild-type cells. Panel B shows the results of corresponding T-cell cytotoxicity assays. The participant's T cells only killed wild-type cells. Panels C and D show the results of innate immune-cell killing assays with natural killer (NK) effector cells and macrophages, respectively. Only double-knockout cells were killed. Panel E shows mean fluorescence intensity of antibody binding against the UP421 wild-type cell, double-knockout cell, or HIP cell subpopulations. Antibodies were only generated against wild-type cells, with IgM antibody binding peaking early (circles with solid line), followed by a class switch to IgG antibodies (squares with dashed line). No antibodies against double-knockout or HIP islet cells were generated (the dashed lines show the background staining). Panels F and G show antibody-mediated complement-dependent cytotoxicity (CDC) and antibody-dependent cell-mediated cytotoxicity (ADCC) with NK effector cells, respectively. Only wild-type islet cells, against which antibodies were measurable, were killed in these assays. Panel H shows the participant's comprehensive immune response orchestrated by peripheral-blood mononuclear cells (PBMCs) and serum containing antibodies and complement. In this assay, both the wild-type islet cells and the double-knockout cells were killed, but the HIP islet cells survived because they escape all the immune components in the participant.



### Postoperative Persistence and Function of HIP Islet-Cell Allografts.

Panel A shows that the participant did not have measurable C-peptide levels before receiving the UP421 islet-cell product. C-peptide levels were measured over the 12-week follow-up period with a high-sensitivity assay, which showed that the levels remained stable near or above 10 pmol per liter. Panel B shows that the participant did not have any C-peptide response to a mixed-meal tolerance test before transplantation, but at 4, 8, and 12 weeks after transplantation, an increase in the C-peptide level was observed, a finding suggestive of functional beta-cell grafts. Panels C and D show the mean insulin doses (the total dose and the dose per kilogram of body weight, respectively) that were administered during the study period. Panel E shows glycated hemoglobin levels over the 12-week follow-up period.

## **Discussion**

The results of this first-in-human study are consistent with immune evasion by allogeneic, hypoimmune-engineered islet cells. These cells, transplanted and engrafted in the forearm muscle of a person with type 1 diabetes, did not induce an immune response and escaped the alloimmune responses induced against nonedited or partially edited cells. The results are also consistent with stable beta-cell function over a 12-week period. Our findings are encouraging in consideration of the reported association between early graft function and long-term clinical outcomes. Although T-cell-mediated immunity and donor-specific antibody surges peaked during the first 3 weeks, the HIP islet cells did not induce a measurable immune-cell or antibody-mediated response throughout the 12-week follow-up period. The absence of an alloimmune response against the HIP islet cells is consistent with our earlier findings in a diabetic cynomolgus monkey that received allogeneic hypoimmune-engineered islet allografts. C-peptide levels in the monkey were stable throughout the 6-month follow-up period. Moreover, a previous study in humanized mouse models of diabetes showed that hypoimmune islets escape the etiologic autoimmune response.

On the basis of previous preclinical studies, the hypoimmune phenotype provides protection against alloimmunity for cell types other than islet cells. Although inducing immune tolerance of allogeneic transplants has long been viewed as a holy grail, our study, although preliminary, suggests that immune evasion is an alternative concept for the circumvention of allorejection.



## Management of Acute Type B Aortic Dissection

*A 74-year-old man presents to the emergency department with a 1-day history of severe chest and back pain. He has a history of hypertension and has run out of medication. He has no history of similar previous events or a relevant family history. He quit smoking 10 years ago. Pedal pulses are palpable. The results of laboratory tests, including troponin levels, and an electrocardiogram are normal. Computed tomographic (CT) angiography of the chest, abdomen, and pelvis reveals an aortic dissection that extends from the left subclavian artery to the right iliac artery. How should this case be managed?*

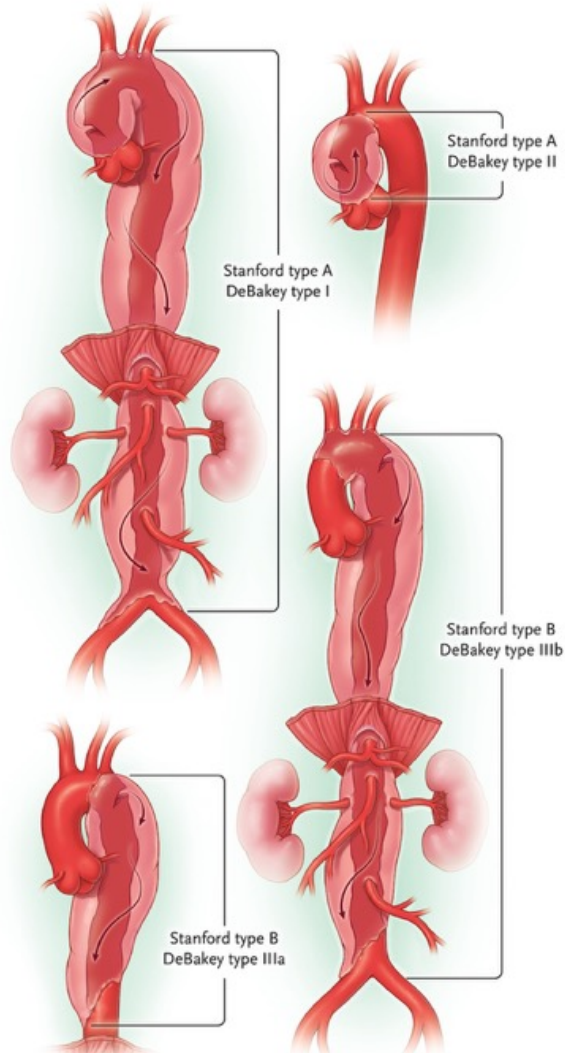
Aortic dissection is a catastrophic event that affects approximately 13,000 persons each year in the United States. Most patients with a type B aortic dissection, in which the origin of the aortic entry tear is distal to the left subclavian artery, are initially treated with medications to reduce blood pressure and myocardial contractility. Surgical or endovascular therapy is reserved for complications, such as aortic rupture or end-organ malperfusion. In this review, we describe the current state of the evidence informing clinical practice for the treatment of type B aortic dissection, as well as areas of controversy and future directions

## KEY POINTS

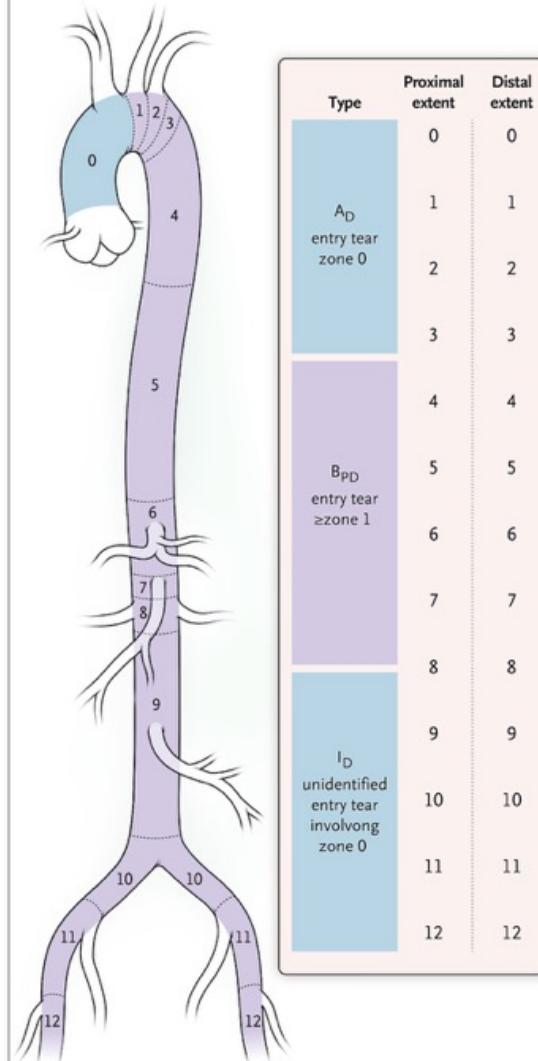
### Management of Acute Type B Aortic Dissection

- Key risk factors for aortic dissection are hypertension and known genetic aortopathy.
- Thoracic endovascular aortic repair (TEVAR) has largely replaced open surgery for patients presenting with complications (rupture or malperfusion).
- Uncomplicated type B aortic dissection is treated medically with blood-pressure control.
- TEVAR or open repair is indicated if complications develop during follow-up.
- Serial imaging and lifelong surveillance are recommended for all patients who have had an aortic dissection.

## A Stanford and DeBakey Classification Systems

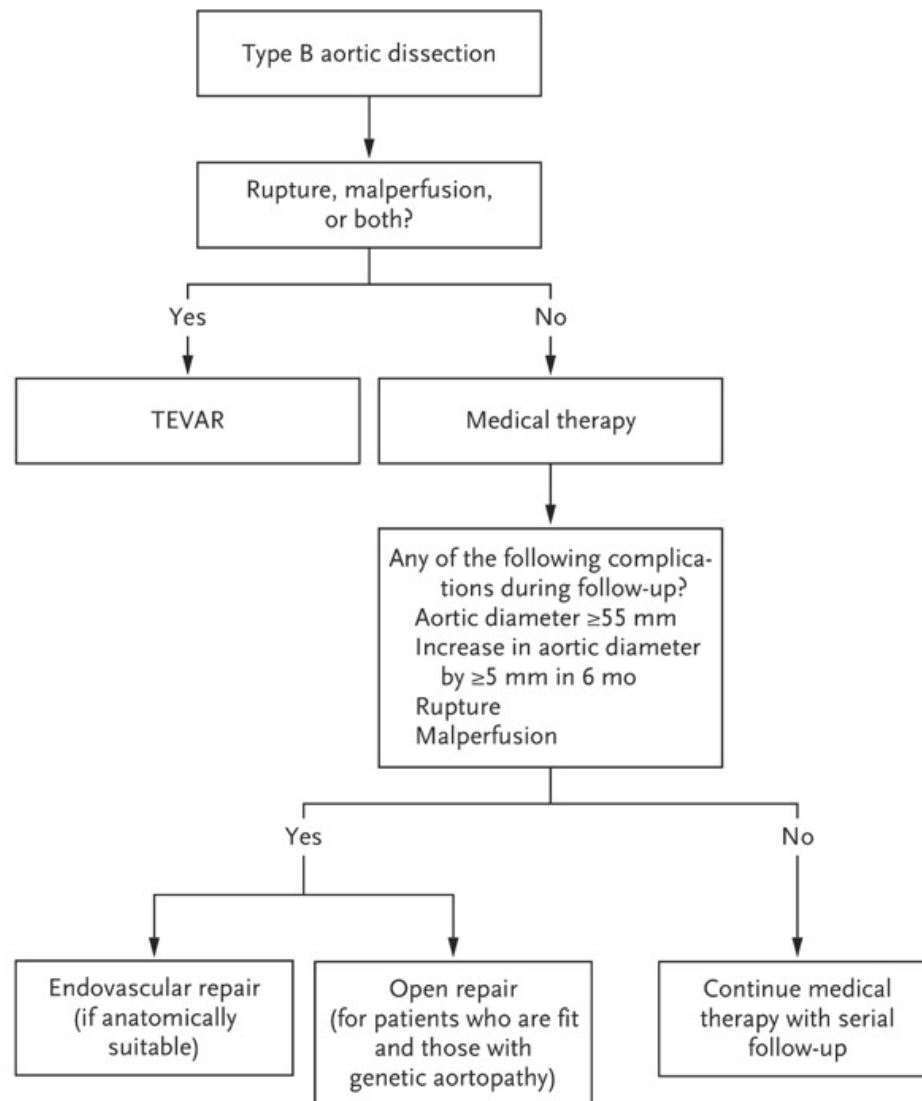


## B SVS–STS Classification System



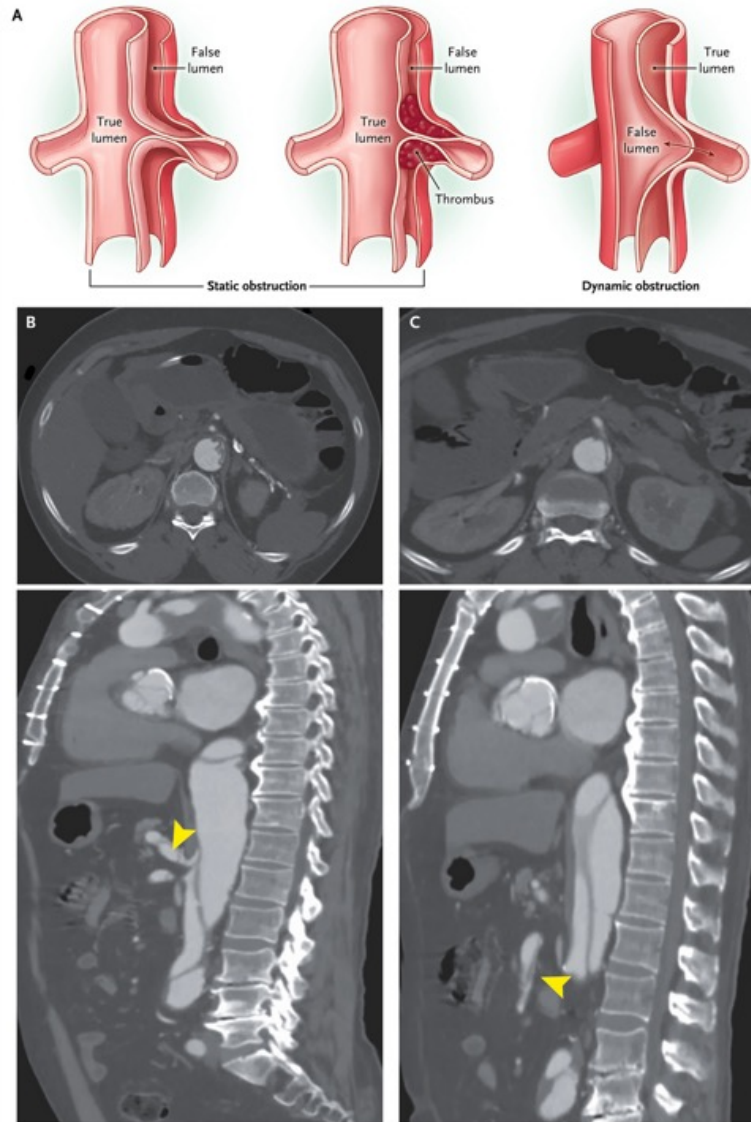
## Classification of Aortic Dissection.

Panel A shows the Stanford and DeBakey classification systems. A Stanford type A dissection involves the ascending aorta, which is defined by the proximal border of the innominate artery. All other dissections not involving the ascending aorta are designated as Stanford type B. If the aortic arch is involved but not the ascending aorta, the dissection is classified as type B; rarely, isolated arch dissections occur that are limited to the arch. In the DeBakey system, the dissection is classified as type I if a tear in the ascending aorta propagates distally to the aortic arch and descending aorta, type II if the dissection involves only the ascending aorta, type IIIa if the tear is beyond the ascending aorta and the dissection involves only the descending thoracic aorta, and type IIIb if the tear is beyond the ascending aorta and the dissection involves the entire descending thoracic and thoracoabdominal aorta and the region below the diaphragm. Panel B shows the Society for Vascular Surgery and the Society of Thoracic Surgeons (SVS–STS) classification scheme, which divides the aorta into 12 zones. A type A dissection has an entry tear in zone 0 and extends distally anywhere from zone 1 to zone 12, whereas a type B dissection has an entry tear distal to zone 1 and can extend distally to zone 12 or propagate in a retrograde manner to zone 0. In type I, the entry tear is unidentified and the dissection involves zone 0. D denotes distal extension, and PD proximal or distal extension.



**Algorithm for the Management of Type B Aortic Dissection.**

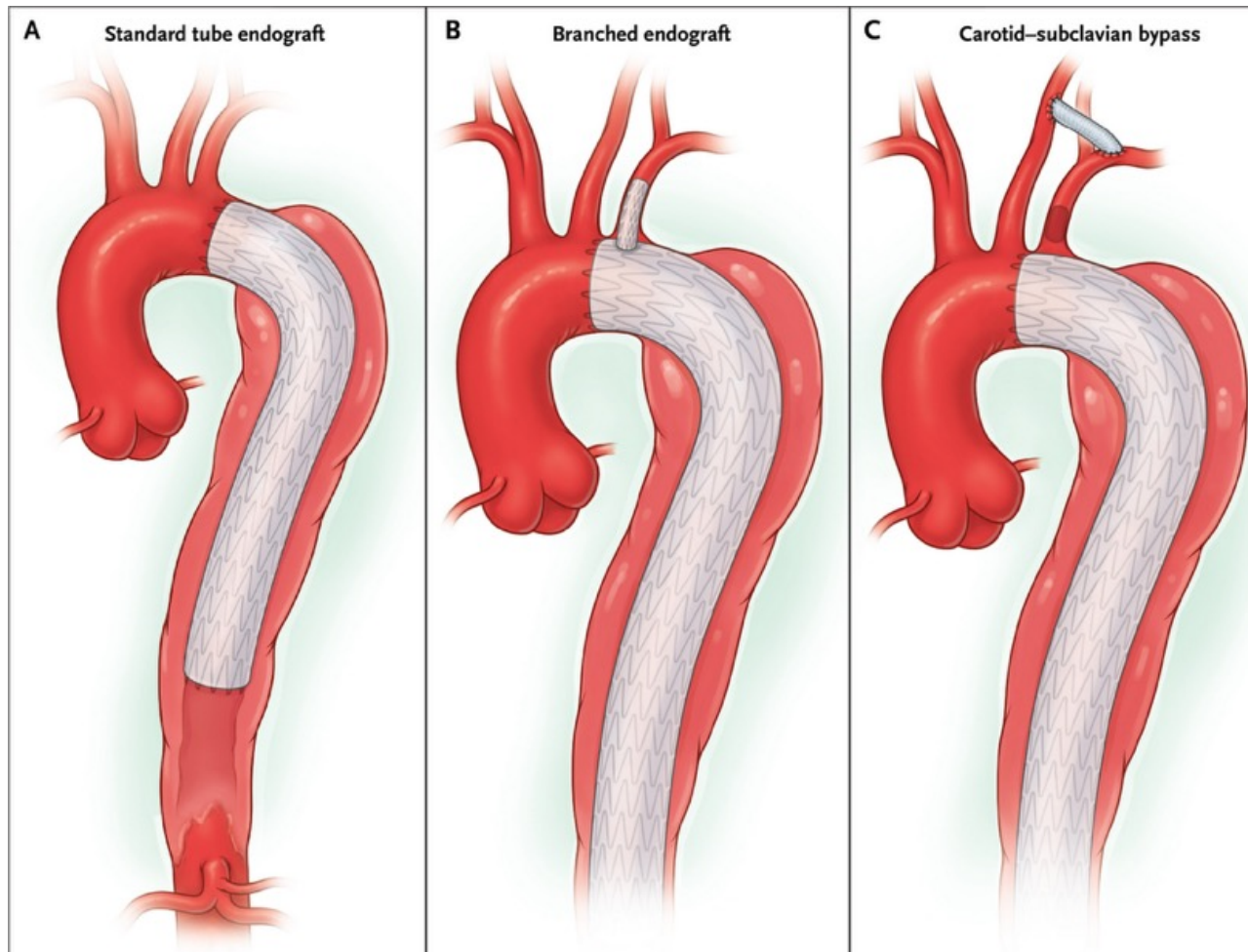
Patients with type B aortic dissection who have rupture or malperfusion are generally treated with thoracic endovascular aortic repair (TEVAR). Patients without rupture or malperfusion may be treated with medical therapy alone, but either endovascular or open repair may be warranted if complications develop.



### Mechanisms of End-Organ Ischemia.

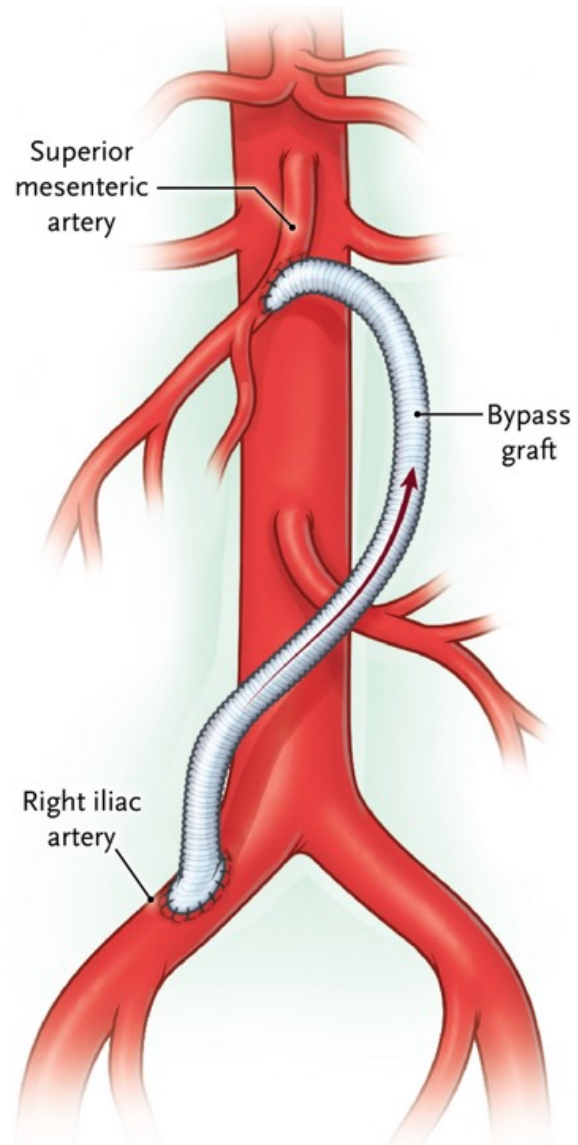
Panel A shows the mechanisms by which an aortic dissection may lead to end-organ ischemia, including static obstruction, in which the side branch is occluded completely by the dissection flap, with or without thrombus. Dynamic branch obstruction occurs when the dissection flap intermittently occludes the side branch. The axial and sagittal computed tomography (CT) images in Panel B (top and bottom, respectively) show malperfusion of the celiac artery caused by an aortic dissection. The arrowhead indicates the false lumen that has extended into the celiac artery. The axial and sagittal CT images in Panel C (top and bottom, respectively) show malperfusion of the superior mesenteric artery caused by an aortic dissection. The arrowhead points to the compressed true lumen that has extended into the superior mesenteric artery.





#### Examples of TEVAR.

Panel A shows an example of standard zone 3 TEVAR to cover a proximal entry tear. Panel B shows zone 2 TEVAR with a thoracic branched endograft to ensure flow into the left subclavian artery. Panel C shows zone 2 TEVAR, with a carotid-subclavian arterial bypass to ensure flow into the subclavian artery and an endovascular plug to occlude the origin of the left subclavian artery to prevent future type II endoleak. Zones refer to SVS-STS classification.



**Right Iliac-Superior Mesenteric Arterial Bypass for Malperfusion.**

Retrograde iliac-superior mesenteric arterial bypass may be used when TEVAR or branch stenting does not resolve malperfusion. The arrow indicates the retrograde flow.

## **Conclusions**

The patient described in the vignette in the introduction has several risk factors for aortic dissection, including male sex and a history of smoking and hypertension, and he presents with severe chest and back pain. The CT angiogram is diagnostic of a type B aortic dissection. He has palpable distal pulses and no clinical or laboratory evidence of malperfusion, which indicates the presence of uncomplicated type B aortic dissection. Current practice includes admission to the intensive care unit for pain management and strict control of blood pressure and heart rate with antihypertensive therapy, along with close clinical and laboratory follow-up in order to allow for early detection of signs of malperfusion or rupture. The development of abdominal or leg pain or worsening chest pain would warrant immediate CT angiography of the chest, abdomen, and pelvis to assess the patient for malperfusion or aortic rupture. If such an acute event developed, TEVAR with coverage of the entry tear would be appropriate. Otherwise, lifelong surveillance with clinical examination and serial imaging to detect aneurysmal degeneration is recommended, with treatment, when appropriate.

A massage gun is a handheld, electric device that provides percussive therapy – rapid, repetitive pulses of pressure and vibration into muscles and fascia to relieve muscle soreness, improve circulation, and increase range of motion. Often used by athletes and individuals for pre- and post-workout recovery, these devices offer a deep-tissue stimulation similar to a vigorous sports massage and come with different attachments and speeds to target specific muscle groups.



## A Fruitful Workup

A 37-year-old woman presented to the emergency department with a 4-day history of acute pain, swelling, and bruising on the upper portion of the left knee after using an electronic massage gun.

Her symptoms had abated slightly after she stopped using the massage gun. She was receiving lifelong anticoagulation with rivaroxaban owing to an unprovoked pulmonary embolism and paradoxical embolic stroke that had occurred 6 years earlier and had been found to be related to an underlying heterozygous factor V Leiden mutation and a patent foramen ovale. She reported no other recent bruising or bleeding apart from chronic menorrhagia.

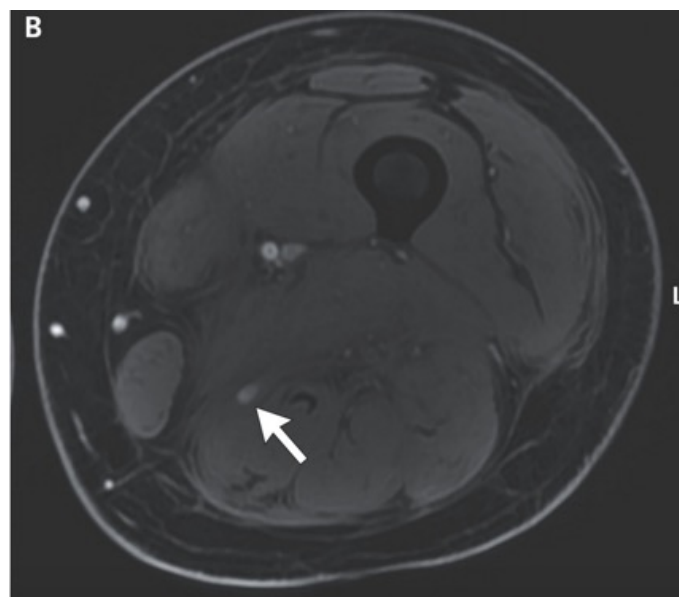
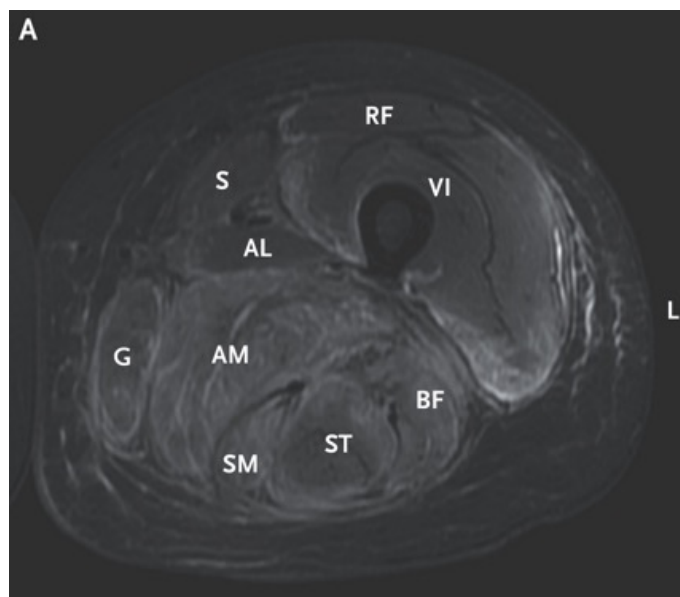
The patient's additional medical history included asthma, migraines, rheumatoid factor seropositivity without clinical arthritis, and five full-term pregnancies with no pregnancy loss. Her medications included an albuterol inhaler, seasonal cetirizine, and tranexamic acid as needed for menorrhagia. She had an epinephrine pen because of previous anaphylactic reactions to tree nuts, bananas, and avocados. She had never smoked and did not drink alcohol. She had no family history of clotting, autoimmune diseases, or blood disorders. Physical examination was notable for nonpalpable ecchymoses of her posteromedial thigh, posterior knee, and posterior calf. Her knee joint was swollen and painful on posterior palpation, but it was not erythematous and had full range of motion. She had no conjunctival pallor or pain with calf flexion, and no cordlike structures were found beneath the skin on palpation. Her vital signs were normal.

The patient's hemoglobin level was 12.4 g per deciliter, platelet count 198,000 per cubic millimeter, and white-cell count 7600 per cubic millimeter. The international normalized ratio was 1.1 (reference range, 0.8 to 1.1), and the partial thromboplastin time was 29.9 seconds (reference range, 25.1 to 36.5).

Ultrasonography and computed tomography (CT) of the left leg showed patent veins, diffuse subcutaneous edema, and no intraarticular fluid collection. She was discharged home with instructions not to use her massage gun. She resumed anticoagulation and scheduled a follow-up visit for hematologic assessment.

The patient returned to the emergency department several weeks later with exertional dyspnea and lightheadedness. She reported no dark or bloody stools, diarrhea, abdominal pain, gas, or nausea. The swelling in her left leg was slightly reduced with the use of compression stockings and leg elevation, but the bruising persisted. She had normal heart sounds, breath sounds, and pulmonary effort at rest. Her blood pressure was 113/74 mm Hg, heart rate 111 beats per minute, respiratory rate 23 breaths per minute, and oxygen saturation 100% while she was breathing ambient air. Orthostatic changes were not assessed. The hemoglobin level had declined to 7.7 g per deciliter, with a mean corpuscular volume of 84.1 fL; the red-cell distribution width was 15.4% (reference range, 11.5 to 14.5), and the platelet count was 261,000 per cubic millimeter. The international normalized ratio was 1.26, and the partial thromboplastin time was 29 seconds. Magnetic resonance imaging of the left leg showed moderate subcutaneous edema and a possible small intramuscular hematoma ([Figure 1](#)).





#### **MRI of the Left Femur without Contrast.**

In Panel A, an axial T2-weighted image, obtained with fat suppression, shows severe edema within the adductor magnus (AM), semimembranosus (SM), semitendinosus (ST), and biceps femoris (BF) muscles. In Panel B, an axial T1-weighted image, obtained with fat suppression, shows a small (0.5 cm by 0.4 cm), T1-weighted, hyperintense focus (arrow) along the anteromedial margin of the SM muscle, a finding suggestive of a small intramuscular hematoma. AL denotes adductor longus, G gracilis, RF rectus femoris, S sartorius, VI vastus intermedius, and VL vastus lateralis.

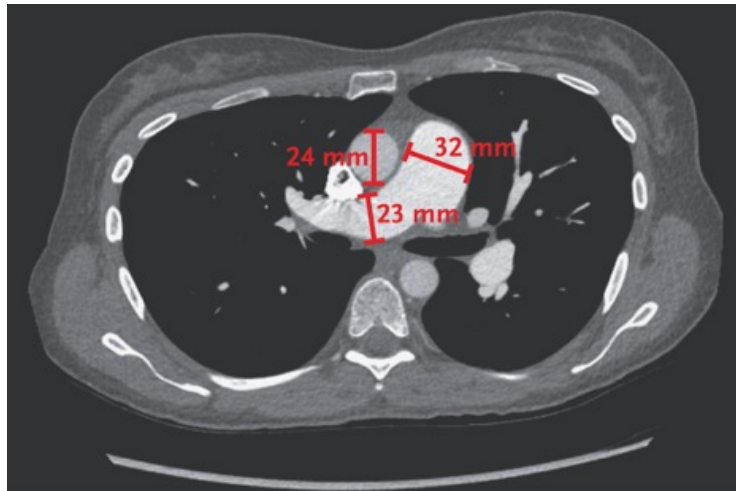
The patient's serum iron level was 12 µg per deciliter (2 µmol per liter; reference range, 50 to 170 µg per deciliter [9 to 30 µmol per liter]), iron-binding capacity 250 µg per deciliter (45 µmol per liter; reference range, 250 to 425 µg per deciliter [45 to 76 µmol per liter]), transferrin saturation 4.6% (reference range, 15 to 50), and ferritin level 55 ng per milliliter (reference range, 16 to 154). Her vitamin B<sub>12</sub> level was 291 pg per milliliter (215 pmol per liter; reference range, 211 to 911 pg per milliliter [156 to 672 pmol per liter]), and the folate level was 13.45 ng per milliliter (30 nmol per liter; reference range, >5.38 ng per milliliter [>12 nmol per liter]). The levels of haptoglobin, lactate dehydrogenase, and indirect bilirubin were normal, and a Coombs test was negative. Her reticulocyte count was 210,000 per cubic millimeter (7.9% of red cells; reticulocyte production index, 2.1), with a reticulocyte hemoglobin content of 21.6 pg (reference range, 28.2 to 36.6).

During her hospitalization, a gynecologist reevaluated her chronic menorrhagia. She described many years of regular cycles but with heavy menstrual bleeding with quarter-sized clots; her bleeding usually lasted 3 to 4 days and required pad changes every 2 to 3 hours. She reported no recent changes in her menstrual bleeding frequency, duration, or magnitude. The results of fecal occult blood testing, esophagogastroduodenoscopy, and colonoscopy were normal.

The patient was discharged home with prescriptions for daily oral iron (650 mg) and vitamin B<sub>12</sub> (1000 µg) and a plan for weekly intravenous infusions of iron sucrose (200 mg). Despite the intravenous iron infusions, she remained severely anemic and received red-cell transfusions. The gynecologist placed a levonorgestrel intrauterine device, which resulted in cessation of menstrual bleeding. Given the ongoing decrease in her hemoglobin level, anticoagulation was withheld. Over the course of 6 weeks, she received five iron infusions and four units of red cells, but her hemoglobin level remained lower than 7.5 g per deciliter. After each transfusion, her hemoglobin level would increase by approximately 1 g per deciliter per unit, but within a week, the level would decrease back to pretransfusion values.

Before further workup was performed, the patient returned to the emergency department (6 weeks after her previous hospitalization), with worsening dyspnea and new chest pain. She also reported night sweats and a weight loss of 15 lb (6.8 kg). Her heart rate was 122 beats per minute, respiratory rate 28 breaths per minute, and oxygen saturation 88% while she was breathing ambient air. She was afebrile. Venous blood gas measurements showed a pH of 7.44 and a partial pressure of carbon dioxide of 21 mm Hg. The hemoglobin level was 7.2 g per deciliter, with a mean corpuscular volume of 77.9 fl. While awaiting further evaluation, she received a transfusion of red cells, and the hemoglobin level increased to 8.4 g per deciliter. Subsequent examination revealed jugular venous distension and a new systolic murmur.

Her N-terminal pro-B-type natriuretic peptide level was 4303 pg per milliliter (up from 57.2 pg per milliliter measured during her previous hospitalization). Electrocardiography revealed sinus tachycardia, right-axis deviation, and mild precordial T-wave inversions. CT angiography of the chest showed no acute pulmonary embolism and clear lung parenchyma but revealed a dilated main pulmonary artery to 32 mm (reference value, <27 mm in women) ([Figure 2](#)). Severe tricuspid regurgitation, right ventricular dilatation, right ventricular systolic dysfunction, and a new pericardial effusion were also shown on echocardiography ([Video 1](#)).



**Contrast-Enhanced Computed Tomographic Angiogram of the Chest.**

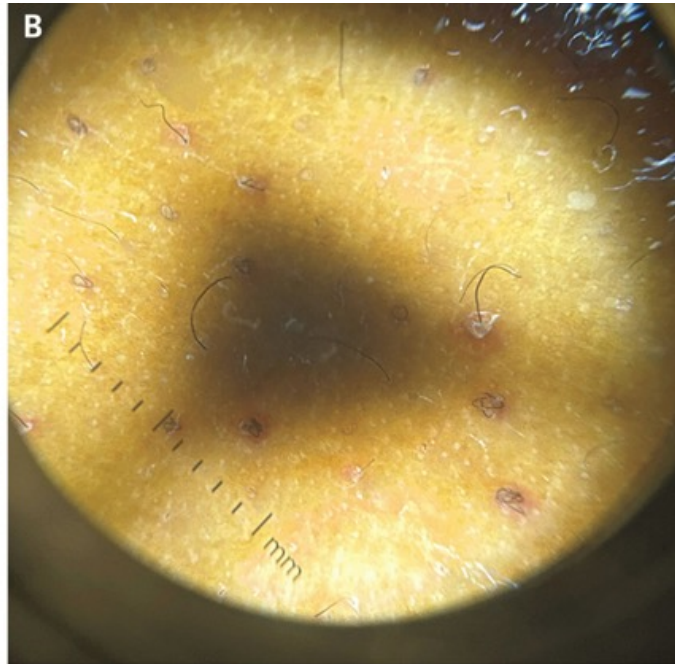
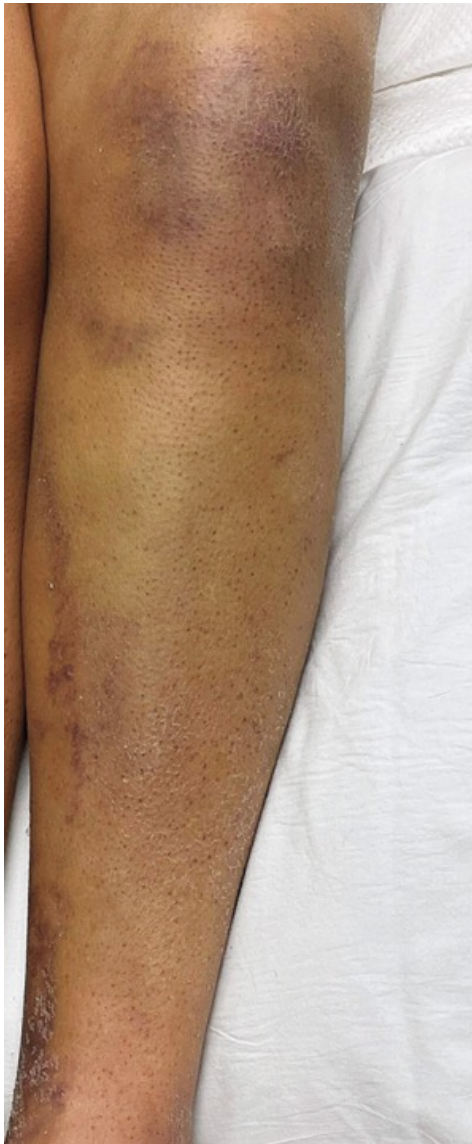
Shown is a dilated main pulmonary artery, a finding consistent with pulmonary arterial hypertension. The ascending aorta measured 24 mm in diameter, the right main pulmonary artery 23 mm in diameter, and the main pulmonary artery 32 mm in diameter.

The patient's indirect bilirubin level was 1.7 mg per deciliter (29  $\mu$ mol per liter); the results of liver tests were otherwise normal. Tests for antibodies against rheumatoid factor, cyclic citrullinated peptide, Scl-70, complement C3 and C4, antinuclear antibodies, and neutrophil cytoplasmic antigens were negative. The results of a monoclonal protein test, serologic tests for human immunodeficiency virus and hepatitis, and hemoglobin electrophoresis were normal. The reticulocyte count was 206,700 per cubic millimeter (5.8% of red cells; production index, 2.6), erythropoietin level 37 mIU per milliliter (reference range, 3 to 19), transferrin saturation 15.6% (reference range, 15 to 50), and ferritin level 111 ng per milliliter (reference range, 11 to 307). The levels of lactate dehydrogenase, haptoglobin, vitamin B<sub>12</sub>, folate, copper, and zinc were normal. A peripheral-blood smear showed microcytic red cells, polychromasia, rare schistocytes, and no immature white cells.

While awaiting further workup for pulmonary hypertension, the patient received treatment with furosemide and supplemental oxygen, which was administered through a nasal cannula at a rate of 2 liters per minute. Overnight, she became hypotensive and had worsening hypoxemia that led to a transfer to the intensive care unit.

Right heart catheterization showed a right atrial pressure of 7 mm Hg (reference range, 2 to 6); a pulmonary artery pressure of 67/26 mm Hg (reference range, 15 to 25/8 to 15), with a mean pressure of 41 mm Hg (reference range, 9 to 18); a pulmonary capillary wedge pressure of 2 mm Hg (reference range, 6 to 12); a cardiac output of 3.13 liters per minute (reference range, 4 to 8); a cardiac index of 2.12 liters per minute per square meter of body-surface area (reference range, 2.5 to 4.0); and pulmonary vascular resistance of 11.9 Woods units (reference value, <2). Her arterial oxygen saturation was 88% while she was receiving supplemental oxygen through a nasal cannula at a rate of 5 liters per minute, and serial oximetry ruled out a left-to-right shunt (i.e., no abrupt increases in blood oxygen saturation were detected within the right heart chambers). Because of her critical illness, a vasoreactivity challenge to assess eligibility for calcium channel blocker pharmacotherapy was not performed. Repeat echocardiography with agitated saline confirmed a right-to-left shunt through her patent foramen ovale ([Video 2](#)). Ventilation–perfusion single-photon emission CT showed mildly heterogeneous radioactive tracer distribution without perfusion defects, which ruled out chronic thromboembolic disease. Therapy with sildenafil and macitentan was initiated. Closer examination of the patient’s legs showed diffuse, red, nonblanching, perifollicular macules ([Figure 3](#)). On dermoscopy, hairs within these follicles were coiled. An oral examination revealed red-purple soft nodules in her gingiva, a finding consistent with gingival hyperplasia.





**Findings on Dermatologic Physical Examination.**

Shown are nonblanching perifollicular macules on the patient's shins with bruising and swelling of her left knee and leg (Panel A); corkscrew hairs and perifollicular hemorrhages, as visualized on dermoscopy (Panel B); and red-purple soft nodules in the upper gingiva (Panel C, arrow).

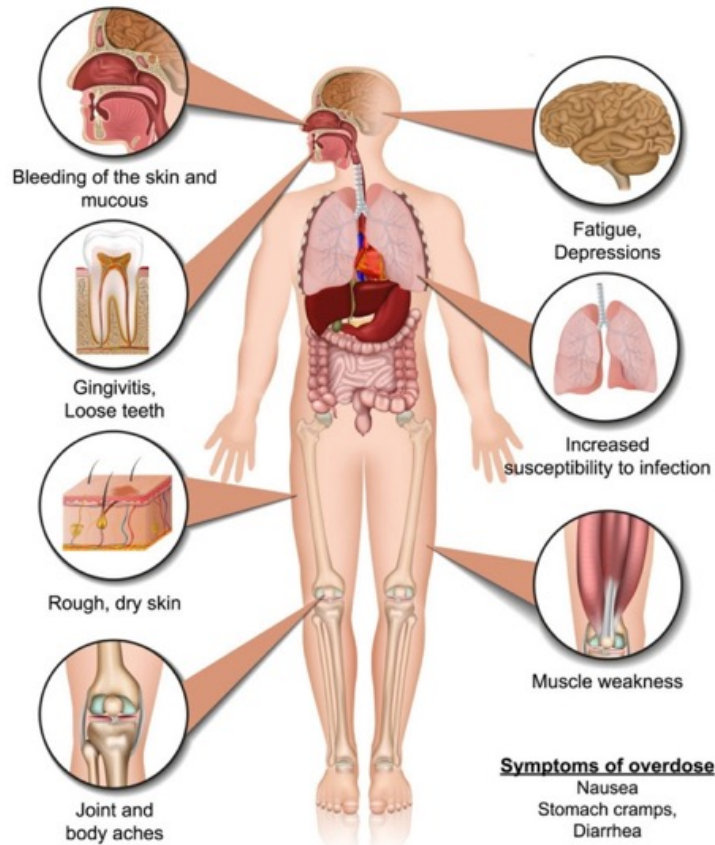
On further questioning, the patient reported avoiding all citrus products for years after hives had developed with the ingestion of citrus fruits. The patient began empirical, oral supplementation with vitamin C (ascorbic acid) at a dose of 1000 mg per day; her vitamin C level before beginning supplementation was undetectable. After 48 hours of oral repletion, she left the intensive care unit. The patient was discharged home with prescriptions for vitamin C, an iron-containing multivitamin, and sildenafil and macitentan for her pulmonary hypertension. Within 2 weeks, her hemoglobin level increased from 7.3 to 9.9 g per deciliter; after 1 month, her hemoglobin level was 12.0 g per deciliter, without further parenteral iron or red-cell transfusions. Furthermore, her cutaneous findings resolved, and rivaroxaban therapy was restarted. After several months, her dyspnea fully resolved, which enabled her to exercise regularly again. She was weaned from both sildenafil and macitentan within 6 months. Follow-up echocardiography showed resolution of all previous abnormalities ([Video 3](#)).

## **Commentary**

Humans cannot synthesize vitamin C and have limited body stores, so inadequate dietary intake can result in clinical manifestations after 1 to 3 months. Common causes of inadequate vitamin C intake include malabsorption disorders and conditions that confer a predisposition to poor intake, such as a restrictive diet, substance abuse, psychiatric illness, low socioeconomic status, and social isolation. Despite the wide availability of produce and fortified foods, serum vitamin C deficiency still occurs in the United States, with an estimated prevalence of 5.9%; contemporary estimates for clinical scurvy, however, remain elusive.

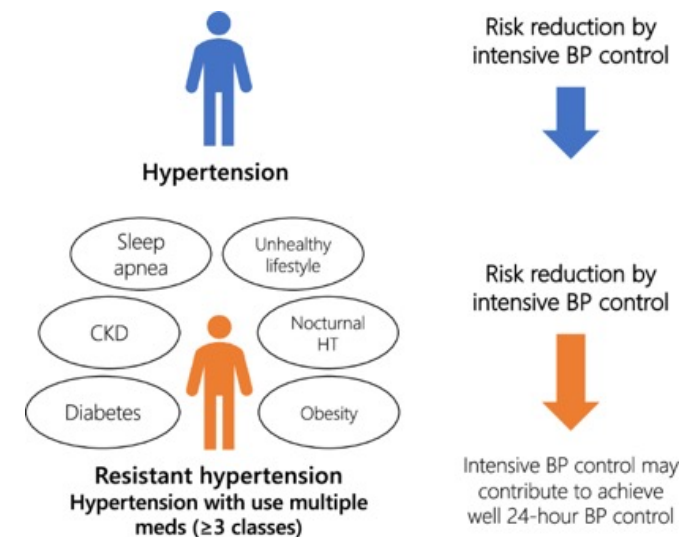
Scurvy has a range of clinical manifestations that are attributable primarily to the role of vitamin C as a cofactor for prolyl and lysyl hydroxylase, which add hydroxyl groups to procollagen residues during collagen synthesis. Hallmark signs of scurvy include perifollicular hemorrhage, corkscrew hairs, ecchymoses, musculoskeletal pain, and gum disease. Although these findings are pathognomonic for scurvy, the disease is often overlooked in the early phase, when the clinical manifestations are nonspecific (e.g., fatigue and lethargy), and because of its presumed rarity in developed nations.

# SCURVY SYMPTOMS



# THE LANCET

Intensive blood-pressure control is an aggressive antihypertensive treatment strategy that aims for a lower systolic blood pressure target, often below 120 mm Hg, compared to standard treatment's target of 130–140 mm Hg or higher. While this approach has been shown to significantly reduce the risk of [major adverse cardiovascular events](#) (MACE), it also carries potential risks, such as increased rates of [hypotension](#), [syncope](#), and potential effects on kidney function. The benefits versus risks depend on the individual's specific health profile, particularly their baseline cardiovascular risk.





# Benefit–harm trade-offs of intensive blood pressure control versus standard blood pressure control on cardiovascular and renal outcomes: an individual participant data analysis of randomised controlled trials

## Summary

**Background** Although intensive blood pressure control is recommended by major guidelines, its overall benefit–harm balance remains uncertain. In particular, it is unclear how net clinical benefit varies by blood pressure target and patient characteristics. We aimed to quantify the benefit–harm trade-offs of intensive blood pressure control versus standard blood pressure control.

**Methods** We conducted a post-hoc, pooled participant-level analysis of six randomised controlled trials (ACCORD BP, SPRINT, ESPRIT, BPROAD, STEP, and CRHCP). Trial selection was based on our collaborative framework, the Blood Pressure Reduction Union-Landmark Evidence, and a targeted literature search, guided by five predefined inclusion criteria: (1) comparison of intensive systolic blood pressure targets (<120 mm Hg or <130 mm Hg) versus standard treatment; (2) reporting of composite major cardiovascular outcomes; (3) enrolment of more than 2000 participants; (4) standardised reporting of treatment-related adverse events; and (5) availability of individual participant data. We also conducted a systematic review in which we searched PubMed for studies published from database inception up to June 15, 2025, with no language restrictions. We used search terms related to cardiovascular outcomes, hypertension, intensive blood pressure lowering, and randomised trials. Study screening and data extraction were independently conducted in pairs by ten reviewers, with discrepancies resolved by discussion or adjudication. Participants in the six trials were randomly assigned to intensive blood pressure treatment (systolic blood pressure target <120 mm Hg or <130 mm Hg) versus standard treatment (systolic blood pressure target <140 mm Hg, <150 mm Hg in older adults, or usual care), depending on the trial design. The primary benefit outcome was a composite of myocardial infarction, stroke, heart failure, and cardiovascular death. The primary harm outcomes were adverse events of interest (eg, hypotension and syncope) and renal-related events. Statistical analyses were performed on an intention-to-treat basis using Bayesian hierarchical models.



**Findings** The initial dataset included 80 676 participants, of whom 80 220 were included in our analyses (intensive blood pressure control group n=40 503; standard blood pressure control group n=39 717). The median age was 64·0 years (IQR 59·0–70·0), 39 043 (48·7%) participants were male, and 41 177 (51·3%) were female. Most participants were Asian (66 290 [82·6%]) or White (8097 [10·1%]). During a median follow-up of 3·2 years (IQR 3·0–3·5), the composite cardiovascular disease outcome occurred in 2158 (5·3%) participants in the intensive blood pressure control group and 2811 (7·1%) participants in the standard blood pressure control group (hazard ratio 0·76, 95% credible interval [CrI] 0·72–0·81;  $p<0\cdot0001$ ). Compared with standard blood pressure control, intensive blood pressure control was associated with a 1·73% absolute risk reduction (95% CrI 1·65–1·81) in cardiovascular disease (number needed to treat 58 [95% CrI 55–61]) and a 1·82% absolute risk increase (95% CrI 1·63–2·01) for adverse events of interest (number needed to harm 55 [95% CrI 49–61]). Overall, intensive blood pressure control showed a favourable benefit–harm profile, with a net benefit of 1·14 (95% CrI 1·03–1·25), using adjudicated weighting. The net benefit remained positive when considering kidney-related adverse events (1·13 [95% CrI 1·01–1·24]).

**Interpretation** Compared with standard blood pressure control, intensive blood pressure control provides a net benefit between the reduction in cardiovascular events and the increase in adverse events, including renal events.

**Funding** National Key Research and Development Program, the Ministry of Science and Technology of China; National Science and Technology Major Project; National Natural Science Foundation of China; China Academy of Chinese Medical Sciences Innovation Fund for Medical Science; and Science and Technology Program of Liaoning Province.

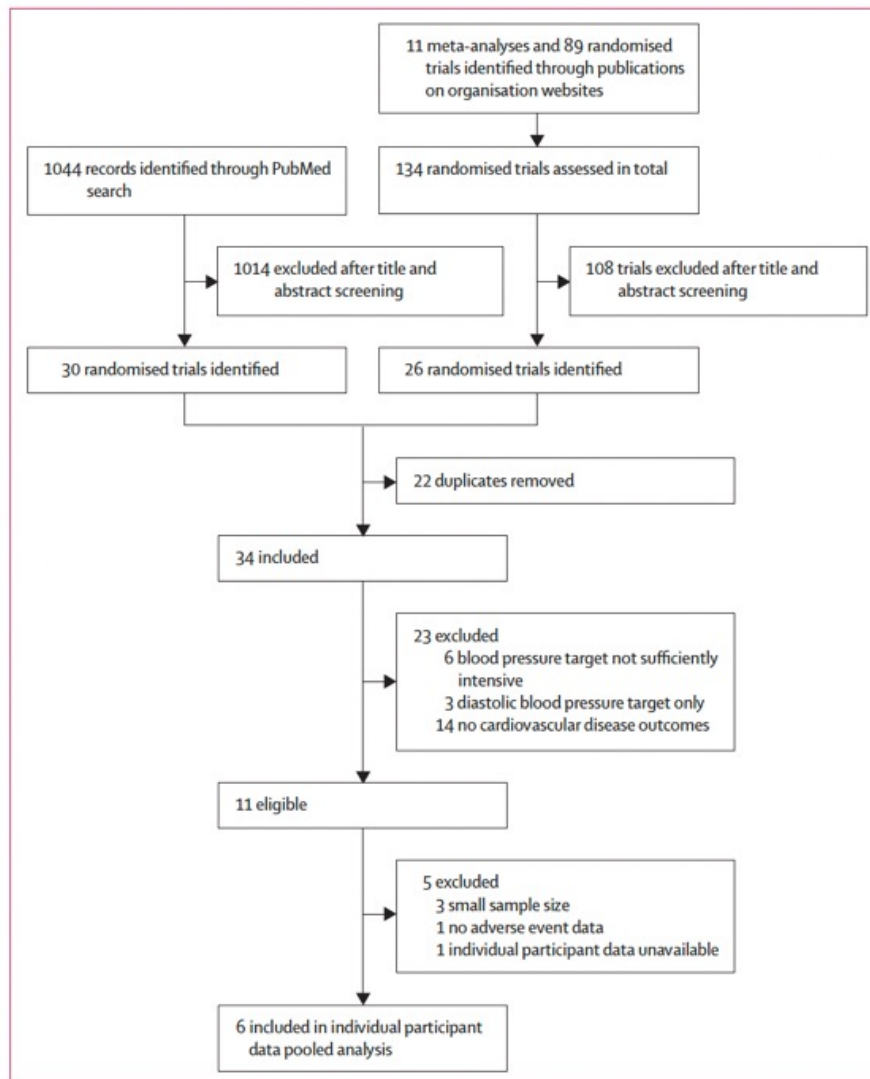
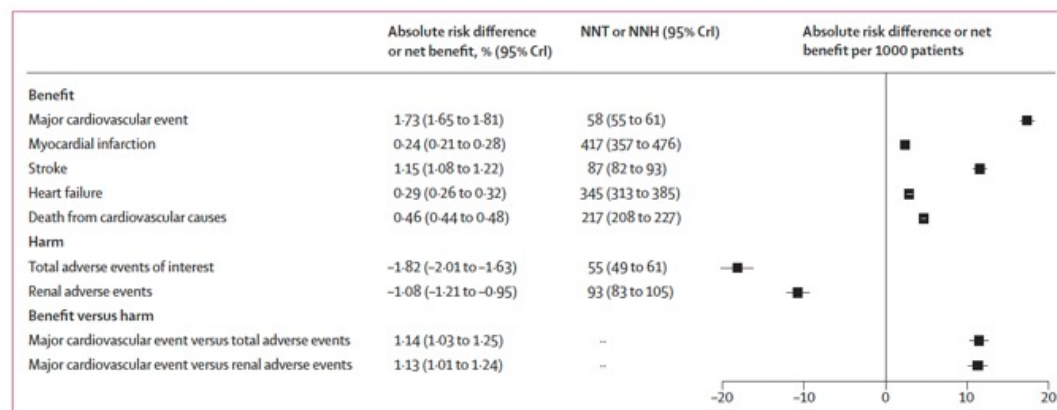


Figure 1: Study flow diagram

	Overall (n=80 220)	Intensive treatment group (n=40 503)	Standard treatment group (n=39 717)
Age, years	64.0 (59.0-70.0)	64.0 (58.5-70.0)	64.0 (59.0-70.0)
Sex			
Female	41 177 (51.3%)	20 801 (51.4%)	20 376 (51.3%)
Male	39 043 (48.7%)	19 702 (48.6%)	19 341 (48.7%)
Race or ethnic group			
Asian	66 290 (82.6%)	33 535 (82.8%)	32 755 (82.5%)
Non-Hispanic White	8097 (10.1%)	4077 (10.1%)	4020 (10.1%)
Non-Hispanic Black	3871 (4.8%)	1897 (4.7%)	1974 (5.0%)
Hispanic	1303 (1.6%)	658 (1.6%)	645 (1.6%)
Other	659 (0.8%)	336 (0.8%)	323 (0.8%)
High school education or above	27 738 (34.6%)	13 919 (34.4%)	13 819 (34.8%)
Smoking status			
Never smoked	49 129 (61.2%)	24 909 (61.5%)	24 220 (61.0%)
Former smokers	13 850 (17.3%)	6957 (17.2%)	6893 (17.4%)
Current smokers	17 241 (21.5%)	8637 (21.3%)	8604 (21.7%)
BMI, kg/m <sup>2</sup>	26.9 (4.4)	26.9 (4.4)	26.8 (4.4)
Systolic blood pressure, mm Hg	148.4 (16.9)	148.7 (17.3)	148.1 (16.6)
Diastolic blood pressure, mm Hg	82.9 (11.5)	83.1 (11.6)	82.6 (11.4)
History of major cardiovascular disease*	14 156 (17.6%)	7304 (18.0%)	6852 (17.3%)
History of stroke	11 132 (13.9%)	5768 (14.2%)	5364 (13.5%)
History of diabetes	26 362 (32.9%)	13 245 (32.7%)	13 117 (33.0%)
History of chronic kidney disease	5273 (6.6%)	2675 (6.6%)	2598 (6.5%)
Use of antihypertensive medications	63 464 (79.1%)	32 557 (80.3%)	30 907 (77.8%)
Antihypertensive medications	1.2 (0.9)	1.2 (0.9)	1.2 (0.9)
Use of aspirin	20 143 (25.1%)	10 176 (25.1%)	9967 (25.1%)
Use of statins	22 343 (27.9%)	11 139 (27.5%)	11 204 (28.2%)
Total cholesterol, mg/dL	182.1 (45.9)	182.5 (46.1)	181.6 (45.6)
LDL cholesterol, mg/dL	100.4 (34.5)	100.7 (34.7)	100.2 (34.3)
HDL cholesterol, mg/dL	48.8 (14.9)	48.9 (15.0)	48.6 (14.8)
Triglycerides, mg/dL	128.4 (90.3-189.5)	129.2 (90.3-189.6)	128.0 (89.5-188.7)
Estimated glomerular filtration rate, mL/min per 1.73 m <sup>2</sup> †	91.9 (19.7)	92.0 (19.7)	91.7 (19.6)
Atherosclerotic cardiovascular disease 10-year risk strata‡			
Low or borderline risk (<7.5%)	15 162 (18.9%)	7788 (19.2%)	7374 (18.6%)
Intermediate risk (7.5-19.9%)	30 080 (37.5%)	15 171 (37.5%)	14 909 (37.5%)
High risk (≥20%)	34 978 (43.6%)	17 544 (43.3%)	17 434 (43.9%)

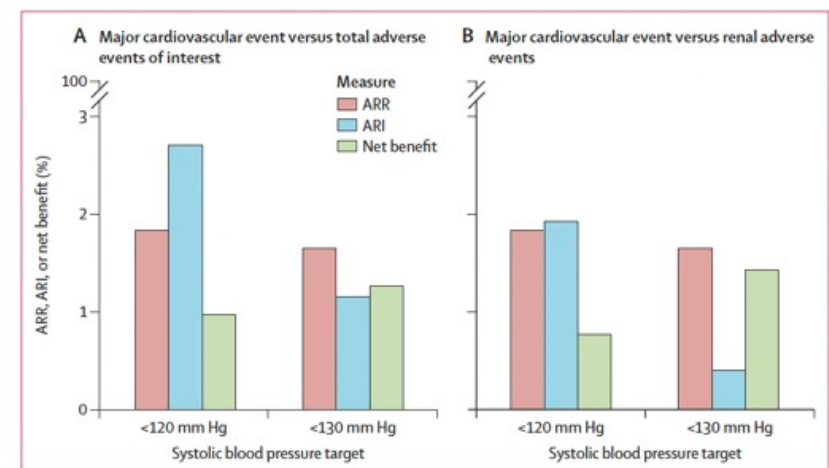
Data are median (IQR), n (%), or mean (SD). \*Major cardiovascular disease includes myocardial infarction, stroke, and heart failure. †Estimated glomerular filtration rate was calculated based on the 2021 Chronic Kidney Disease Epidemiology Collaboration creatinine equations. ‡Atherosclerotic cardiovascular disease risk was calculated based on the American College of Cardiology and American Heart Association Pooled Cohort Equations.

Table: Baseline characteristics of participants in the six included trials<sup>1,3,5-2,21</sup>



**Figure 3: Net benefit analysis comparing intensive versus standard blood pressure control**

Major cardiovascular events included myocardial infarction, stroke, heart failure, and cardiovascular death. Total adverse events of interest included hypotension, syncope, injurious fall, arrhythmia, angio-oedema and renal adverse events. Renal adverse events included acute kidney injury, renal failure, end-stage renal disease or dialysis, a reduction of 50% or more in estimated glomerular filtration rate in patients with chronic kidney disease at baseline, or a reduction of 30% or more in estimated glomerular filtration rate to <60 mL/min per 1.73 m<sup>2</sup> in patients without chronic kidney disease at baseline. All NNT and NNH values were based on a median follow-up of 3.2 years (IQR 3.0–3.5). CrI=credible interval. NNH=number needed to harm. NNT=number needed to treat.



**Figure 4: Net benefits of intensive versus standard blood pressure control in trials with different systolic blood pressure targets (<120 mm Hg and <130 mm Hg)**

(A) Major cardiovascular events versus total adverse events of interest, weighted at 1.0:3.1. (B) Major cardiovascular events versus renal adverse events, weighted at 1.0:1.8. Net benefit is defined as the absolute risk reduction minus the weighted absolute risk increase, expressed as a percentage. Values greater than 0% indicate a net benefit; values of less than 0% indicate net harm. Trials with a systolic blood pressure target of <120 mm Hg were ACCORD BP,<sup>21</sup> SPRINT,<sup>2</sup> ESPRIT,<sup>6</sup> and BPROAD,<sup>7</sup> and those with a systolic blood pressure target of <130 mm Hg were STEP<sup>3</sup> and CRHCP.<sup>8</sup> ARI=absolute risk increase. ARR=absolute risk reduction.



## Research in context

### Evidence before this study

We systematically searched PubMed for randomised controlled trials evaluating intensive blood pressure lowering and its effect on cardiovascular outcomes. The search strategy included comprehensive combinations of MeSH terms and keywords related to cardiovascular disease (eg, "myocardial infarction", "stroke", "heart failure", "mortality"), hypertension (eg, "high blood pressure", "prehypertension"), and treatment intensity (eg, "intensive", "strict", "tight"). Filters for randomised controlled trials were applied. The search covered studies published from database inception to June 15, 2025, with no language restrictions. Eligible studies were randomised controlled trials comparing intensive blood pressure control (defined as systolic blood pressure targets <130 mm Hg or <120 mm Hg) versus standard treatment, reporting cardiovascular events and adverse events. Our search ultimately identified six randomised controlled trials: ACCORD BP, SPRINT, ESPRIT, BPROAD, STEP, and CRHCP. These trials focused primarily on relative risk reduction without a comprehensive net-benefit assessment that accounts for both cardiovascular benefits and potential adverse events, particularly renal complications. Reliable estimates of the benefits and harms of intensive blood pressure control, and how these vary by blood pressure target and patient characteristics, are crucial for optimising treatment decisions. Emerging evidence from recent large, high-quality trials provides an opportunity to address this gap.

### Added value of this study

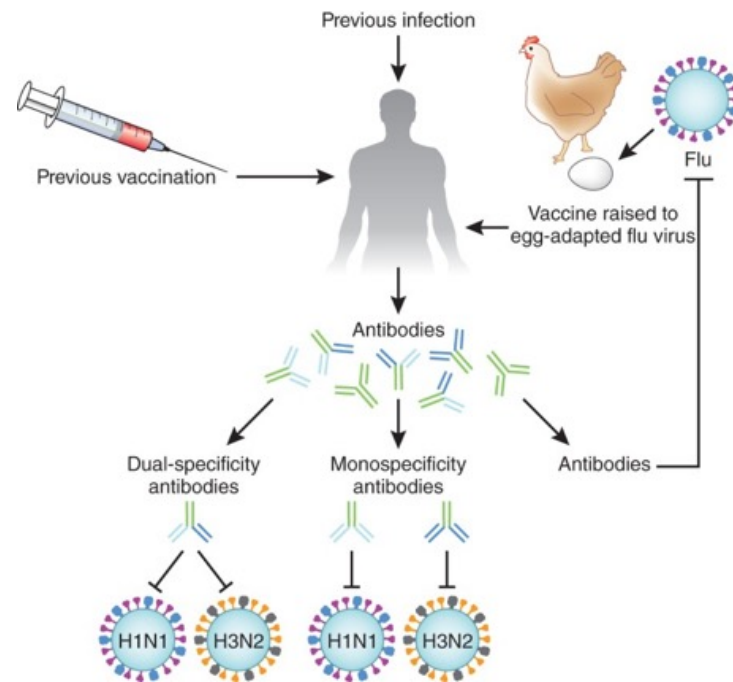
This pooled analysis of individual participant data was conducted to contextualise the findings from existing

randomised controlled trials within the broader scientific landscape and to inform guideline recommendations for hypertension management, ultimately enhancing clinical decision making. To our knowledge, this study provides the first pooled analysis of individual participant data explicitly assessing the benefit-harm trade-off of intensive blood pressure control across six pivotal randomised controlled trials, encompassing 80 220 participants. It addresses key clinical uncertainties by quantifying both the cardiovascular benefits and the potential harms, particularly renal adverse events. Net benefit varied by systolic blood pressure target (120 mm Hg vs 130 mm Hg) and patient characteristics, highlighting the need for individualised blood pressure management based on risk profiles. This approach provides deeper insight into treatment effects across diverse populations, supporting more precise and evidence-based clinical decision making.

### Implications of all the available evidence

Our findings provide robust evidence supporting a net-benefit-based approach to hypertension management, shifting the focus from cardiovascular risk reduction alone to a more patient-centred framework that integrates both benefits and potential harms. These insights offer important implications for refining blood pressure guidelines and underscore the importance of individualised strategies to optimise outcomes while avoiding both overtreatment and undertreatment.

Influenza vaccination is recommended annually for nearly everyone six months and older by health organizations like the [CDC](#) to prevent the flu and its serious complications. Everyone should get a flu shot each season, though some children may need two doses. The best time to get vaccinated is generally September or October, as it takes about two weeks for protection to develop.



# Influenza vaccination to improve outcomes for patients with acute heart failure (PANDA II): a multiregional, seasonal, hospital-based, cluster-randomised, controlled trial in China

## Summary

**Background** Influenza vaccination is widely recommended to prevent death and serious illness in vulnerable people, including those with heart failure. However, the randomised evidence to support this practice is limited and few people are vaccinated in many parts of the world. We aimed to determine whether influenza vaccination can improve the outcome of patients after an episode of acute heart failure requiring admission to hospital in China.

**Methods** We undertook a pragmatic, multiregional, parallel-group, cluster (hospital)-randomised, controlled, superiority trial over three winter seasons in China. Participating hospitals were located in the counties of 12 provinces with the capability of establishing a point-of-care service to provide free influenza vaccination to a sufficient number of patients before their discharge, if allocated to the intervention group. No such service was used in hospitals allocated to usual care (control) but patients were informed of fee-for-service influenza vaccination being available at local community medical centres, as per usual standard of care. Hospitals were randomised (1:1) in each year, stratified by province and up to three times (ie, new randomisation for each season), to include eligible adult (aged  $\geq 18$  years) patients with moderate to severe heart failure (New York Heart Association class III or IV) and no contraindication to influenza vaccination. Patient enrolment was conducted over three consecutive winter seasons, from October in each year to March of the following year, between 2021 and 2024. All patients received usual standard of care and were followed up at 1, 3, 6, and 12 months after their hospital discharge by trained study personnel using a standardised protocol. The primary outcome was a composite of all-cause mortality or any hospital readmission over 12 months, excluding events that occurred within 30 days after hospital discharge at all sites and in the summer season only for sites in northern China. The effect of the intervention was assessed at an individual level in the modified intention-to-treat population (all randomly assigned patients with available information until the time of last follow-up, excluding censored events) with a two-level hierarchical logistic regression model that included study period (year) as a fixed effect, and hospital and hospital-period as random effects, with the censored events excluded. The trial is registered at the Chinese Clinical Trial Registry (ChiCTR2100053264).



**Findings** Of 252 hospitals assessed for eligibility, 196 hospitals agreed to join and were randomised in three batches at the beginning of each winter season from October, 2021, but 32 hospitals subsequently withdrew before any patients were included. Overall, 7771 participants were enrolled at 164 hospitals in each winter season between Dec 3, 2021, and Feb 14, 2024, with 3570 assigned to the influenza vaccination group and 4201 to the usual care (control) group. The primary outcome occurred in 1378 (41·2%) of 3342 patients in the vaccination group and in 1843 (47·0%) of 3919 patients in the usual care group (odds ratio 0·83 [95% CI 0·72–0·97];  $p=0\cdot019$ ). The result was consistent in the sensitivity analysis. The number of participants with a serious adverse event was significantly lower in the vaccination group (1809 [52·5%] of 3444) than the usual care group (2426 [59·0%] of 4110; odds ratio 0·82 [0·70–0·96];  $p=0\cdot013$ ).

**Interpretation** Influenza vaccination during a hospital admission in patients with acute heart failure can improve their survival and reduce likelihood of readmission to hospital over the subsequent 12 months. The integration of influenza vaccination into inpatient care could offer a widely applicable strategy for an underserved high-risk patient group, that is relevant to resource-limited and possibly resource-rich settings.

**Funding** Sanofi and the Chinese Society of Cardiology.

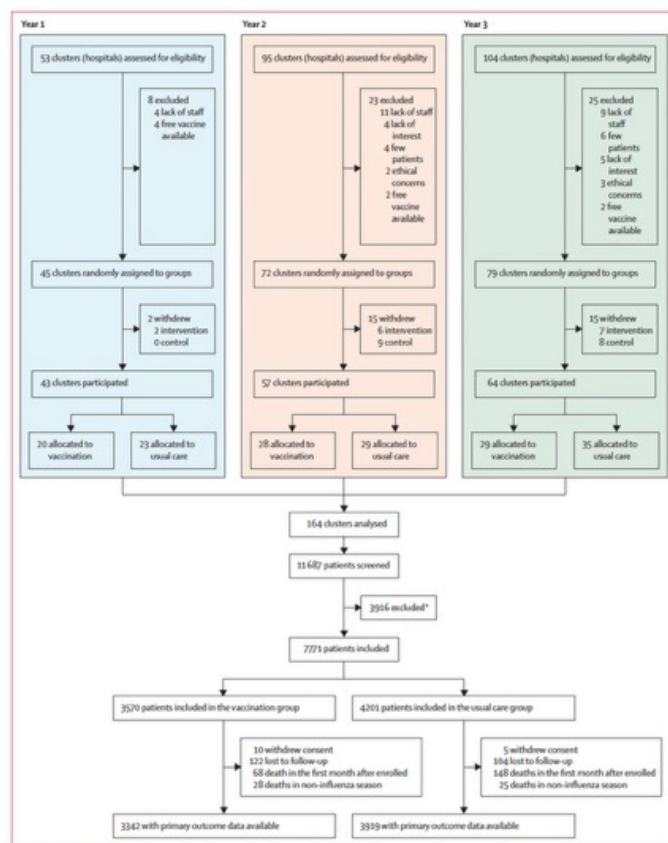


Figure 1: Trial profile

\*The main reason for exclusion was refusal to participate in the study (n=3550), for the full list of reasons see appendix p.24.

	Influenza vaccination (n=3570)	Usual care (n=4201)
Age, years	71.7 (11.0)	72.0 (11.5)
Sex		
Female	1682/3570 (47.1%)	1983/4201 (47.2%)
Male	1888/3570 (52.9%)	2218/4201 (52.8%)
Ethnicity		
Han Chinese	3389/3570 (94.9%)	4150/4201 (98.8%)
Other	181/3570 (5.1%)	51/4201 (1.2%)
Level of education		
Primary school or below	2630/3568 (73.7%)	2975/4200 (70.8%)
Secondary school or above	938/3568 (26.3%)	1225/4200 (29.2%)
Type of medical insurance		
Urban employees or residents	1095/3570 (30.7%)	1957/4200 (46.6%)
Rural cooperative medical care	2313/3570 (64.8%)	2131/4200 (50.7%)
Other	162/3570 (4.5%)	112/4200 (2.7%)
Medical history		
Hypertension	2043/3566 (57.3%)	2330/4201 (55.5%)
Coronary artery disease	1252/3566 (35.1%)	1545/4201 (36.8%)
Diabetes	754/3566 (21.1%)	1007/4201 (24.0%)
Atrial fibrillation or atrial flutter	1006/3566 (28.2%)	1140/4201 (27.1%)
Cerebrovascular disease	680/3566 (19.1%)	867/4201 (20.6%)
Heavy drinking*	186/3566 (5.2%)	225/4201 (5.4%)
Current smoker†	397/3566 (11.1%)	449/4201 (10.7%)
Vital signs		
Systolic blood pressure, mm Hg	136.1 (24.7); n=3566	136.8 (25.4); n=4199
Diastolic blood pressure, mm Hg	82.0 (15.7); n=3566	82.5 (16.1); n=4199
Heart rate, bpm	87.2 (21.9); n=3566	89.1 (21.9); n=4199
NYHA class		
III	1923/3566 (53.9%)	2281/4201 (54.3%)
IV	1643/3566 (46.1%)	1920/4201 (45.7%)
BMI, kg/m <sup>2</sup>	23.9 (4.0); n=3055	24.0 (4.2); n=3426
Laboratory results		
Sodium, mmol/L	139.5 (4.4); n=3512	139.2 (4.5); n=4120
Potassium, mmol/L	4.2 (0.6); n=3515	4.2 (0.6); n=4123
eGFR, mL/min per 1.73 m <sup>2</sup>	71.2 (23.8); n=3493	69.3 (24.3); n=4077
Natriuretic peptide tests		
BNP, ng/L	1197 (481–2586); n=440	1002 (420–2207); n=495
NT-proBNP, ng/L	3176 (1183–7637); n=2783	3940 (1458–8657); n=3240

(Table 1 continued on next page)

	Influenza vaccination (n=3570)	Usual care (n=4201)
(Continued from previous page)		
Echocardiographic parameters		
LVEF ≥40%	2467/3286 (75.1%)	2928/3829 (76.5%)
Moderate or severe mitral regurgitation	1021/3286 (31.1%)	1128/3829 (29.5%)
Interventions in the hospital		
Use of antibiotics	1369/3563 (38.4%)	1471/4179 (35.2%)
Use of intravenous inotropes	833/3563 (23.4%)	1070/4179 (25.6%)
Intravenous vasodilators	1628/3563 (45.7%)	1964/4179 (47.0%)
Percutaneous coronary revascularisation	154/3558 (4.3%)	158/4185 (3.8%)
Other cardiac procedure	77/3558 (2.2%)	48/4185 (1.1%)
Medications at hospital discharge		
Spironolactone	2631/3416 (77.0%)	299/3991 (7.5%)
ARB, ACEI or ARNI	2147/3416 (62.9%)	2407/3991 (60.3%)
Beta blocker	2288/3416 (67.0%)	2415/3991 (60.5%)
SGLT2 inhibitor	902/3416 (26.4%)	955/3991 (23.9%)
Diuretic	2302/3416 (67.4%)	2757/3991 (69.1%)
Length of hospital stay, days	8.6 (4.2); n=3558	8.6 (4.0); n=4184
Influenza vaccination given	3368/3566 (94.4%)	21/4201 (0.5%)†

Data are n, n (%), mean (SD), or median (IQR). ACEI=angiotensin-converting enzyme inhibitor. ARB=angiotensin receptor blocker. ARNI=angiotensin receptor-neprilysin inhibitor. BNP=B-type natriuretic peptide. eGFR=estimated glomerular filtration rate. bpm=beats per minute. LVEF=left ventricular ejection fraction. NT-proBNP=N-terminal pro-B-type natriuretic peptide. NYHA=New York Heart Association classification system for heart failure. \*Heavy drinking defined according to consumption for more than 5 days within 1 month: more than four shots of liquor or five cans of beer in men, and more than three shots of liquor or more than four cans of beer in women. †Smoking one cigarette or more per day in 1 month. ‡Includes 12, three, and six patients who had the vaccine before, during, and after admission to hospital, respectively.

Table 1: Baseline characteristics and patient management

	Influenza vaccination (n=3570)	Usual care (n=4201)	Effect size (95% CI)	p value	Adjusted p value*
<b>Primary outcome</b>					
All-cause mortality or hospital readmission at 12 months	1378/3342 (41.2%)	1843/3919 (47.0%)	OR 0.83 (0.72 to 0.97); RR 0.90 (0.86 to 0.94)	OR: 0.019; RR: <0.0001†	..
Adjusted mortality or hospital admission at 12 months‡	1243/3037 (40.9%)	1614/3487 (46.3%)	OR 0.85 (0.72 to 0.99)	0.042	..
Cluster level regression of primary outcome incidence§	0.40 (0.11); n=77	0.46 (0.14); n=87	-0.037 (-0.073 to -0.002)	0.037	..
<b>Secondary outcomes</b>					
All-cause mortality at 12 months	335/3342 (10.0%)	500/3919 (12.8%)	OR 0.76 (0.69 to 0.84)	<0.0001	0.0005
Hospital readmission at 12 months	1182/3342 (35.4%)	1587/3919 (40.5%)	OR 0.83 (0.70 to 0.99)	0.037	0.060
All-cause mortality or hospitalisation at 6 months	1018/3449 (29.5%)	1393/4010 (34.7%)	OR 0.84 (0.72 to 0.97)	0.018	0.053
All-cause mortality at 6 months	263/3449 (7.6%)	398/4010 (9.9%)	OR 0.74 (0.61 to 0.90)	0.0025	0.010
Hospital readmission at 6 months	882/3449 (25.6%)	1213/4010 (30.2%)	OR 0.83 (0.70 to 0.98)	0.030	0.060
<b>Serious adverse events during follow-up</b>					
Events reported	2863	4113	..	..	..
Patients with at least one event	1809/3444 (52.5%)	2426/4110 (59.0%)	OR 0.82 (0.70 to 0.96)	0.013	..
Sites with at least one event§	0.52 (0.14); n=77	0.58 (0.14); n=87	-0.042 (-0.079 to -0.004)	0.030	..
<p>Data are n/N (%), median (IQR), and mean difference (95% CI). OR=odds ratio. RR=risk ratio. *Holm-Sidak correction applied to control the family-wise error rate. Each ordered p value was compared to a sequential threshold in the formula: <math>\alpha_i = 1 - (1 - \alpha)^{1/(m - i + 1)}</math>. †p value was calculated using the Chi-square test. ‡Adjusted model included age, sex, New York Heart Association class, history of ischaemic heart disease (myocardial infarction, coronary stent insertion, coronary artery bypass surgery, or coronary artery disease), left ventricular ejection fraction (&lt;40% vs ≥40%), renal function (estimated glomerular filtration rate &lt;30 mL/min per 1.73 m<sup>2</sup> vs ≥30 mL/min per 1.73 m<sup>2</sup>).</p> <p>§Cluster level analysis conducted using weighted mixed linear regression. The model was weighted proportionally to the inverse of the binomial variance, with intervention and period as fixed effects, and hospital as a random effect.</p>					
<b>Table 2: Primary and secondary outcomes, and safety of influenza vaccination</b>					



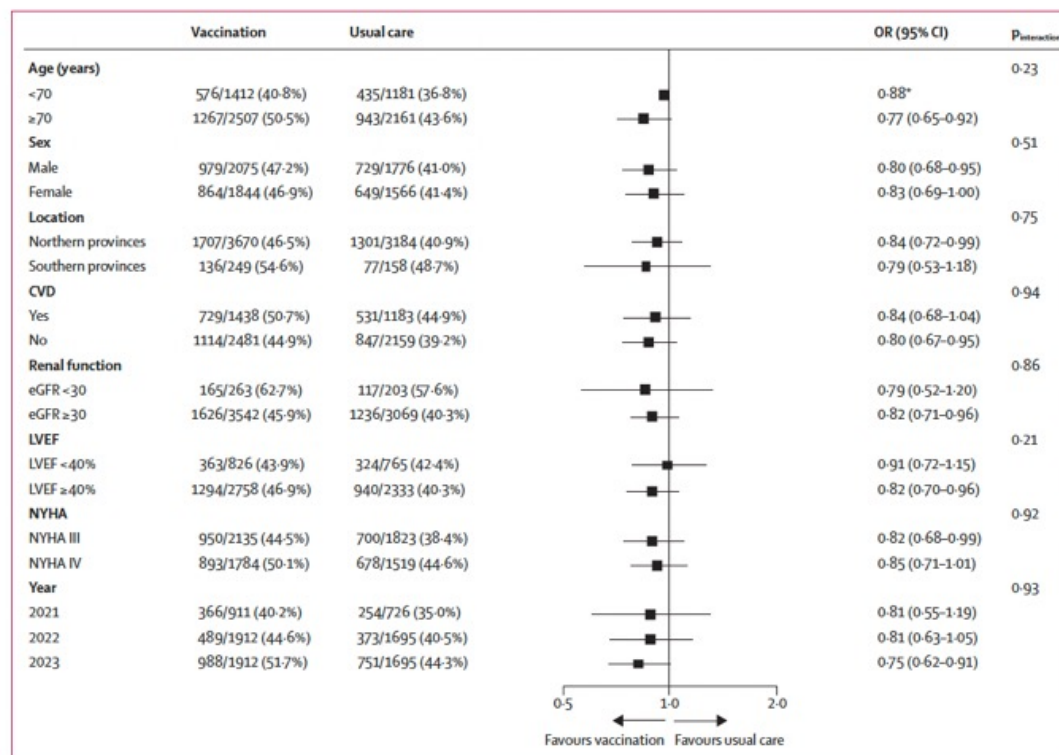


Figure 2: Forest plot of the primary outcome according to subgroups

CVD=cardiovascular disease. LVEF=left ventricular ejection fraction. eGFR=estimated glomerular filtration fraction. NYHA=New York Heart Association. OR=odds ratio. \* 95% CIs unable to be calculated due to convergence issues from small numbers in the model.

## Research in context

### Evidence before this study

We searched PubMed (from Jan 1, 1970, to May 1, 2025) and Embase (from Jan 1, 1947, to May 1, 2025) on May 10, 2025, with no language or data restrictions, for publications with relevant text words in the title or abstract or keywords that included: “influenza” AND “cardiac”. Our search yielded seven randomised controlled trials, predominantly focused on patients with coronary artery disease. One trial of 2532 patients with recent myocardial infarction reported that the use of influenza vaccination early after the onset of myocardial infarction reduced the risk for a composite cardiovascular outcome compared with placebo. Similarly, a trial of 658 patients with stable coronary disease and another trial involving 439 patients with an acute coronary syndrome reported that influenza vaccination reduced a composite cardiovascular outcome compared with placebo and a non-vaccinated group, respectively. Only one previous randomised trial limited to patients with heart failure was found. It enrolled 5129 patients to show that influenza vaccination did not significantly reduce a composite cardiac outcome, but it was associated with reduced rates of all-cause hospitalisation and community-acquired pneumonia.

### Added value of this study

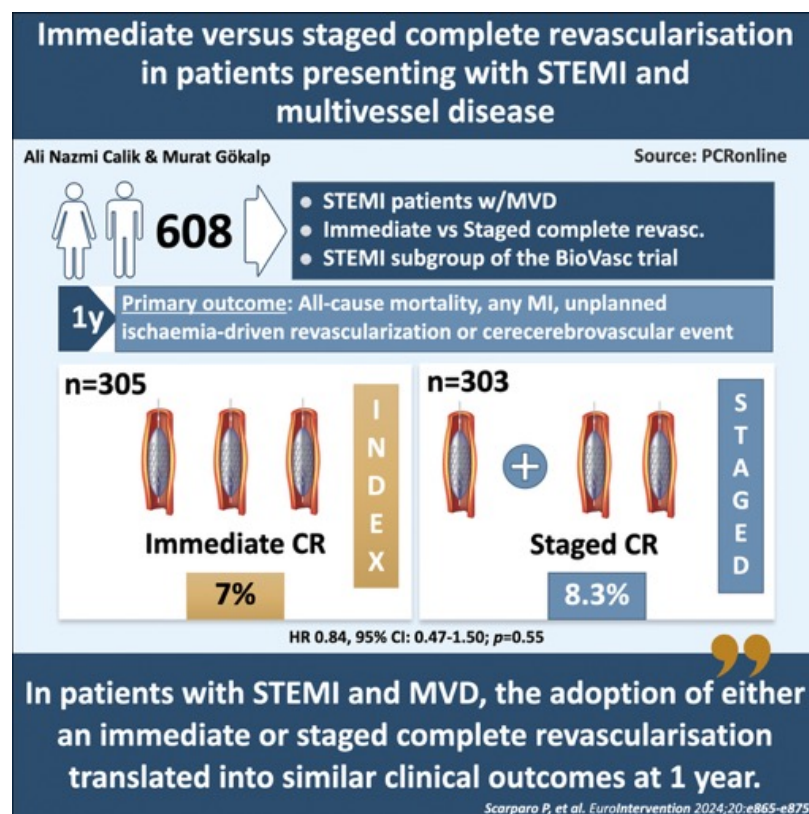
To our knowledge, this study is the first randomised trial to systematically implement an in-hospital influenza vaccination programme for high-risk patients with advanced heart failure (New York Heart Association class III or IV). By training ward staff to administer the vaccine and through a temporary point of vaccination service, the intervention embedded influenza

vaccination into routine care pathways. The intervention achieved a 94.4% vaccination rate compared with 0.5% in the usual care group, proving that hospital-based vaccination during an admission for acute heart failure is both feasible and transformative for coverage. Through the conduct across 164 county-level hospitals in China, this trial has shown that systematic in-hospital vaccination reduces the odds of the composite risk of all-cause mortality or rehospitalisation by 17% within 12 months. These findings extend previous evidence by focusing on a high-risk and understudied population to quantify the benefits of a potentially applicable treatment for low-resource settings and establish a scalable model to overcome systemic barriers to accessing vaccination.

### Implications of all the available evidence

Our trial provides strong evidence to support in-hospital use of influenza vaccination for patients admitted with acute heart failure as a potentially transformative strategy to improve their outcome. By integrating vaccination into inpatient care, the strategy overcomes systemic barriers such as frailty, limited mobility, and provider hesitancy, with the ability to achieve near-universal coverage in a historically underserved high-risk patient group. The significant reduction in post-discharge adverse outcomes highlights the phase of hospitalisation for acute heart failure as a critical window for prevention, challenging the traditional separation of acute management and preventive care. As shown through the conduct of the trial across a diverse range of locations of hospitals in China, this approach can be adaptable to resource-limited settings.

Immediate revascularization addresses all significant lesions during the initial procedure, while staged revascularization treats only the culprit lesion initially and defers other lesions to a later date. Evidence suggests that immediate complete revascularization in patients with acute coronary syndrome (ACS) and multivessel coronary artery disease (MVD) may lead to a lower risk of unplanned revascularization and recurrent heart attacks compared to staged revascularization. However, there is no significant difference in overall major adverse cardiovascular and cerebrovascular events (MACEs) or mortality between the two strategies at one year, and guidelines offer different recommendations depending on the ACS type.





# Immediate versus staged complete revascularisation during index admission in patients with ST-segment elevation myocardial infarction and multivessel disease (OPTION-STEMI): a multicentre, non-inferiority, open-label, randomised trial

## Summary

**Background** The optimal timing of complete revascularisation for patients with ST-segment elevation myocardial infarction (STEMI) and multivessel coronary artery disease remains unclear. We aimed to assess whether immediate complete revascularisation was non-inferior to staged complete revascularisation during the index admission.

**Methods** We conducted an open-label, randomised, non-inferiority trial at 14 hospitals in South Korea. Patients aged 19 years or older with STEMI and multivessel disease who had undergone percutaneous coronary intervention (PCI) for a culprit lesion were randomly assigned 1:1 to immediate complete revascularisation (PCI for non-culprit lesions during the index procedure) or staged complete revascularisation (non-culprit PCI on another day during the index admission). Web-based, permuted-block randomisation (using mixed block sizes of two or four) was implemented at each participating centre to allocate patients. Non-culprit lesions with 50–69% stenosis were evaluated by fractional flow reserve. Study participants and study investigators were aware of treatment allocation, but members of the independent clinical committee reviewing primary and secondary endpoints were masked to treatment allocation. The primary endpoint was a composite of death from any cause, non-fatal myocardial infarction, or any unplanned revascularisation at 1 year in the intention-to-treat population, and the non-inferiority margin was set at a hazard ratio (HR) of 1.42; if the upper boundary of the one-sided 97.5% CI of the HR was less than 1.42, immediate complete revascularisation would be considered non-inferior to staged complete revascularisation. Reported adverse events consisted of procedural complications, other complications during admission, and in-hospital clinical events occurring during the index admission. This trial is registered with the Clinical Research Information Service (KCT0004457) and ClinicalTrials.gov (NCT04626882). Long-term follow-up is ongoing.

**Findings** Between Dec 30, 2019, and Jan 15, 2024, 994 patients were enrolled and randomly assigned to immediate revascularisation (n=498; immediate group) or staged revascularisation (n=496; staged group). The primary endpoint occurred at 1 year in 65 patients (13%) in the immediate group and 53 patients (11%) in the staged group (HR 1·24 [95% CI 0·86–1·79];  $p_{\text{non-inferiority}}=0·24$ ). Rates of stroke, major bleeding, and contrast-induced nephropathy did not differ significantly between the two groups. Cardiogenic shock during the index hospitalisation occurred in 18 (4%) of 498 patients in the immediate group and nine (2%) of 496 patients in the staged complete revascularisation group.

**Interpretation** Among patients with STEMI and multivessel disease, immediate complete revascularisation was not shown to be non-inferior to staged complete revascularisation during the index admission in terms of incidence of a composite of death from any cause, non-fatal myocardial infarction, or any unplanned revascularisation at 1 year. This finding might inform future clinical guidelines on the role and optimal use of immediate complete revascularisation during the index admission.

**Funding** Boston Scientific.

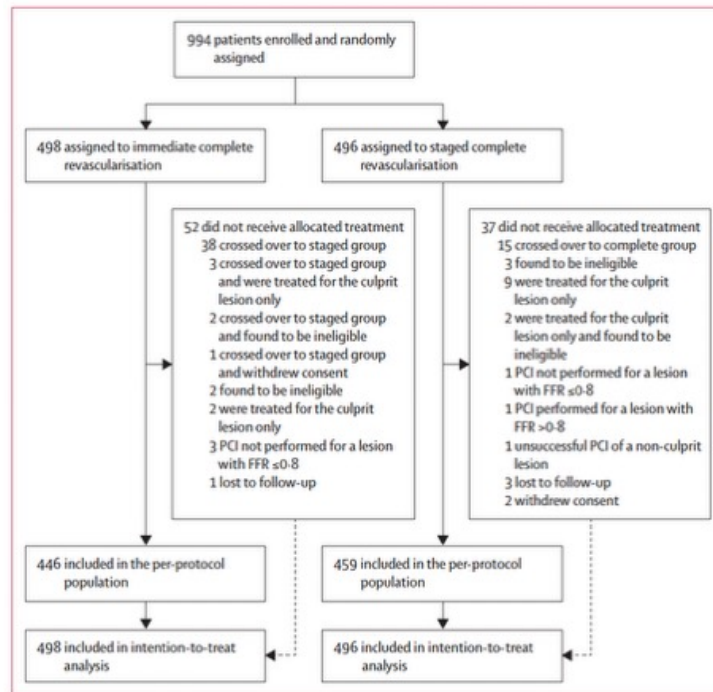


Figure 1: Trial profile  
FFR=fractional flow reserve. PCI=percutaneous coronary intervention.

	Immediate complete revascularisation group (n=498)	Staged complete revascularisation group (n=496)
<b>Patient characteristics</b>		
Age, years	66.0 (57.0-76.0)	65.0 (58.0-76.0)
Sex		
Male	396 (80%)	393 (79%)
Female	102 (20%)	103 (21%)
BMI, kg/m <sup>2</sup>	24.0 (22.1-26.0)	24.2 (22.0-26.3)
Missing data	3 (<1%)	1 (<1%)
Current smoker	205 (41%)	202 (41%)
Former smoker	97 (19%)	85 (17%)
<b>Baseline clinical characteristics</b>		
Hypertension	245 (49%)	253 (51%)
Diabetes	211 (42%)	205 (41%)
Use of insulin	8 (2%)	9 (2%)
Dyslipidaemia	295 (59%)	280 (56%)
Family history of premature coronary artery disease*	34 (7%)	37 (5%)
Previous percutaneous coronary intervention	49 (10%)	50 (10%)
Previous myocardial infarction	40 (8%)	36 (7%)
Previous heart failure	22 (4%)	20 (4%)
Previous cerebrovascular disease	40 (8%)	38 (8%)
Previous peripheral artery disease	9 (2%)	8 (2%)
Previous chronic kidney disease†	37 (7%)	34 (7%)
Receiving dialysis	6 (1%)	4 (<1%)
Location of infarct		
Anterior	215 (43%)	230 (46%)
Inferior	250 (50%)	233 (47%)
Lateral	109 (22%)	124 (25%)
Posterior	54 (11%)	48 (10%)
Isolated posterior	15 (3%)	19 (4%)
Left bundle-branch block	6 (1%)	3 (<1%)
Systolic blood pressure, mm Hg	120 (110-140)	120 (110-140)
Diastolic blood pressure, mm Hg	80 (64-80)	80 (61-80)
Heart rate, beats per minute	77 (65-90)	80 (67-90)
Killip class ≥2	171 (34%)	158 (32%)
Left ventricular ejection fraction	50.3% (11)	49.7% (11)
Missing data	10 (2%)	3 (<1%)
Symptom to balloon time, min	133 (72-261)	137 (72-240)
Door to balloon time, min	69 (55-89)	69 (56-90)
Radial access	371 (74%)	379 (76%)
Arteries with stenosis		
2	392 (79%)	397 (80%)
3	106 (21%)	99 (20%)
Location of culprit lesion		
Left anterior descending artery	221 (44%)	234 (47%)
Left circumflex artery	62 (12%)	67 (14%)
Right coronary artery	215 (43%)	195 (39%)
Location of non-culprit lesions		
Left anterior descending artery	222 (45%)	212 (43%)
Left circumflex artery	218 (44%)	215 (43%)
Right coronary artery	162 (33%)	167 (34%)

(Table 1 continued on next page)

	Immediate complete revascularisation group (n=498)	Staged complete revascularisation group (n=496)
<b>Procedural characteristics</b>		
Thrombus aspiration	109 (22%)	105 (21%)
Use of glycoprotein IIb/IIIa inhibitor	42 (8%)	45 (9%)
Guidance of intravascular imaging	118 (24%)	139 (28%)
Intravascular ultrasonography	55 (11%)	43 (9%)
Optical coherence tomography	63 (13%)	96 (19%)
Time to staged procedure, days	NA	3 (2-4)
Missing data	NA	26 (5%)
Fractional flow reserve in non-culprit lesions‡	278/654 (43%)	351/649 (54%)
Missing data	2 (<1%)	4 (<1%)
Mean value of fractional flow reserve	0.86 (0.08)	0.85 (0.08)
Fractional flow reserve >0.80	238/278 (86%)	280/351 (80%)
Fractional flow reserve ≤0.80	40/278 (14%)	71/351 (20%)
Revascularisation for non-culprit lesions	410/654 (63%)	359/649 (55%)
Stents used per patient in index procedure	2 (1-2)	1 (1-1)
Stents used per patient in index plus staged procedures	NA	2 (1-2)
Mean diameter of stents in index procedure, mm	3.08 (0.38)	3.09 (0.42)
Missing data	17 (3%)	17 (3%)
Mean diameter of stents in index plus staged procedures, mm	NA	3.07 (0.38)
Missing data	NA	17 (3%)
Total length of stents in index procedure, mm	48 (29-68)	32 (24-48)
Missing data	6 (1%)	17 (3%)
Total length of stents in index plus staged procedures, mm	NA	48 (31-76)
Missing data	NA	16 (3%)
Contrast use in index procedure, mL	180 (140-225)	130 (100-180)
Contrast use in index plus staged procedures, mL	NA	220 (170-298)
Fluoroscopy time for index procedure, min	16.4 (11.3-23.1)	9.5 (6.5-14.6)
Missing data	47 (9%)	43 (9%)
Fluoroscopy time for index plus staged procedures, min	NA	18.5 (13.3-27.6)
Missing data	NA	41 (8%)
Total radiation area dose in index procedure, cGy·cm <sup>2</sup>	8140 (5416-11980)	5388 (3693-8388)
Missing data	51 (10%)	46 (9%)
Total radiation area dose in index plus staged procedures, cGy·cm <sup>2</sup>	NA	8985 (6151-13601)
Missing data	NA	43 (9%)
Total length of hospital stay, days	4 (3-6)	5 (4-8)

Data are mean (SD), median (IQR), n (%), or n/N (%). NA=not applicable. SYNTAX=synergy between percutaneous coronary intervention with taxus and cardiac surgery. Percentages for location of non-culprit lesion sum to more than 100% because some patients had lesions in more than one artery. \*Defined as diagnosis of the disease in a male first-degree relative before age 55 years or in a female first-degree relative before age 65 years. †Defined as either a history of chronic kidney disease or receipt of dialysis. ‡Data were obtained at the angiographic core laboratory. §Fractional flow reserve not done in specified patients despite diameter stenosis between 50% and 69% by visual assessment; no patients with diameter stenosis ≥70% by visual assessment received fractional flow reserve.

Table 1: Baseline and procedural characteristics



	Immediate complete revascularisation group (n=498)	Staged complete revascularisation group (n=496)	Hazard ratio (95% CI)*
<b>Primary endpoint</b>			
Death from any cause, non-fatal myocardial infarction, or any unplanned repeat revascularisation	65 (13%)	53 (11%)	1.24 (0.86–1.79); p <sub>non-inferiority</sub> =0.24
<b>Secondary endpoints</b>			
Death from any cause	37 (7%)	26 (5%)	1.44 (0.87–2.38)
Any non-fatal myocardial infarction	19 (4%)	25 (5%)	0.77 (0.42–1.39)
Spontaneous (not procedure-related) myocardial infarction	16 (3%)	17 (3%)	0.95 (0.48–1.89)
Procedure-related myocardial infarction	3 (<1%)	8 (2%)	0.38 (0.10–1.42)
Any unplanned repeat revascularisation	28 (6%)	24 (5%)	1.19 (0.69–2.05)
Death from cardiac cause	28 (6%)	21 (4%)	1.35 (0.77–2.37)
Death from non-cardiac cause	9 (2%)	5 (1%)	1.83 (0.63–5.13)
Target lesion revascularisation	10 (2%)	9 (2%)	1.12 (0.46–2.76)
Target vessel revascularisation	17 (4%)	10 (2%)	1.73 (0.79–3.77)
Non-target vessel revascularisation	17 (4%)	16 (3%)	1.08 (0.55–2.14)
Hospitalisation for unstable angina	27 (6%)	36 (8%)	0.75 (0.46–1.24)
Hospitalisation for heart failure	21 (4%)	25 (5%)	0.85 (0.48–1.52)
Stroke†	18 (4%)	14 (3%)	1.31 (0.65–2.64)
Definite or probable stent thrombosis	10 (2%)	8 (2%)	1.26 (0.50–3.20)
Acute stent thrombosis	8 (2%)	1 (<1%)	8.00 (1.00–63.97)
Major bleeding‡	14 (3%)	21 (4%)	0.66 (0.34–1.31)
Contrast-induced nephropathy§	25/492 (5%)	32/492 (7%)	0.77 (0.45–1.32)¶

Data are n (Kaplan–Meier estimated % at 1 year), hazard ratio (95% CI), or n/N (%), unless otherwise stated. \*Hazard ratios are for immediate complete revascularisation compared with staged complete revascularisation at 1 year; 95% CIs for secondary endpoints have not been adjusted for multiplicity and should not be used to infer treatment effects. †Ischaemic stroke occurred in 14 patients in the immediate group and 12 patients in the staged group; haemorrhagic stroke occurred in four patients in the immediate group and two in the staged group. ‡Bleeding Academic Research Consortium type 3 or 5 indicates major bleeding. §Defined as an increase in serum creatinine level by at least 0.5 mg/dL ( $\geq 44.2 \mu\text{mol/L}$ ) or an increase in serum creatinine level to at least 1.25 times the baseline level within 72 h of contrast agent exposure. ¶Odds ratio (with 95% CIs calculated using unadjusted logistic regression) is shown instead of hazard ratio. ||Ten patients (six in the immediate group and four in the staged group) with end-stage renal disease were excluded from the analysis.

**Table 2: Primary and secondary endpoints in the intention-to-treat population**

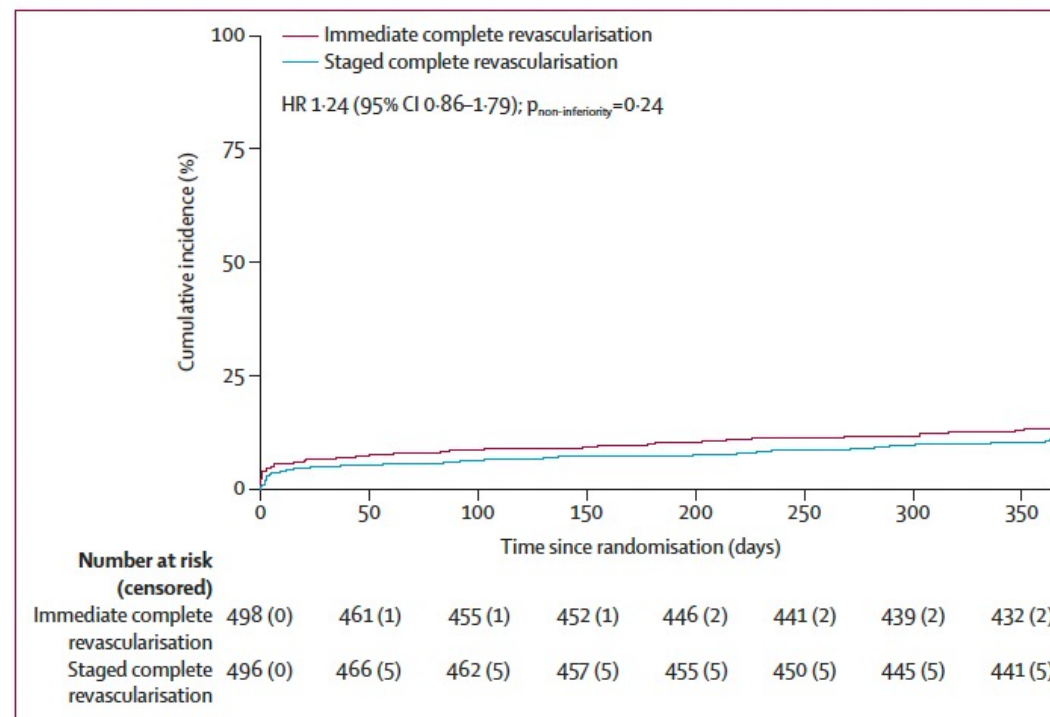


**Figure 2: Kaplan–Meier curves for cumulative incidence of the primary endpoint at 1 year**  
The primary endpoint was a composite of death from any cause, non-fatal myocardial infarction (both spontaneous and procedure-related), or any unplanned revascularisation. HR=hazard ratio.

	Immediate complete revascularisation group (n=498)	Staged complete revascularisation group (n=496)
<b>Procedural complications</b>		
No-reflow phenomenon	22 (4%)	23 (5%)
Coronary artery perforation	3 (<1%)	3 (<1%)
Coronary artery perforation requiring pericardiocentesis	2 (<1%)	1 (<1%)
Fractional flow reserve-related complications	0/278	3/351 (<1%)*
Need for cardiopulmonary resuscitation	6 (1%)	8 (2%)
Need for mechanical circulatory support†	3 (<1%)	3 (<1%)
<b>Complications during hospitalisation</b>		
Cardiogenic shock	18 (4%)	9 (2%)
Cardiogenic shock in patients with Killip II or III	15/171 (9%)	8/158 (5%)
Need for mechanical circulatory support†	10 (2%)	5 (1%)
New or worsening of heart failure	16 (3%)	15 (3%)
Pulmonary complications‡	9 (2%)	12 (2%)
Anaphylactic reaction to contrast agent	1 (<1%)	0
Critical limb ischaemia	1 (<1%)	1 (<1%)
Mechanical complications of myocardial infarction	2 (<1%)	1 (<1%)
Need for mechanical ventilation	18 (4%)	10 (2%)
Vascular access site-related complications	7 (1%)	7 (1%)
<b>In-hospital clinical events</b>		
Death from any cause	13 (3%)	6 (1%)
Non-fatal myocardial infarction	13 (3%)	13 (3%)
Any unplanned repeat revascularisation	12 (2%)	9 (2%)
Unplanned revascularisation for non-culprit lesions before planned staged procedure	NA	1 (<1%)
Death from cardiac cause	13 (3%)	6 (1%)
Death from non-cardiac cause	0	0
Target lesion revascularisation	9 (2%)	6 (1%)
Target vessel revascularisation	10 (2%)	6 (1%)
Non-target vessel revascularisation	5 (1%)	4 (<1%)
Stroke	7 (1%)	4 (<1%)
Definite or probable stent thrombosis	9 (2%)	5 (1%)
Major bleeding	7 (1%)	14 (3%)

Data are n (%), or n/N (%). NA=not applicable. \*Ventricular tachycardia in one patient, coronary dissection in one patient, and significant bradycardia requiring transient pacing in one patient. †All mechanical circulatory supports were venoarterial extracorporeal membrane oxygenation. ‡Pulmonary complications included pneumonia, pulmonary thromboembolism, and pulmonary haemorrhage.

Table 3: Adverse events during the index hospitalisation

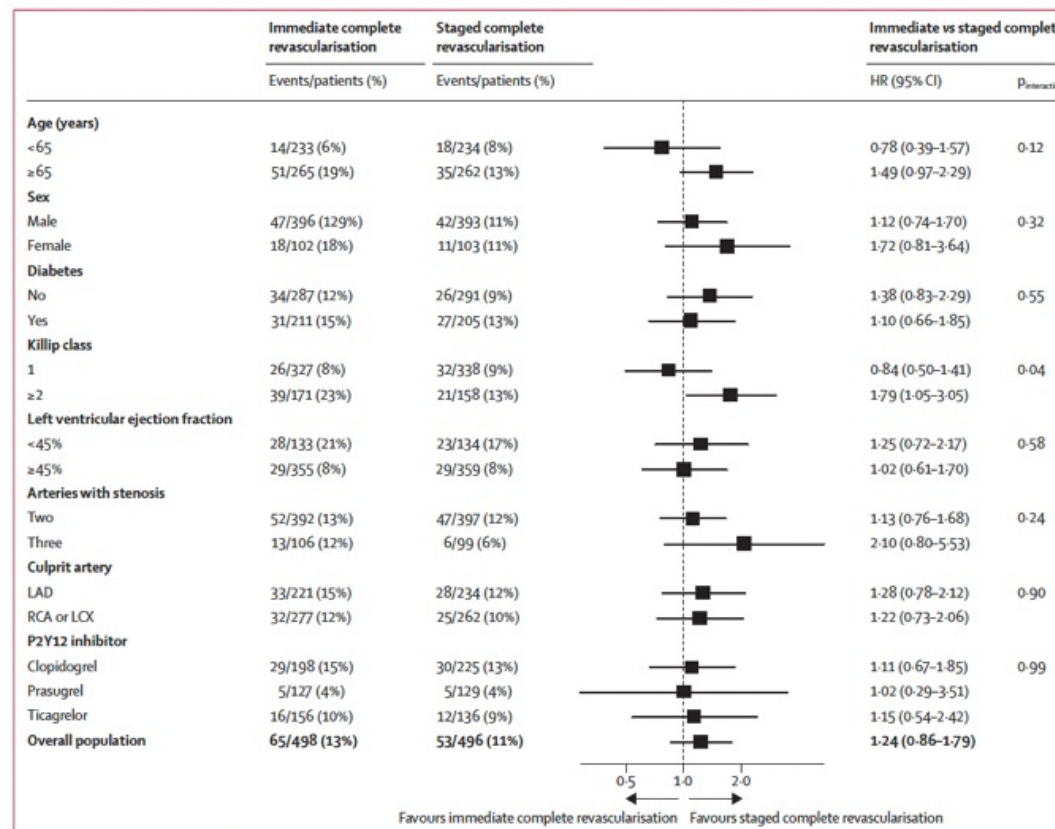


Figure 3: Subgroup analysis of the primary endpoint

The forest plot shows numbers of patients with events in the treatment groups overall and in prespecified subgroups at 1 year. The widths of the CIs have not been adjusted for multiplicity and should not be used to infer definitive treatment effects. HR=hazard ratio. LAD=left anterior descending artery. RCA=right coronary artery.







## The *Lancet* Countdown on health and plastics

Plastics are a grave, growing, and under-recognised danger to human and planetary health. Plastics cause disease and death from infancy to old age and are responsible for health-related economic losses exceeding US\$1.5 trillion annually. These impacts fall disproportionately upon low-income and at-risk populations. The principal driver of this crisis is accelerating growth in plastic production—from 2 megatonnes (Mt) in 1950, to 475 Mt in 2022 that is projected to be 1200 Mt by 2060. Plastic pollution has also worsened, and 8000 Mt of plastic waste now pollute the planet. Less than 10% of plastic is recycled. Yet, continued worsening of plastics' harms is not inevitable. Similar to air pollution and lead, plastics' harms can be mitigated cost-effectively by evidence-based, transparently tracked, effectively implemented, and adequately financed laws and policies. To address plastics' harms globally, UN member states unanimously resolved in 2022 to develop a comprehensive, legally binding instrument on plastic pollution, namely the Global Plastics Treaty covering the full lifecycle of plastic. Coincident with the expected finalisation of this treaty, we are launching an independent, indicator-based global monitoring system: the *Lancet* Countdown on health and plastics. This Countdown will identify, track, and regularly report on a suite of geographically and temporally representative indicators that monitor progress toward reducing plastic exposures and mitigating plastics' harms to human and planetary health.

### Panel 1: Lessons learned from other global health threats

Successes achieved in the control of other environmental health threats offer lessons for the control of the plastic crisis. Clean air legislation has reduced ambient air pollution in multiple countries, thus improving air quality and preventing millions of premature deaths.<sup>30</sup> Lead has now been removed from automotive petrol in every nation, resulting in sharp reductions in children's blood lead levels and increases in cognitive function among children, and contributing to decreased risks of hypertension, heart disease, and stroke in adults.<sup>31</sup> The Montreal Protocol on Substances that Deplete the Ozone Layer has considerably reduced emissions of ozone-depleting chlorofluorocarbons and their alternatives, leading to the recovery of the stratospheric ozone layer and helping to prevent deaths from malignant melanoma.<sup>32,33</sup> The Minamata Convention on Mercury is coordinating a global phase-out of mercury to protect infants and children from developmental neurotoxicity.<sup>34</sup>

These interventions have proven highly cost-effective. For example, each dollar invested in air pollution control in the USA since 1970 is estimated to have yielded an economic benefit of US\$30 by reducing health-care costs and increasing the economic productivity of a healthier, longer-lived population.<sup>30</sup> The removal

of lead from petrol has benefitted the health of entire nations by increasing intelligence, human capital, and economic productivity. In the USA, lead removal is estimated to have added \$200 billion to the economy in each annual birth cohort since 1980—an aggregate benefit of more than \$8 trillion in the past four decades.<sup>31</sup>

Two key lessons emerge from these interventions. First, health matters. The recognition that an environmental threat damages human health, especially children's health, is far more probable to catalyse public engagement and drive meaningful change across every level of society than a conversation that focuses solely on the environment. Second, data matter. Data are needed to identify the sources of a health threat, measure the extent and severity of exposure across populations, quantify health effects, track time trends and geographic patterns, assess the effectiveness of interventions, and guide course corrections. Data play a key role also in countering disinformation and attempts at greenwashing, such as the false claims by the plastic industry that all plastics can be recycled,<sup>35-37</sup> or that plastic waste can safely be burned for energy and to generate plastic credits in industries, such as in cement production.<sup>38,39</sup>



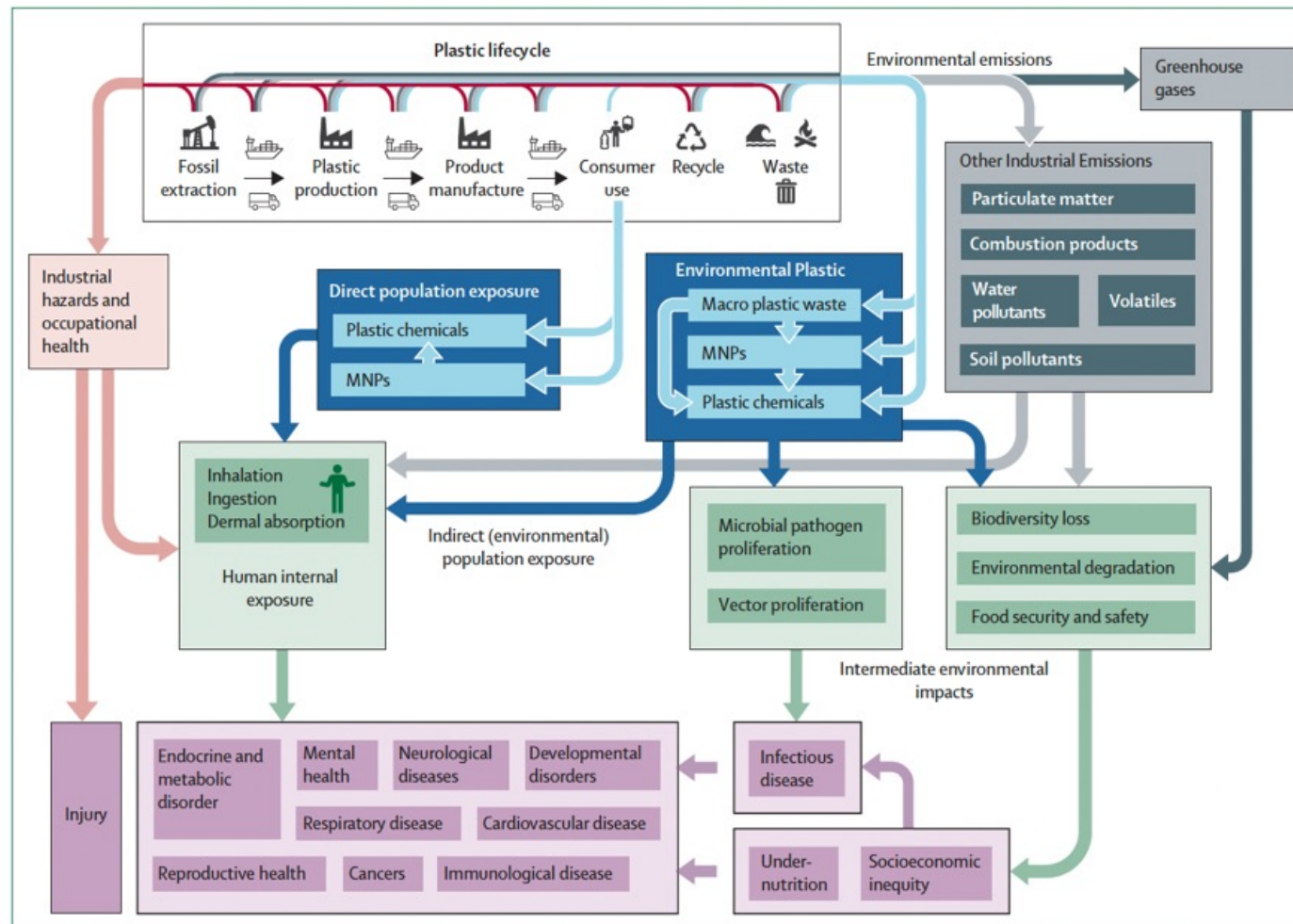


Figure 2: The potential impacts of plastics on health across the plastic lifecycle  
MNP=microplastic and nanoplastic particle.

### Panel 2: Summary of key findings from the Minderoo–Monaco Commission

The Minderoo–Monaco Commission on plastics and human health presented a comprehensive assessment of plastics-associated harms to human and ecosystem health.<sup>23</sup> Key findings were the following:

- Current patterns of plastic production, use, and disposal cause disease, disability, and death at every stage of the plastic lifecycle.
- Infants and young children are highly susceptible to plastics-associated harms. Early-life exposures to plastics and plastic chemicals are linked to increased risks of miscarriage, prematurity, stillbirth, low birthweight and birth defects of the reproductive organs, neurodevelopmental impairment, impaired lung growth, and childhood cancer. Early-life exposures to plastic chemicals can contribute to reduced human fertility and increased risks of non-communicable diseases, such as cancer, diabetes, and cardiovascular disease in adult life.
- Plastic production is highly energy-intensive, releases more than 2 gigatonnes of CO<sub>2</sub>, equivalent and other climate-forcing greenhouse gases to the atmosphere each year, and harms health by accelerating climate change.
- Increasing plastic production is the main driver of worsening harms to human and planetary health.
- Because less than 10% of plastic is recycled and plastic waste can persist in the environment for decades, an estimated 8 billion tonnes of plastic waste or 80% of all plastic ever made, now pollute the planet.<sup>25</sup>
- The ocean is the ultimate destination for much plastic waste, and each year, an estimated 10–12 million tonnes of plastic enter the ocean. Many plastics appear to resist breakdown in the ocean and could persist for decades.
- Microplastic and nanoplastic particles (MNPs), which result from the breakdown of larger plastic materials, are an emerging threat to health. While the health impacts of MNPs are still incompletely understood, increasing numbers of studies report the presence of microplastics in multiple human tissues and are beginning to link MNPs to disease.
- Plastic is expensive. It is responsible for health-related economic losses that include health-care costs (eg, costs of physician services, hospitalisation, and medications) and productivity losses (eg, lost economic output or earnings resulting from disease, disability, or premature death). In 2015, the health-related costs of plastic production amounted to almost US\$600 billion globally—more than the gross domestic product of New Zealand or Finland.<sup>23</sup> Chemicals in plastics, such as PBDE (flame retardant), bisphenol (BPA; monomer), and di(2-ethylhexyl)phthalate (DEHP; plasticiser) are responsible for additional health-related economic costs. In the USA alone, the annual costs of diseases caused by PBDE, BPA, and DEHP exceed \$675 billion.
- These estimates undercount the full costs of plastics-related health damages because they examine only a few countries and only a subset of plastic chemicals. The costs are externalised by fossil fuel and plastic manufacturing industries and borne by governments and taxpayers.
- Current patterns of plastic production, use, and disposal are unsustainable and socially and environmentally unjust. Plastics-associated harms disproportionately damage disempowered and marginalised populations.<sup>54</sup> Addressing these inequities will require a multifaceted approach that centres on justice and incorporates equity and inclusivity into all levels of policy and decision making.

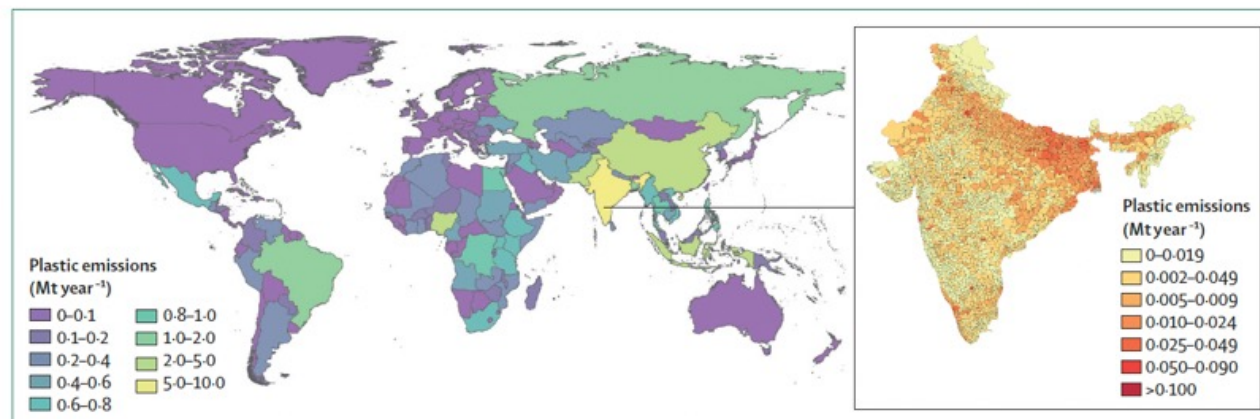


Figure 3: Macroplastic waste generation by country and by municipality for India, 2020  
Adapted from Cottom and colleagues.<sup>68</sup> Mt=megatonnes.

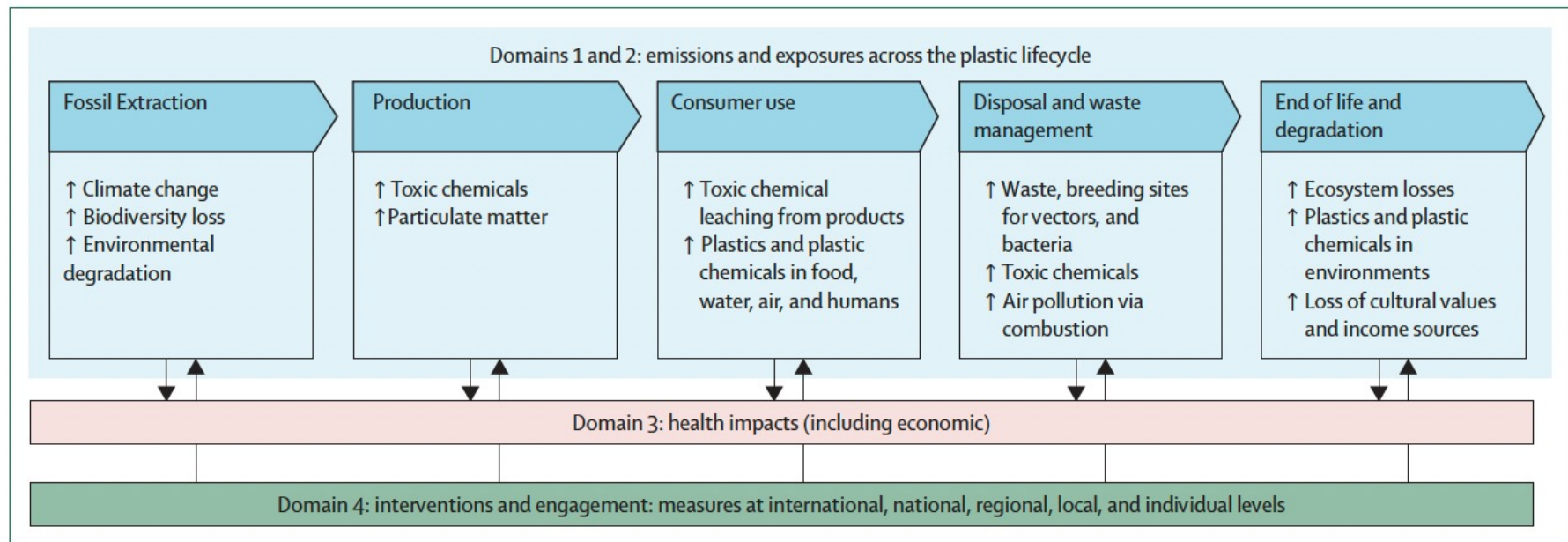
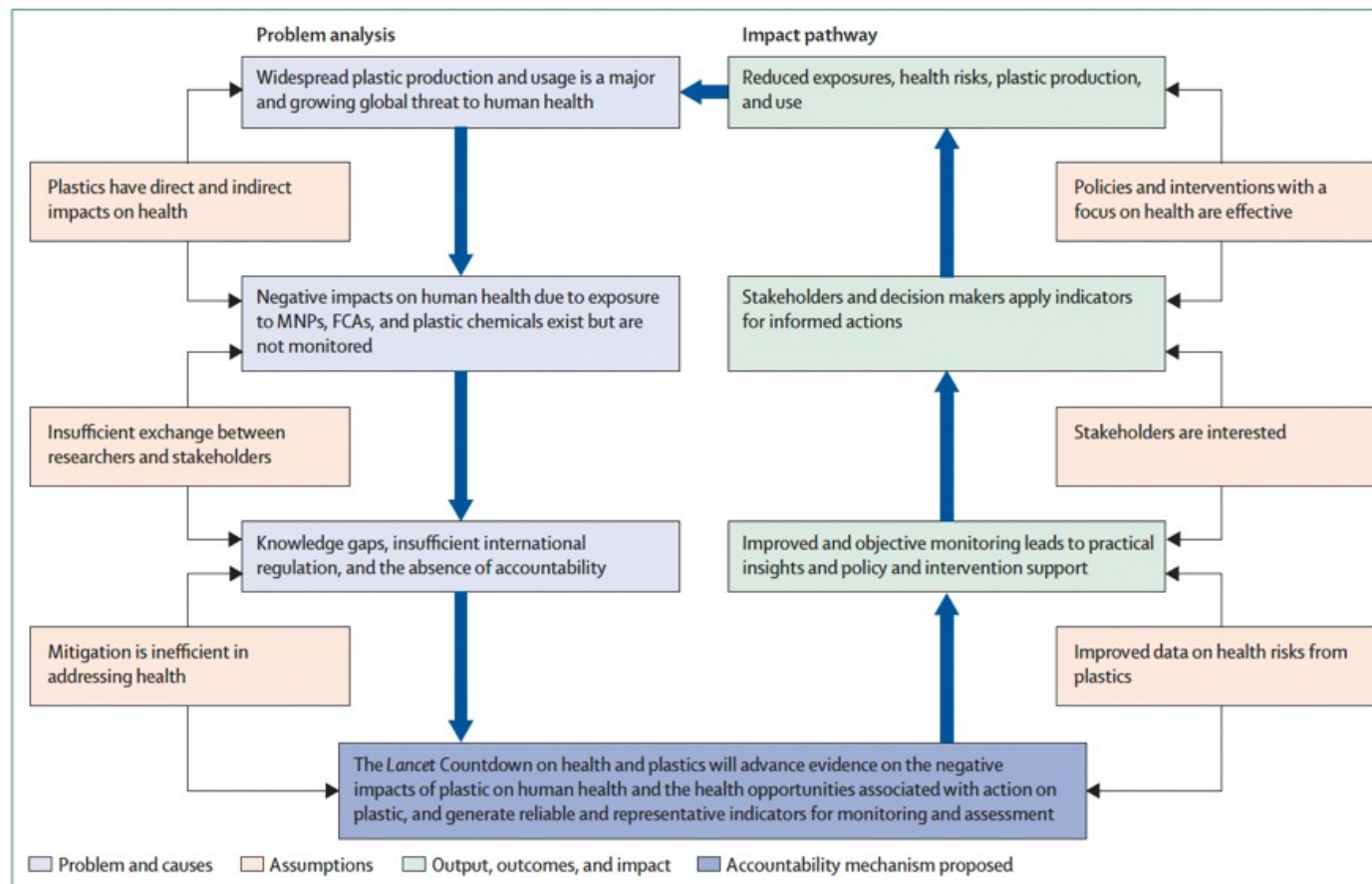


Figure 4: Conceptual domains in the Lancet Countdown on health and plastics





**Figure 5: Schematic representation of impact pathways for the Lancet Countdown on health and plastics based on the theory of change**  
 On the left side, the problem analysis outlines the growing threat of plastic production and pollution, highlighting gaps in monitoring, the need for strengthening the science-policy interface, limited industry accountability, and insufficient regulatory interventions for health protection across the plastic lifecycle. On the right side, the impact pathway envisions a series of outcomes starting with improved data on health risks from plastics, which will enable stakeholders and decision makers to apply health-focused indicators to leverage effective actions. Figure adapted from the Dutch Research Council.<sup>195</sup> FCA=food contact articles. MNP=microplastic and nanoplastic particle.

## Conclusion

The world is in a plastics crisis. This crisis has worsened alongside the other planetary threats of our time and is contributing to climate change, pollution, and biodiversity loss. Long unseen and unaddressed, the magnitude of the plastics crisis is now widely recognised, and its implications for both human and planetary health are increasingly clear.

An estimated 8000 Mt of plastic waste pollute the environment.<sup>25</sup> MNPs and multiple plastic chemicals are found in the most remote reaches of the planet<sup>112–114</sup> and in the bodies of marine and terrestrial species worldwide, including humans.<sup>18</sup> The 2023 analysis by

the Minderoo–Monaco Commission on plastics and health found that plastics harm human health at every stage of the plastic lifecycle, that these health-related damages result in massive economic losses that are borne by society, and that plastics-associated harms fall disproportionately on low-income people and at-risk populations (panel 2).<sup>23</sup>

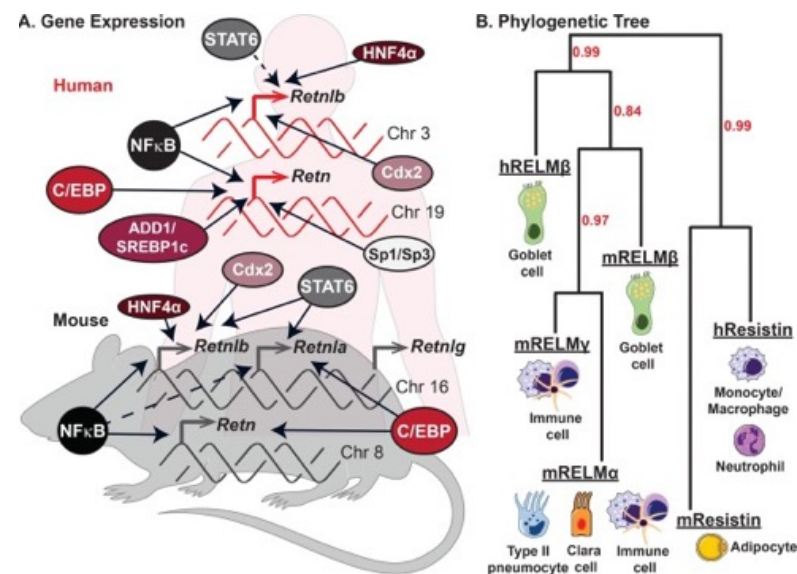
Three factors are responsible for worsening of the plastic crisis. The first and most fundamental is that global plastic production is accelerating.<sup>57</sup> Current increases in production are projected to continue, and in the absence of intervention, global plastic output is on track to nearly triple by 2060.<sup>24</sup> Inadequate recovery and recycling, coupled with a lack of operationalised circularity, is a second driver. Despite decades of effort, less than 10% of plastics are recycled, and thus 90% are either burned, landfilled, or accumulate in the environment.<sup>60</sup> Unlike paper, glass, steel, and aluminium, chemically complex plastics cannot be readily recycled. It is now clear that the world cannot recycle its way out of the plastic pollution crisis. The persistence of plastics is a third key driver. Most plastics do not biodegrade in the environment, nor do they break down into their constituent elements; instead, they fragment into ever smaller particles (eg, MNPs) that can

persist for decades in salt and fresh water, on land, and in living organisms. Polymers, such as PVC and some plastic chemicals (eg, PFAS) that are based on carbon–halogen bonds, are especially durable. The consequence is that at least 80% by the weight of all plastic ever made is still present in the environment (figure 1). For much of this plastic, its ultimate repository is the ocean.<sup>180</sup>

The plastic crisis is not inevitable. Although there is much we still do not know about plastics' harms to human health and the global environment, and more research is certainly needed, we have enough data now to know that these harms are already considerable, and there is enough information on trends in plastic production to recognise that in the absence of intervention, they will get worse.

Control of the plastics crisis will require continuing research coupled with the science-driven interventions—laws, policies, monitoring, enforcement, incentives, and innovations—that have successfully and cost-effectively controlled other forms of pollution and catalysed systems change.<sup>30,32,34</sup>

Resistin-like molecule Y is a protein from the resistin-like molecule (RELM) family that is not documented in current scientific literature; however, the family consists of other members like [RELM- \$\alpha\$](#) , [RELM- \$\beta\$](#) , [RELM- \$\gamma\$](#) , and Resistin, all of which are cysteine-rich secreted proteins involved in diverse physiological processes, including immune responses, inflammation, metabolism, and growth, and are implicated in various diseases.





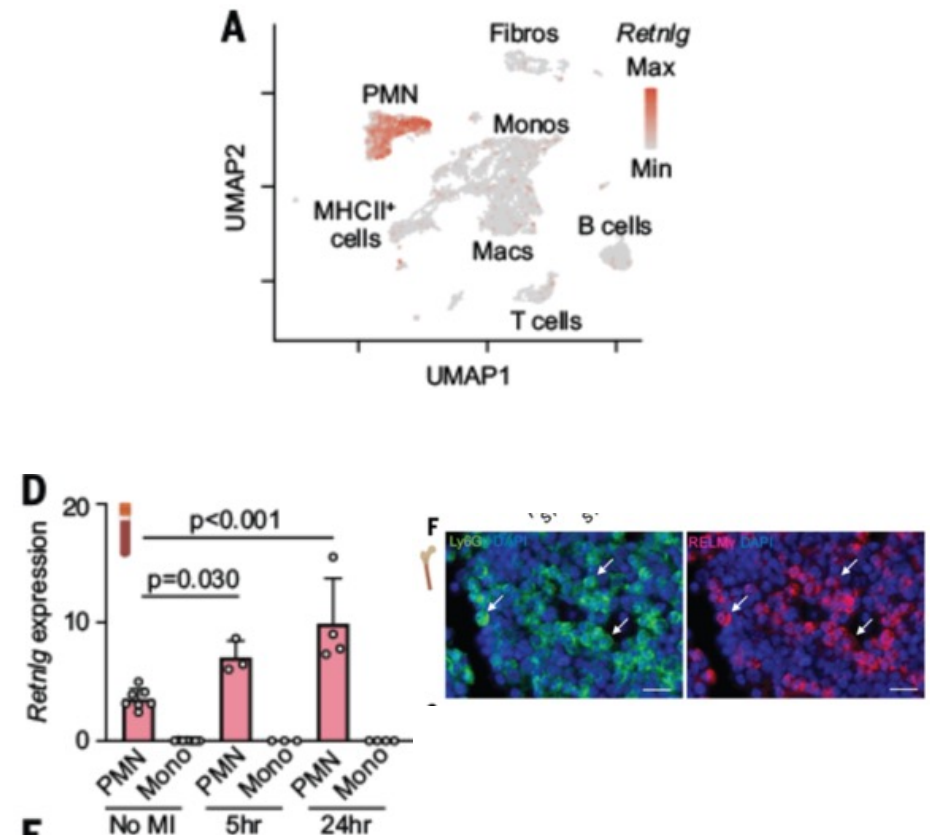


## Poking holes in the heart's rhythm

The mammalian innate immune system has evolved over millions of years as a first line of defense against pathogens and tissue injury. But what emerges when immunity encounters the syndromes of advanced age, wherein the selective evolutionary pressure is relatively short? In the case of human heart disease, the confrontation can lead to unintended and grave consequences. Kumowski *et al.* report that in mice, misdirected **cross-talk between neutrophils and cardiac tissue predisposes the heart to arrhythmia and cardiac death and can inflict damage beyond the heart. Antimicrobial peptides normally released by neutrophils to fight infection damage the cell membrane of cardiomyocytes, causing ion leaks that disrupt the heart's electrical activity.** These peptides may offer a new target for limiting tissue injury and death from ischemic heart disease.

# Resistin-like molecule $\gamma$ attacks cardiomyocyte membranes and promotes ventricular tachycardia

Ventricular tachycardia disrupts the heart's coordinated pump function, leading to sudden cardiac death. Neutrophils, which are recruited in high numbers to the ischemic myocardium, promote these arrhythmias. Comparing neutrophils with macrophages, we found that resistin-like molecule  $\gamma$  (*Retnlg* or RELM $\gamma$ ) was the most differentially expressed gene in mouse infarcts. reLM $\gamma$  is part of a pore-forming protein family that defends the host against bacteria by perforating their membranes. In mice with acute infarcts, leukocyte-specific *Retnlg* deletion reduced ventricular tachycardia. RELM $\gamma$  elicited membrane defects that allowed cell exclusion dyes to enter the cardiomyocyte interior and also caused delayed afterdepolarizations and later cardiomyocyte death, both of which are strong arrhythmogenic triggers. Human resistin likewise attacked membranes of liposomes and mammalian cells. We describe how misdirected innate immune defense produces membrane leaks and ventricular arrhythmia.

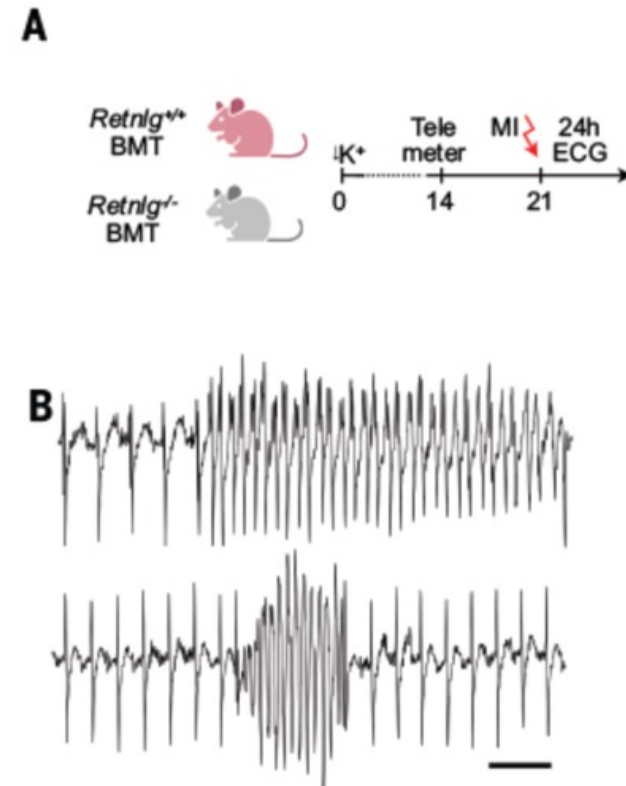




## RELMγ causes membrane defects in liposomes and cardiomyocytes

Next, we sought to determine the mechanism by which RELMγ elicits arrhythmia. Known RELM functions can be divided into two categories: (i) enhancing inflammation and (ii) defending against bacteria by attacking their membranes. We first studied whether infarct leukocyte frequencies, which may modulate arrhythmogenesis, were altered in Retnlg<sup>-/-</sup> BMT. Using flow cytometry of acute infarcts, remote myocardium, and blood, we found no differences in circulating and recruited leukocytes between Retnlg<sup>-/-</sup> BMT mice and Retnlg<sup>+/+</sup> BMT mice, nor were there differences in stromal cell numbers. These data were confirmed by histology, which also revealed comparable myocardial fibrosis and vascularization. Cardiomyocyte size and left ventricular weight were similar in the two cohorts. Comparing the inflammatory response to ischemia in Retnlg<sup>-/-</sup> BMT and Retnlg<sup>+/+</sup> BMT mice with MI, we detected no differences. Retnlg deletion did not affect other inflammatory neutrophil functions such as provision of oxidative stress or NETosis. Therefore, we subsequently focused on the membrane pore-forming properties of RELMγ.

Retnlg (resistin-like gamma) is a gene and protein, also known as FIZZ3 or RELMγ, that belongs to the resistin-like molecule family and is primarily expressed in hematopoietic (blood-forming) tissues and the colon. It functions as a probable hormone and cytokine, promoting myeloid cell chemotaxis (movement). Retnlg plays a role in the inflammatory and metabolic processes of mice and rats and has been linked to intestinal regulation of insulin sensitivity.



**RELMγ deficiency reduces arrhythmia.**

The detrimental roles of neutrophils after clinical reperfusion and in the heart are widely documented. Yet neutrophils also have woundhealing properties. As such, the en masse blockade of this cell type is problematic, and targeting neutrophil effectors, such as reactive oxygen species and myeloperoxidase, have yet to benefit clinical reperfusion. Thus, new targets are needed to rescue nonregenerative, but salvageable, cardiomyocytes. Kumowski et al. also reported a similar neutrophil attack mechanism on neuronal cells after experimental stroke in a mouse model. Misdirected injury response by neutrophils could be relevant to other scenarios, where different mechanisms selectively regulate the deployment of RELMs in various contexts.

# ‘Gray rocking’ is a way to deal with difficult people. Here’s how it works.



Gray rocking is “a communication tool that involves being less engaged during an emotionally toxic interaction,” explained Brianne Markley, a psychologist at the Cleveland Clinic. ✦


By responding to goading comments with a blank expression and calm, neutral tone — imagining you’re a dull gray rock, in other words — “you’re not adding fuel to an already volatile fire,” said Chloe Nazra Lee, a resident physician in the Department of Psychiatry at the University of Rochester Medical Center in New York.

The theory is that if you’re interacting with someone who is trying to manipulate or gaslight you, or has narcissistic personality disorder or displays narcissistic traits, they probably “want to get a rise out of you,” explained Julia Babcock, a clinical psychologist and professor at the University of Houston. “Even negative attention reinforces them, so you give them no reinforcement.” (This is different from stonewalling, when one person refuses to communicate at all, an approach that can damage relationships, Lee said.)

"Passiv-aggressiv" (im Deutschen) bezeichnet ein Verhalten, bei dem jemand seine negative Einstellung oder Aggression nicht direkt, sondern indirekt und verdeckt ausdrückt, zum Beispiel durch Ignorieren von Anweisungen, Aufschieben von Aufgaben, Sarkasmus oder durch Vortäuschen von Unfähigkeit.

Gaslighting ist eine Form der psychischen Manipulation, bei der eine Person die andere durch Lügen, Leugnen und Verunsichern dazu bringt, an der eigenen Wahrnehmung und dem eigenen Verstand zu zweifeln. Der Begriff leitet sich vom englischen Theaterstück und Film "Gaslight" ab, in dem die Frau systematisch von ihrem Mann daran gehindert wird, die Realität zu erkennen.

## When to use the gray rock method

Scientists haven't really studied the gray rock method in clinical settings. And some experts stressed that this technique is not recommended if you think someone might become violent. If you have concerns about your safety in a relationship, you should seek professional support immediately, Markley said. Depending on the situation, "it might not be safe to totally disengage from an abusive person," she said. 

It could be a reasonable strategy to "be a gray rock" when dealing with someone you interact with only occasionally, such as an annoying neighbor or co-worker, "but when there is a narcissist in your house, that's different," said Sandra Graham-Bermann, the director of the Child Resilience and Trauma Lab and a professor of psychology and psychiatry at the University of Michigan.

In situations where you don't feel unsafe but do have to interact with a difficult person, the gray rock method is "just good advice on how you manage" them, Graham-Bermann said. "You don't give extra attention; limit your engagement and protect yourself."

## How to be a gray rock

### **Center yourself**

Maybe you're about to enter a situation with a person you suspect will try to provoke you. Beforehand, repeating a mantra might allow you to tap into that gray rock mindset, Babcock said. She recommended a sky and weather metaphor from psychotherapist and acceptance and commitment therapy (ACT) trainer Russ Harris: "The observing self is like the sky, while thoughts, sensations and images are like the weather. The weather constantly changes throughout the day. And whatever it is, the sky always has room for it. No matter how bad the weather, no matter how violent the thunderstorm, no matter how severe the sun, the sky cannot be damaged in any way."

### **Keep responses calm and neutral**

Think: a flat affect, neutral tone of voice, limited eye contact and brief, disinterested replies. Hopefully, the other person will get the message that you're not engaged in the conversation, Babcock said. "It is really not fun to talk with somebody who has that blank expression and doesn't seem to be absorbing" what you're saying, she said.